

UNIVERSITÀ
DEGLI STUDI
DI PADOVA

UNIVERSITÀ DEGLI STUDI DI PADOVA

DIPARTIMENTO DI MEDICINA MOLECOLARE

SCUOLA DI DOTTORATO DI RICERCA IN: BIOMEDICINA

CICLO XXV

SETTING UP OF AN INNOVATIVE PROCEDURE FOR REDOX PROTEOMICS

**AND ITS APPLICATION FOR DEFINITION OF THE REDOX
STATUS OF CELLS WITH HIGH METASTATIC POTENTIAL**

Direttore della Scuola: Ch.mo Prof. Giorgio Palù

Supervisore: Ch.mo Prof. Fulvio Ursini

Dottorando: Mattia Zaccarin

ABBREVIATIONS

2D	Two-dimensional
5-IAF	5-(Iodoacetamido)fluorescein
Ab	Antibody
ACN	Acetonitrile
APS	Ammonium persulfate
BSA	Bovine serum albumine
CCB	Coomassie Colloidal Blue
CID	Collision induced dissociation
CSCs	Cancer Stem Cells
DIGE	Differential in Gel Electrophoresis
DOC	Sodium deoxycholate
DTNB	3,3'-dithio-bis(6-nitrobenzoic acid)
DTT	Dithiothreitol
EDTA	Ethylenediaminetetraacetic acid
EMT	Epithelial to mesenchymal transition
ESI	Electrospray ionization
FA	Formic acid
G6PDH	Glucose-6-phosphate dehydrogenase
GSH	Reduced glutathione
HPDP	N-[6-(Biotinamido)hexyl]-3'-(2'-pyridyldithio)propionamide
HRP	Horseradish peroxidase
IAA	Iodoacetic acid
IAM	Iodoacetamide
LC	Liquid chromatography
m/z	Mass to charge ratio
MS	Mass Spectrometry
MS/MS	Tandem mass spectrometry
MW	Molecular weight
NEM	N-ethylmaleimide
PAGE	Polyacrylamide electrophoresis
PBS	Phosphate buffered saline
PEP	Posterior Error Probability
PPP	Pentose phosphate pathway
Q-TOF	Quarupole – Time of flight
RNS	Reactive nitrogen species
ROS	Reactive oxygen species
RPC	Reverse phase chromatography
Rt	Retention time
SDS	Sodium dodecyl sulphate
TCA	2,2,2-Trichloroacetic acid
TCEP	Tris(2-carboxyethyl)phosphine
TEMED	Tetramethylethylenediamine
TrisHCl	Trishydroxymethylaminomethane hydrochloride
Wb	Western blotting

CONTENTS

ABBREVIATIONS	1
1. ABSTRACT	5
RIASSUNTO	6
2. INTRODUCTION	8
2.1 REDOX STATUS OF PROTEINS.....	8
2.1.1 <i>Reactivity of Cysteine residues</i>	9
Disulfides.....	10
Thiyl radical	11
Sulfenic acid	12
Reaction of thiols with hydrogen peroxide	13
2.1.2 <i>Redox switches</i>	14
2.1.3 <i>Structural and functional disulfides</i>	17
2.2 OXIDATION RATE AND REDUCTION RATE	20
Specificity and reversibility of redox signalling	20
Dynamic equilibrium: oxidation and reduction rate	21
2.2.1 <i>Electrophiles and nucleophiles formation</i>	23
Sources of biologically relevant ROS.....	24
Antioxidant defense mechanisms	25
2.2.2 <i>Nrf2-Keap1 feedback loop</i>	27
Nrf2 in cancer prevention and promotion: dual roles of Nrf2.....	28
2.3 EVENTS RELATED TO MALIGNANCY ARE REDOX REGULATED.....	29
2.3.1 <i>Oxidation</i>	31
DNA and lipids.....	31
Proteins.....	32
Non receptor tyrosine kinases (PTKs): Src.....	33
Rat Sarcoma genes product (Ras) and the Raf/MEK/ERK pathway	33
PI3K/AKT pathway and protein tyrosine phosphatases: PTP1B and PTEN	34
2.3.2 <i>Reduction</i>	35
2.3.3 <i>Localization</i>	37
GSH/GSSG redox potential in cellular compartments.....	37
Redox regulation of cell migration and adhesion	38
2.4 METHODOLOGICAL APPROACH: TRADITIONAL AND INNOVATIVE METHODS FOR DISULFIDE BONDS ASSESSMENT.....	40
2.4.1 <i>Disulfide proteome of complex samples</i>	42
3. MATERIALS AND METHODS	44
3.1 CELL CULTURES	44
3.2 SUB-CELLULAR FRACTION ENRICHMENT	44
3.2.1 <i>Protein assay</i>	45
3.2.2 <i>DTNB assay</i>	45
3.3 DIFFERENTIAL “REDOX” LABELLING.....	46
Alkylation of free thiols.....	46
Reduction of oxidized thiols.....	46
HPDP Labelling.....	46
Enrichment of labelled proteins	46
Alkylation of formerly oxidized thiols	47
3.3.1 <i>HPDP assay</i>	48

3.3.2	<i>Electrophoresis</i>	48
3.3.3	<i>Western blotting</i>	48
3.4	SAMPLE PREPARATION FOR MS ANALYSIS	49
3.5	Q-TOF ANALYSIS	49
3.6	G6PDH ENZYMATIC ACTIVITY MEASUREMENT	50
3.7	DATA ANALYSIS.....	51
3.7.1	<i>Input data</i>	52
3.7.2	<i>Identification</i>	52
3.7.3	<i>Quantification</i>	54
3.7.4	<i>Results filtering and score ranking</i>	55
4.	RESULTS	57
4.1	DEVELOPMENT OF LABEL FREE METHODOLOGY TO CHARACTERIZE AND DIFFERENTIALLY QUANTIFY OXIDATIVELY MODIFIED PROTEINS IN COMPLEX SAMPLE.....	57
4.1.1	<i>Differential redox labelling</i>	57
4.1.1.1	Trapping of the native redox state of thiols	57
4.1.1.2	Reduction of oxidized thiols.....	58
4.1.1.3	Labelling reaction.....	59
4.1.1.4	Critical aspects of elution	59
4.1.2	<i>Quantification of extracted proteins</i>	60
4.1.2.1	Ion abundance linearity	60
4.1.2.2	Workflow development: from identification to quantification	62
4.1.2.3	Workflow validation	64
4.1.2.4	Decision-making criteria	65
4.2	DIFFERENCES IN M2 AND M2T REDOXOME	67
4.2.1	<i>Differential protein list</i>	68
4.2.2	<i>Differential proteins characterization</i>	71
4.2.3	<i>“Totally reduced” controls</i>	72
4.2.4	<i>Mapping of specific modifications</i>	73
4.3	REDOX ENVIRONMENT OF M2 AND M2T CELL LINES	75
4.4	G6PDH ACTIVITY	75
4.4.1	<i>G6PDH activity is affected by redox status</i>	75
4.4.2	<i>G6PDH reduced and oxidized forms</i>	78
4.5	NRF2 PATHWAY GENE EXPRESSION DATA	79
5.	DISCUSSION	81
5.1	REDOX PROTEOMICS: A TECHNICAL CHALLENGE	81
5.1.1	<i>General strategies to screen for protein thiol modifications</i>	81
Loss of selective labelling due to thiol modification	81	
Selective reduction of reversible protein thiol modifications	82	
Selective reaction of particular protein thiol modifications.....	83	
5.1.2	<i>The “biotin-switch” method</i>	83
5.2	INNOVATIVE PROCEDURE FOR REDOX PROTEOMICS	84
Unmodified thiols blocking.....	85	
Selective reduction	86	
Affinity purification	86	
5.2.1	<i>Label-free approach: computational analysis</i>	86
The choice of the features quantification approach	87	
Reproducibility and relative-quantification criteria.....	88	
5.2.2	<i>Limits and improvements of the approach</i>	89

5.3 G6PDH AS PUTATIVE MASTER REGULATOR OF REDOX EQUILIBRIUM.....	90
5.3.1 <i>Cancer metabolism and ECM detachment</i>	90
5.3.2 <i>G6PDH redox regulation</i>	92
5.4 CONCLUDING REMARKS	93
6. REFERENCES	95
OTHER STUDIES CARRIED OUT DURING PHD PROGRAM	104
AKNWOLEDGMENTS	105

1. ABSTRACT

BACKGROUND: The cysteine (Cys) proteome includes 214.000 Cys with thiol and other forms. Of these, only a relatively small subset functions in cell signalling. Redox-active Cys are more susceptible to oxidation, and their oxidized form is more susceptible to reduction. Specific proteomic techniques are required to identify these modifications and to study their regulation in different cell processes that are collectively known as *redox proteomics*. Thus, it is of interest to be able to identify both the proteins and the cysteine residues affected, and to quantify the extent of the modification involved. The quantification of differences between two or more physiological states of a biological system is among the most challenging technical tasks in proteomics: liquid chromatography coupled to mass spectrometry (LC-MS) based quantification methods have gained increasing robustness and reliability over the past five years. Many authors still share a view of redox signalling in which the fate of the cell is dependent mainly on the intensity and duration of pro-oxidant stimulus: here we sustain the involvement of an equilibrium encompassing the action of both nucleophiles and electrophiles at the same time.

AIM: The dual aim of my PhD work has been both to develop suitable methodology to identify and quantify redox-active proteins in complex samples and to apply it to the study of a cellular model of breast cancer (MCF10A) engineered to reproduce malignancy.

METHODS: In order to pursue this aim, I took advantage of an approach integrating differential chemical sample labelling (*non-isotopic*) with Cys reactive probes (NEM, IAM, HPDP) and chromatographic purification of redox-sensitive proteins, with subsequent LC-MS/MS analysis and computational data handling for *OpenMS*-based label-free quantification. All the steps of this methodology have been developed and validated in close collaboration with experts from both the biochemistry and bioinformatics field.

RESULTS: We obtained an efficient cost-effective and isotopes-free methodology to characterize the *redoxome* in complex protein samples. Application of our quantification protocol to benchmark dataset leads to 100% correct estimates of under/over expression of the protein moiety. Application of the methodology to the breast cancer cellular model lead to identification of more than 300 proteins and allowed us to group-up unchanged and differentially oxidized redox-sensitive proteins in the more malignant cells in respect to their less aggressive counterpart.

CONCLUSION: Despite the commonly accepted association between cancer and higher oxidative-stress, this study links higher breast cancer cells malignancy to a finely tuned dynamic equilibrium in which selected protein targets are oxidized in the context of a more reduced cell environment. Preliminary results point at the enzyme G6PDH as a crucial regulator of this redox process.

RIASSUNTO

STATO DELL'ARTE: Il proteoma include 214.000 cisteine in forma di gruppi tiolici liberi od altra forma. Di queste, solamente un insieme relativamente ristretto ha un ruolo nella mediazione di segnali cellulari. Tali cisteine, attive dal punto di vista dell'ossido-riduzione, sono più sensibili all'ossidazione e la loro forma ossidata è più facilmente riducibile. Sono dunque necessarie specifiche tecniche di proteomica, globalmente indicate con il termine *proteomica delle ossido-riduzioni*, per identificare tali modifiche e studiarne la regolazione in diversi processi cellulari. Risulta quindi determinante la capacità di identificare sia le proteine che i residui coinvolti e di quantificarne il grado di modificazione. E proprio la quantificazione delle differenze tra due o più stati di un sistema biologico, si colloca tra gli obiettivi tecnicamente più sfidanti della proteomica: nel corso degli ultimi cinque anni, tecniche basate sulla spettrometria di massa associata a cromatografia in fase liquida hanno progressivamente guadagnato affidabilità e robustezza. Molti autori condividono tuttora una visione delle ossido-riduzioni nella mediazione del segnale in cui il destino cellulare dipende principalmente dall'intensità e dalla durata degli stimoli ossidanti: nel presente lavoro si vuole invece sostenere il coinvolgimento di un equilibrio che includa l'azione concomitante sia di specie nucleofile sia di specie elettrofile.

OBIETTIVO: Il duplice obiettivo del mio lavoro di Dottorato è stato sia lo sviluppo di una metodologia idonea all'identificazione e quantificazione di proteine, attive dal punto di vista delle ossido-riduzioni, in campioni complessi, sia l'applicazione di tale metodologia allo studio di un sistema cellulare ingegnerizzato di carcinoma mammario (MCF10A) caratterizzato da diversi gradi di malignità.

METODI: Al fine di perseguire tale obiettivo ho tratto vantaggio da un approccio che integra la marcatura chimica differenziale (*non-isotopica*) per mezzo di sonde reattive con i residui di cisteina (NEM, IAM, HPDP) e la purificazione cromatografica delle proteine attive dal punto di vista ossido-riduttivo, alla successiva analisi LC-MS/MS ed elaborazione informatizzata dei dati mediante *OpenMS* per una quantificazione *label-free*. Tutti i passaggi di tale metodologia sono quindi stati messi a punto e validati in stretta collaborazione con esperti biochimici e bioinformatici.

RISULTATI: E' stato sviluppato un metodo efficiente ed economico, non basato sull'utilizzo di marcatori isotopici, per la caratterizzazione delle proteine attive dal punto di vista ossido-riduttivo in campioni proteici complessi. L'applicazione del protocollo di quantificazione ad un campione test ha dato il 100% di stime corrette di sovra/sotto-espressione della miscela proteica. L'applicazione del metodo allo studio del modello cellulare di carcinoma mammario ha portato all'identificazione di più di 300 proteine ed ha permesso il raggruppamento di quelle sensibili dal punto di vista ossido-riduttivo in gruppi non differenziali e

sovra- o sotto-ossidate nelle cellule più maligne rispetto alla loro controparte meno aggressiva.

CONCLUSIONI: Nonostante sia comunemente riconosciuta l'associazione tra fenomeni neoplastici ed uno stress ossidativo, questo studio collega la maggiore malignità di un modello cellulare di carcinoma mammario ad un complesso equilibrio ossido-riduttivo. In questo contesto, specifici bersagli proteici sono ossidati mentre viene mantenuto un ambiente cellulare complessivamente ridotto. Risultati preliminari evidenziano poi l'enzima G6PDH come possibile elemento chiave nella regolazione di tale equilibrio.

2. INTRODUCTION

2.1 Redox status of proteins

Despite some ostensible formalism clarification of essential definitions, speaking of redox proteomics is not just a mere semantic task. Redox status is a term that has been used to describe the ratio of the convertible oxidized and reduced forms of a specific redox couple and it should not be extended to description of the general redox environment of a cell since the latter is a reflection of the state of sets of redox couples. Moreover, we should also distinguish a redox pair from a redox couple, since the former refers to both oxidizing and reducing species involved in a reaction while the latter describes the behaviour of the reducing specie and its corresponding oxidized form.

So a more precise definition of redox status of a redox couple could be intended as the half-cell reduction potential of that couple while redox environment of a linked set of redox couples (redox pairs) is the summation of the products of the reduction potential and reducing capacity of the linked redox couples present. In these definitions reducing capacity refers to the concentration of reducing equivalents available (strength of the redox buffer). Each protein in the cell could be seen as a redox couple on its own and thus described as an electrochemical cell. Nernst equation allows us to determine the reduction potential for the half-cell (E_{red}) which is the potential when the half reaction takes place at cathode (a measure of the tendency of the oxidizing agent to be reduced).

So given the Nernst equation for the half cell reaction:

$$E_{red} = E_{red}^{\theta} - \frac{RT}{zF} \ln \frac{a_{Red}}{a_{Ox}}$$

Where:

E_{red} = Half-cell reduction potential at the temperature of interest

E_{red}^{θ} = Standard reduction potential

R = Universal gas constant = $8.314472 \text{ J K}^{-1} \text{ mol}^{-1}$

T = Absolute temperature in K

z = Number of moles of electrons transferred in the cell half-reaction

F = Faraday constant = $9.64853399 \cdot 10^4 \text{ C mol}^{-1}$

$a_{Red/Ox}$ = Chemical activity of the reductant/oxidant specie.

a = activity coefficient * $[\text{Red/Ox}]$

For low concentrations activity coefficient = 1 and $a = [\text{Red/Ox}]$

Overflying chemical and mathematical details we can then obtain the Nernst equation for the one electron process: $\text{Ox} + e^- \rightarrow \text{Red}$

$$E_{\text{red}} = E_{\text{red}}^{\theta} - \frac{RT}{F} \ln \frac{[\text{Red}]}{[\text{Ox}]}$$

So we can state that each protein is characterized by its own redox status which could be described by means of the reduction potential of the redox couple considered. Definitely the redox status of a protein is the ratio of its reduced and oxidized form. Moreover, the Nernst equation could be used to determine the electromotive force between two redox couples (ΔE). Given species being oxidized (E_1) and species being reduced (E_2) we then have: $\Delta E = E_2 - E_1$.

If ΔE is zero, there is no electron flow. When ΔE is not zero the sign determines the direction of electron flow (the direction of the redox reaction). As an example, given a ratio of NADPH/NADP⁺ of 100:1 Reduction potential (E_{red}) for this couple is equal to -374 mV from Nernst equation. This very negative reduction potential supports the idea that the NADPH/NADP⁺ couple is a major driving force for maintaining the reducing environment in cells and tissues. Moreover, as the redox state of couples such as NADPH/NADP⁺ change, they can force changes in other redox pairs, for example signalling proteins.

If we go deeper into considering the redox status of a protein we should analyse which are the modifications characterizing its reduced or oxidized status. Obviously, the targets of such modifications are amino acid (AA) residues and, specifically the ones having “redox-reactive” side chain functional group.

2.1.1 Reactivity of Cysteine residues

Regulation of protein function via post-translational modification (PTM) has always been a leading area of interest in the struggle to comprehend both normal and pathological cellular processes. PTMs study is a growing area of interest supported by advances in high throughput proteomics. Intracellular signalling mediated by reversible phosphorylation of serine (Ser), threonine (Thr) and tyrosine (Tyr) residues of proteins is the best characterized PTM process. More recently multiple modifications of arginine (Arg) and lysine (Lys) residues have come to the fore. For example, Lys can undergo methylation, acetylation and hydroxylation; and can also be covalently cross-linked to different proteins in ubiquitination and similar processes, as well as transglutamination [Begg et al., 2006]. Modifications of Lys mediate diverse processes from epigenetics, to protein fate and structural processes. In addition to these two basic residues, another residue which undergoes multiple modifications but which has received considerably less attention is cysteine (Cys). The diversity of modifications of Cys is extensive and crucial to sustainable life in the oxidizing environment of this planet [Wouters et al., 2010; Nagahara et al., 2009]. Despite their importance Cys modifications are often transitory and refractory to analysis [Riederer, 2009]. Interestingly, Cys has one of the shortest sidechains whereas Lys and Arg have among the longest, extending up to 6.5 Å (Lys) or 7.5 Å (Arg) from the polypeptide backbone [Wouters et al., 2011]. As a result, surface modifications of

Arg and Lys are tethered far from the backbone, almost like labels on the protein. In contrast, modifications of Cys residues occur closer to the protein surface and are often accompanied by conformational changes of the backbone. In addition, Cys has the unique ability to form disulfide bonds, enabling some spectacular redox-driven conformational changes. Thiols are unable to undergo autoxidation in the absence of a catalyst, but several free metal ions markedly increase the rate of autoxidation. Other factors, such as temperature, type of buffer, type of catalyst, and oxygen concentration, are important. Moreover it has been observed that the rate of autoxidation depends on pH, indicating the participation of the thiolate species in the reaction [Bindoli et al., 2008]. The oxidation status of sulfur in different “reactive sulfur species” [Gregory et al., 2001] that we are going to see is summarized in table 2.a

Table 2.a

Reactive Species	Structure	Oxidation status of sulfur	Electrons required for complete reduction to thiol status (-2)
Thiyl radical	RS•	-1	1
Disulfide	RSSR	-1	2
Disulfide-S-monoxide	RS(O)SR	+1;-1	4
Disulfide-S-dioxide	RS(O) ₂ SR	+3;-1	6
Sulfenic acid	RSOH	0	2
Hydroxyl radical	HO•	-1	1
Peroxide	ROOR	-1	2
Superoxide	O ₂ ⁻	-0.5	3

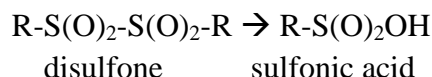
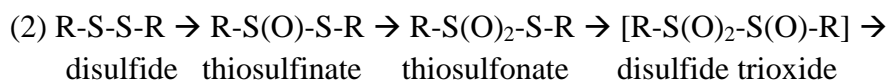
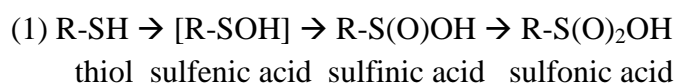
Disulfides

In biochemistry, the most familiar oxidation reaction of thiols involves the well-known thiols/disulfide redox transition:



Disulfides are formed under mild oxidizing conditions and usually do not proceed to further oxidation in the cell. However both thiols (1) and disulfides(2) can form oxygen derivatives as follow (from Bindoli et al., 2008. Intermediates reported in

brackets are unstable) and both pathways are interconnected leading to the sulfonic species which are the highest oxidized species of sulphur:

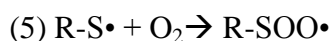
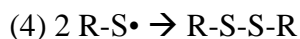
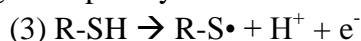


Oxidation of disulfides is generally favoured by anhydrous conditions and finally results in the formation of sulfonic acids after scission of the S-S bond. Thiolsulfonates are the first members of the disulfide oxidation products and occur naturally in biologic systems such as the well-known component of garlic alliin (diallyldisulfide monoxides) exhibiting antibacterial and fungicidal properties. Thiolsulfonates can be easily reduced to the corresponding disulfides by thiols with the intermediate formation of sulfenic acid, hence revealing their importance in the biologic redox processes.

Thiosulfonates are endowed with antimicrobial properties and act as protectants against ionizing radiation. These compounds hydrolyze in the presence of water to the corresponding sulfinic acids and disulfides and their reaction with thiols leads to sulfenic acid and disulfides.

Thiyl radical

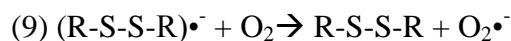
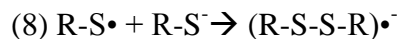
Thiols can also be oxidized by radiation of different energies such as $\alpha/\beta/\gamma$ -rays and UV light. In this case reactions proceed through the formation of a thiyl radical (3) (thiyl radicals can also be formed by transition metal-catalyzed oxidation of thiols) which, in addition to dimerization to a disulphide (4), can interact with oxygen forming a thioperoxyl radical intermediate (5):



Thioperoxyl radicals can interact with the parent thiols, leading to the formation of sulfenic acid (6) [Wardman P., 1998] and regeneration of the thiyl radical (7):

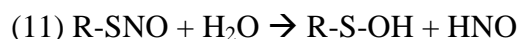
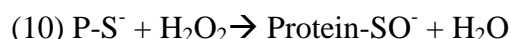


A well-established reaction of the thyl radical is its interaction with the thiolate anion, forming first the strong reductant disulfide radical anion (8), which, in turn, forms superoxide anion on reaction with oxygen (9) [Wardman P., 1998]:



Sulfenic acid

Sulfenic acid (R-SOH) is the first member of sulphur oxy-acids and, although unstable and highly reactive, has gained growing interest in biologic systems. Because of their instability, sulfenic acids are viewed as reaction intermediates, and are difficult to isolate. Sulfenic acids are formed after the reaction of the thiolate group with hydrogen peroxide (10) and other hydroperoxydes (alkylhydroperoxides and peroxyxynitrite) or from hydrolysis of S-nitrosothiols (11) and after reaction of thiols with thiosulfinates (12):



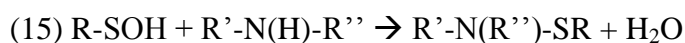
It is noteworthy that the rate of formation of sulfenic acid from many thiolates via reaction with hydrogen peroxide is too slow to happen *in vivo*, and even if it did form the presence of millimolar GSH in cells would convert it rapidly to protein-S-S-G mixed disulfide form (14) [Bindoli et al., 2008]. The same could happen also for the sulfenamide subsequently formed from sulfenic acid (15) as in the case of PTP1B [Salmeen et al., 2003]. Sulfenic acids can however find stabilizing conditions in some proteins, like apolar microenvironment that limits solvent accessibility and allows the stability of the –SOH residue by hydrogen bonding. Probably the most important factor in stabilizing sulfenic acids in proteins is the absence of proximal thiol groups or other nucleophiles. Indeed a thiol group would rapidly interact with the sulfenic moiety forming a disulfide (13) [Allison WS., 1976]:



This reaction is particularly relevant in enzymes involved in redox signalling, as the reaction of sulfenic acid residues with glutathione, present in high concentrations in cells, leads to the formation of a mixed disulfide (i.e. glutathionylation of specific proteins (14):



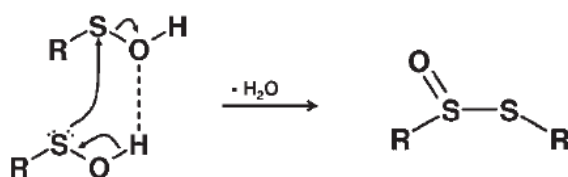
The formation of mixed disulfides, together with that of sulfenamides(15) [Salmeen et al., 2003] prevents over-oxidation of the cysteine residues to sulfinic and sulfonic acids:



Moreover sulfenic acids can undergo both electrophilic and nucleophilic reactions, according to different reaction conditions [Allison WS., 1976]. For instance, sulfenic acids are reactive toward nucleophilic reagents such as dimedone (5,5'-dimethyl-1,3-cyclohexanedione) or TNB⁻ (2-nitro-5-thiobenzoate anion) derived from the reduction of the thiol reagent DTNB (5,5'-dithiobis(2-nitrobenzoic acid)). Indeed dimedone and TNB⁻ are used to identify cysteine sulfenic acids in proteins. Finally sulfenic acids can easily condense to form a thiosulfinate (16) [Bindoli et al., 2008]:



In this reaction (16) dehydration of sulfenic acids proceeds through the formation of a dimer in which the two sulfenic acids are hydrogen-bonded and involves a nucleophilic attack exerted by the sulfenic acid sulfur on the sulfur of the second sulfenic acid molecule (reaction from Bindoli et al., 2008 to follow):



This reaction is a clear example of both the nucleophilic and electrophilic character of these acids.

Reaction of thiols with hydrogen peroxide

The reaction of protein thiols with hydrogen peroxide is of particular relevance for biologic systems. It is known that thiols could be oxidized by hydrogen peroxide in the absence of metal catalysis [Bindoli et al., 2008]. Moreover studies on the sulphhydryl enzyme glyceraldehyde-3-phosphate dehydrogenase [Little et al., 1969] demonstrated that peroxide treatment did not involve disulfide formation but rather oxidation of protein thiol to a sulfenic acid residue. Moreover the reaction was pH dependent, indicating the involvement of a thiolate group acting as a nucleophile on hydrogen peroxide (see 10 above) [Bindoli et al., 2008]. The peroxide-inactivated enzyme can be reactivated if quickly treated with an excess of low molecular weight thiols, but if such treatment is delayed, the inhibition becomes irreversible, thus indicating that the sulfenic residue undergoes further oxidation to sulfonic acid [Little et al., 1969]. Reaction kinetic of low molecular weight thiols with H₂O₂ falls in the range of 18-26 M⁻¹ s⁻¹ and turns out to be of

scarce significance in biological context. Similarly proteins containing low pK_a thiols despite 20 – 30 fold increased rate constant with H_2O_2 , are still far from competing against glutathione peroxidases and peroxiredoxins which are orders of magnitude more efficient in reducing hydrogen peroxide [Winterbourn et al., 1999]. This point to the fact that deprotonation of the thiol group alone is not sufficient to bring the interaction of hydrogen peroxide in proteins to a level comparable to that of thiol or selenium peroxidases. Moreover a study of the second-order rate constants of various proteins with hydrogen peroxide [Stone, 2004] indicates that only peroxidases and the bacterial sensor OxyR exhibit rate constants on the order of 10^5 - $10^6 M^{-1} s^{-1}$ whereas phosphatases and other enzymes such as glyceraldehyde-3-phosphate dehydrogenase and papain are in the range of 10 - $10^2 M^{-1} s^{-1}$. This sustain the idea that, to react rapidly with hydrogen peroxide, the low pK_a of cysteine is not a sufficient condition, but the thiolate requires a proper environment defined by specific amino acid residues able to stabilize the transition state intermediate [Tosatto et al., 2008].

2.1.2 Redox switches

Cysteine is a rarely used amino acid that accounts for about 2% of the amino acids in eukaryotic proteins and about 1% in proteins from eubacteria and archaea. As reported above the large, polarizable sulfur atom in its thiol group is electron-rich and highly nucleophilic; hence, cysteines can undergo a broad range of chemical reactions. Nevertheless, despite the fact that all cysteines, from a chemical point of view, are “reactive”, not all of them could act as *redox switches*. Here we may look at redox switches as specific protein-cysteine-thiols characterized by peculiar reactivity which make them target of choice for oxidative modification. As we have seen the intrinsic reactivity of protein thiols depends not only on their pK_a but also on other structural features, such as their accessibility. For example, although the $-SH$ of bovine albumin has a much lower pK_a [Lewis et al., 1980] than glutathione (GSH), it has a relatively low apparent reactivity which probably depends on steric hindrance. On the other hand we have also seen that peroxidases are reasonable targets acting as both redox signal sensors and transducers: indeed peroxidases bear cysteine residues highly reactive with H_2O_2 . Definitely redox signaling often implies a post-translational protein modification of cysteine residues and a particular cysteine residue may be differentially modified in response to diverse stimuli. Post-translationally modified cysteines are not necessarily directly involved in the catalytic activities of enzymes, but may function at an allosteric site and, thus, regulate the enzymatic activities or other protein functions through structural changes. So a large part of biological properties and functions involving protein structure as well as enzyme catalysis and redox-signalling pathways depends on the redox properties of the thiol group present both in protein and in low-molecular-weight molecules [Bindoli et al., 2008]. Nevertheless the maintenance of intracellular redox homeostasis was

thought to be mainly controlled by the GSH/GSSH ratio. Thus, with GSH and its enzymes as the main actors, the contribution of protein –SH groups (PSH) as a molecular entity capable of reacting with electrophiles and oxygen-derived species was generally considered to be negligible. Anyway this assumption does not consider the fact that PSH may play an antioxidant role, as GSH does, and at the same time perform more specific regulatory functions [Di Simplicio et al., 1998].

So their structural environment and pKa value make cysteine redox-sensitive and make proteins potentially redox regulated. Most cytoplasmic protein thiols have pKa values greater than 8.0, which render the thiol groups predominantly protonated and largely non-reactive at intracellular pH [Giles et al., 2001]. Thiol groups of redox-sensitive cysteines, on the other hand, have characteristically much lower pKa values, ranging from as low as ~ 3.5 in thiols transferase to ~5.1-5.6 in protein tyrosine phosphatases. The low pKa values of redox-sensitive cysteines arise primarily from stabilizing charge-charge interactions between the thiolate anion and neighbouring positively charged or aromatic side chains. So under physiological pH conditions, these thiols are therefore present as deprotonated, highly reactive thiolate anions [Brandes et al., 2009].

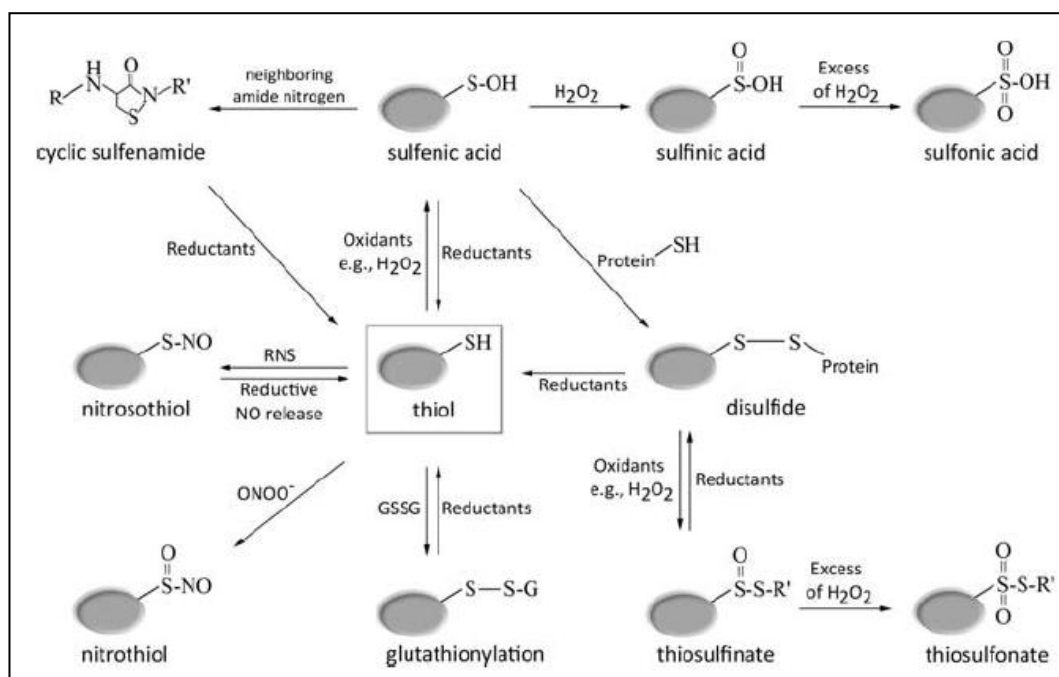


Fig. 2.a Oxidative thiol modifications

Oxidation of cysteine thiol groups by H_2O_2 leads to sulfenic acid ($R-SOH$) formation. Sulfenic acids are either stabilized by nearby charges or react with neighboring thiols or proximal nitrogen to form disulfide bonds ($R'-S-S-R''$) or sulfenamide bonds ($R'-S-NH-R'$), respectively. In the presence of high H_2O_2 concentrations, overoxidation to sulfinic ($R-SO_2H$) or sulfonic acid ($R-SO_3H$) occurs. Although a few protein-specific sulfenic acid reductases have been identified, overoxidation is still considered to be largely irreversible in vivo. Alternatively, reaction of thiolate anions (RS^-) with oxidized cysteines of other proteins or low molecular weight thiols such

as glutathione (GSSG) leads to mixed disulfide bond formation (R'-S-S-R'') or S-glutathionylation (R-S-SG), respectively. Overoxidation of disulfide bonds in the presence of strong oxidants can cause thiosulfinate (R'-SO-S-R'') or irreversible thiosulfonate (R'-SO₂-S-R'') formation. Most oxidative thiol modifications are reduced by members of the glutaredoxin (Grx) system and thioredoxin (Trx) system (reductants), which draw their reducing power from cellular NADPH. Exposure of thiolate anions to reactive nitrogen oxide species causes S-nitrosothiol formation, whereas treatment with peroxynitrite yields S-nitrothiol formation. The exact mechanism by which individual RNS cause oxidative thiol modifications in vivo is still under investigation. [From Brandes et al., 2009]

Thiolate anion are highly susceptible to oxidation by electrophiles and can undergo a wide spectrum of oxidative modifications, including: sulfenic (SOH), sulfinic (SO₂H) and sulfonic (SO₃H) acids, disulfide bonds (PSSP) or nitrosothiols (SNO). Cysteine sulfenic acids and their deprotonated cysteine-sulfenates are frequently formed upon reaction of protein thiols with H₂O₂ and represents reactive and versatile oxidation products. As we have seen, sulfenic acids are highly reactive and thus often considered metastable intermediates undergoing further reactions to form stable modifications, such as disulfides with other protein thiols or glutathione (S-glutathionylation) [Fig. 2.a]. Most oxidative modifications are fully reversible in vivo and utilize dedicated oxidoreductases, such as thioredoxin or glutaredoxin system, to quickly restore the original redox state upon the cell's return to nonstress conditions. It appears that it is the reaction rate with these dedicated oxidoreductases that often determines the lifespan of oxidized proteins and supports their accumulation even in an overall reducing environment [Leichert at al., 2004]. The type and extent of oxidative modifications in redox-regulated proteins depends on the type of oxidative pulse, its intensity, duration and distance with respect to sensor/transducers. Even small changes in the basal level of intracellular electrophiles can cause oxidative modifications in proteins that are specifically sensitive to these oxidants: such proteins are those bearing so called "redox-switches".

So redox signalling does not simply represent non-specific oxidative damage and candidate redox-switches cysteines balance diverse redox signalling responses to multiple stimuli. The susceptibility of cysteine residues to modification by a defined electrophile is dictated by a combination of factors including the pK_a of the thiol and the local pH of the intracellular compartment: for example, the high intra-mitochondrial pH (8.0 – 8.5) may be one reason mitochondrial protein thiols are particularly susceptible to modification and play a key role in cell signalling [Murphy, 2011]. Other factors are the accessibility of the thiol within protein structure and the reactivity of the thiols-modifying agent: a thiol having a pK_a of 7.4 for example will be 50% deprotonated at physiological pH, that is to say it will be in its more nucleophilic thiolate form. Thus lower pK_a thiols, which are more likely to be deprotonated at physiological pH, are favoured in their reaction with electrophiles and are more suitable candidates as redox-switches [Higdon et al., 2012]. Localization of thiol residues within a protein also seems to be

important in dictating their relative susceptibilities to modification: the most accessible thiol residue is more likely to be modified than those less accessible [Fig. 2.b].

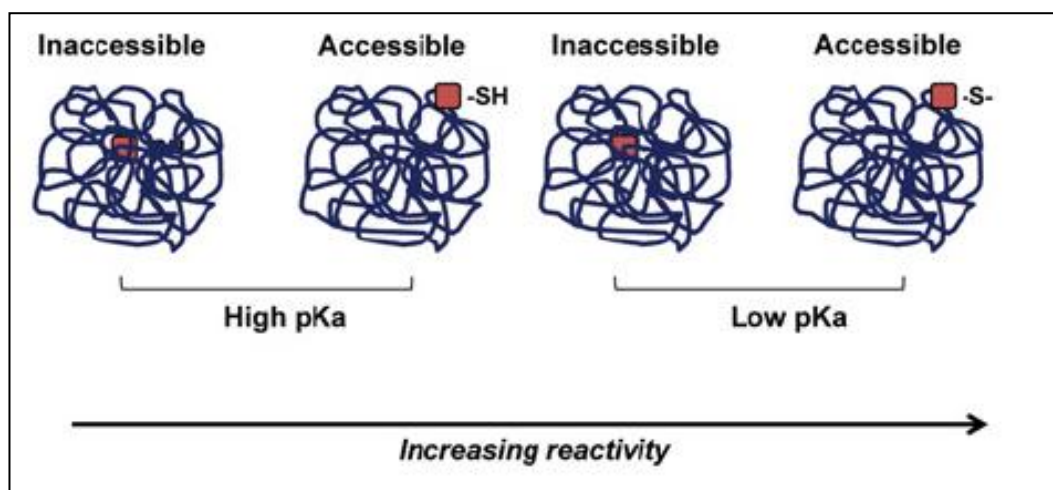


Fig. 2.b Factors which determine susceptibility to thiol modification and cellular thiol targets

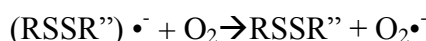
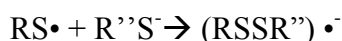
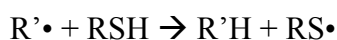
The local protein environment is a very important determinant of thiol reactivity. For example, an inaccessible, high pKa protein thiol would be considered the least prone to modification. However, a low pKa accessible thiol would be a highly sensitive target. [From Higdon et al., 2012]

Thus the combination of steric and biochemical factors result in a functional hierarchy for the activation of cellular signalling pathways on exposure of cells to an electrophile. The first pathways to respond are those which are the closest to the site of formation or exposure to the electrophile. The functional consequence of these factors is that the “first responders to electrophile exposure” are not necessarily the most abundant thiol-containing proteins [Higdon et al., 2012].

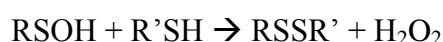
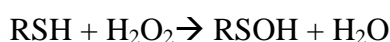
2.1.3 Structural and functional disulfides

Taking protein chemistry into account a disulfide bond is purely the covalent link between two sulfur atoms generated by the oxidation of two cysteines residues. Such bonds are important for the stabilization of the native structure of proteins and determination of their arrangements into wild type or recombinant proteins can provide insights into their folds as well as information to guide structural determination by NMR or X-ray crystallography. The very first determination of the amino acid sequence of Insulin by Sanger (1959) was indeed accompanied by investigation of its disulfide arrangement in order to complete the description of its primary chemical structure. Also characterization of the disulfides of ribonuclease by Spackman et al. (1960) was another informative study into the determination of such protein structural element. Summarizing what we have seen above (§ 2.1.1) Various pathways can lead to the formation of disulfides:

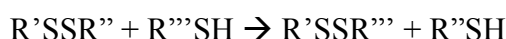
- (a) free radical oxidation of the thiol, evolving to disulfide with a proximal thiol, through the formation of the intermediate disulfide anion radical [Mottley et al., 2001]



- (b) Nucleophilic displacement reaction in the presence of a hydrogen peroxide producing a sulfenic acid residue [Dickinson et al., 2002].



- (c) Thiol-disulfide exchange reaction [Maiorino et al., 2007]



Mechanism (a) is more likely to be involved as antioxidant mechanism in the presence of oxidizing free radicals, while pathways (b) and (c) are relevant for the formation and reshuffling of disulfides in proteins respectively. Beside mechanisms underlying their formation, as stated at the beginning of this paragraph, intra-protein disulfide bonds are classically viewed as part of the tertiary structure of the protein and their formation is an important step in protein folding. Similarly, many disulfide bonds are important in the quaternary structure of proteins (ie – in the formation of homo or hetero multimers). Nevertheless, aerobic organisms maintain a reduced state in the cell despite the highly oxidizing environment (21% oxygen, at sea level) where they live and we have seen (§ 2.1.2) that the redox state of protein thiols is then dependent on their cellular location [Ghezzi, 2005]. In the cytoplasm, the environment is highly reduced, mainly due to the high intracellular concentration of GSH, and the GSH/GSSG ratio is 30–100. For this reason cysteine residues of cytoplasmic proteins are mainly present as free thiols, both in mammalian cells and bacteria. It is generally thought that the only disulfide bonds in the cytoplasm are transient ones formed as a part of the oxidation-reduction reactions of enzymes. In contrast, extracellular proteins are mainly disulfide proteins, because of the oxidative extracellular environment. On the other hand, structural disulfide bonds are formed during the folding process in the endoplasmic reticulum as this intracellular compartment is different from the cytosol in that it is highly oxidizing, with a GSH/GSSG ratio of approx. 1 [Hwang et al., 1992]. Recent studies of redox proteomics have challenged the belief that cytosolic proteins only have free cysteines, showing that many disulfide bonds are formed in a large number (~100) of cytoplasmic proteins in cardiomyocytes and neuronal cells exposed to oxidants [Brennan et al.,

2004; Cumming et al., 2004]. Evidence that a substantial amount of glutathione is present as mixed disulfide with proteins also points in this direction. However, most of these disulfide bonds are different from those important for the structural integrity of proteins. These non-structural disulfide bonds differ from structural ones in that the former are reversible, and both reduced and oxidized forms of these proteins coexist. For a comparison, redox potentials in thiol-disulfide oxidoreductases range from -95 mV to -330 mV, whereas structural disulfides may have potentials as low as -470 mV. In other words, such structural disulfides would never be found as dithiols under normal physiological conditions.

In his exhaustive review Wouters [Wouters et al., 2010] pointed out at least 14 different kinds of non-structural disulfides as those contradicting Richardson and Thornton rules (RT rules from now on) and called them “forbidden disulfides”. Very briefly, Richardson and Thornton pinpointed constraints in protein backbone where disulfides between resident cysteine residues could not form if not at the cost of strain introduction into protein structure.

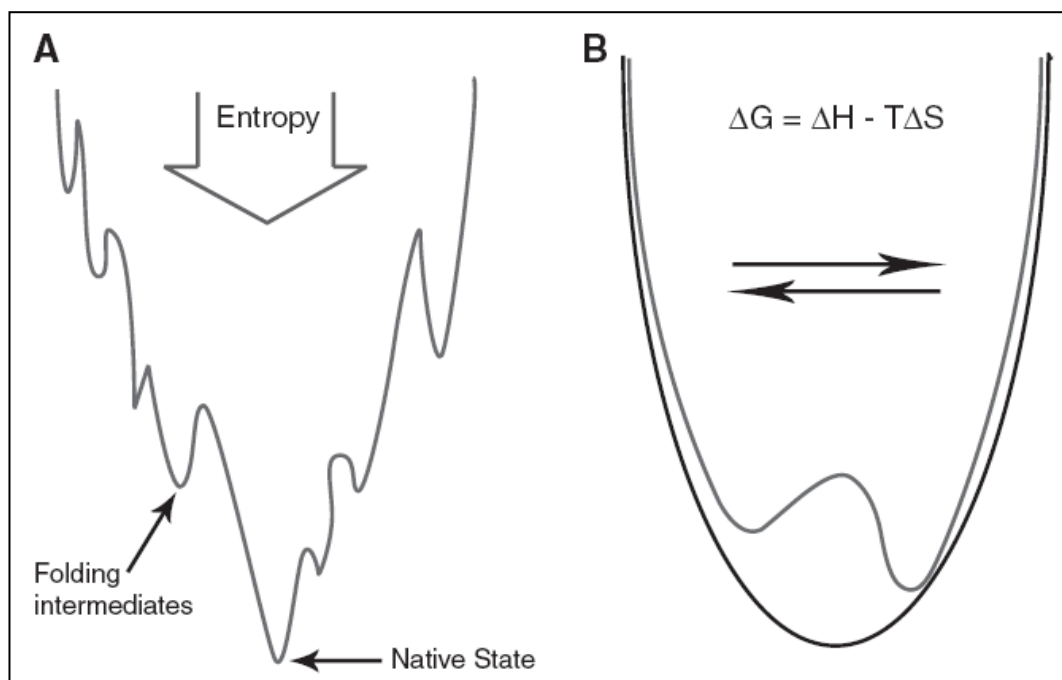


Fig. 2.c Comparison of the folding funnels for (A) a minimally frustrated fold (B) A functional protein with two states.

In a two-state forbidden disulfide switch, the entropic term could be traded off against the enthalpic term to produce two states that are not separated by a large Gibb’s free energy (light gray in B). The minimally frustrated fold is shown in dark gray in B for comparison. [From Wouters et al., 2010]

Thus, in reference to secondary structure, disulfides between cysteine pairs should not be found on (a) adjacent β -strands, (b) in a single helix/strand (c) on non adjacent strand of the same β -sheet. And in reference to primary structure disulfide bonds should not occur (d) between cysteine pairs adjacent in the

sequence [Wouters et al., 2010 and references therein]. From a thermodynamic point of view forbidden disulfides are defined as a “bi-stable switch” [Wouters et al., 2010]: a bi-stable switch is characterized by two states, both of which must contain sufficient stored potential energy to help drive the switch into the opposite state in response to the appropriate signal. Forbidden disulfides may operate as bi-stable switches by trading off different terms in the Gibb’s free energy: forming the disulfide bond decrease the entropy of the chain, however, for forbidden disulfides there is a significant cost in terms of enthalpy to form the bond because of the abnormal stereochemistry adopted by the protein chain (Fig. 2.c). Definitely disulfides disobeying RT rules are likely candidates to act as redox switches.

2.2 Oxidation rate and reduction rate

Specificity and reversibility of redox signalling

Changes in cellular redox environment can initiate signalling cascades and lead to biological consequences, such as proliferation, differentiation, apoptosis etc. This phenomenon could be pointed out as redox regulation, a term defined as “a reversible post-translational alteration in the properties of a protein, typically the activity of an enzyme, as a result of change in its oxidation state”. Authors of this definition made a clear distinction between redox regulation and terminal oxidation, which they defined as “an irreversible reaction that parks protein for degradation” and is implicitly understood to impair protein function. On the other hand, the term redox signalling, despite some interchange ability with redox regulation, extends the meaning to include entire chains involving cascades of redox reactions, eventually leading to changes in gene expression.

So far we have seen that different kinds of electrophiles in cell, together with specific proteins cysteine residues with particular reactivity, have the requisites to account for signalling functions. In a very simplified view we could say that every signal needs to fulfil at least two requisites: (a) it should be specific (b) it should be reversible (c) its action should be limited in time and space. As for the specificity it is often conferred by protein-protein interaction or just by limiting reactivity of signalling molecules in respect to signalling sensors/transducers. Nevertheless, in the case of *redox signalling* it is not so “easy” to speak of specificity, since electrophiles acting as signalling molecules are often characterized by high chemical reactivity without specificity for targets to react with and, considering for example hydroperoxides, we cannot even invoke interaction specificity. Of course among candidate signalling molecules it is possible to pinpoint hydrogen peroxide as preferential choice instead of far more aggressive species like radicals the reactivity of whom is almost diffusion-rate limited. Moreover, we have seen previously that only specific cysteine residues in proteins will undergo oxidative switching in response to electrophiles. The combination of aforementioned elements can thus confer some degree of

specificity even to redox signalling. Furthermore, another possible mechanism of specificity is in that proteins bearing redox sensitive cysteine residues like peroxidases/thioredoxins could act themselves both as sensors and transducers of the signal: thus protein-protein interaction also takes its role in redox signalling. As for the reversibility of redox signalling: first we already demonstrated that cysteine residues acting as redox switches are characterized by reversible oxidative modification (see above); second, the cell is constitutively endowed with complex enzymatic oxidants scavenging machinery (peroxidases, redoxins, reductase system). Despite historical limiting view of such antioxidant defence system as a merely instrument to counteract deleterious oxidative damage, the whole apparatus could act as a finely tuned switch-off mechanism in the context of redox signalling. Finally, limited action in time and space of redox signalling could be achieved by both switching off mechanisms *and* localized production inside the cell of signalling molecules. Indeed, as we will see later, different localized and specific sources of electrophiles could be found inside the cell.

Dynamic equilibrium: oxidation and reduction rate

One misleading aspect of redox signalling is that, differently from other well-known signalling pathways like phosphorylation, the transduction of an initiating stimulus in redox signalling does not involve targeted action of signal transducers upon signal effectors but rather the alteration of the whole redox homeostasis inside the cell. Clearly such phenomenon is sufficiently wide spread to make it difficult to think at the aforementioned specificity criteria for redox signalling.

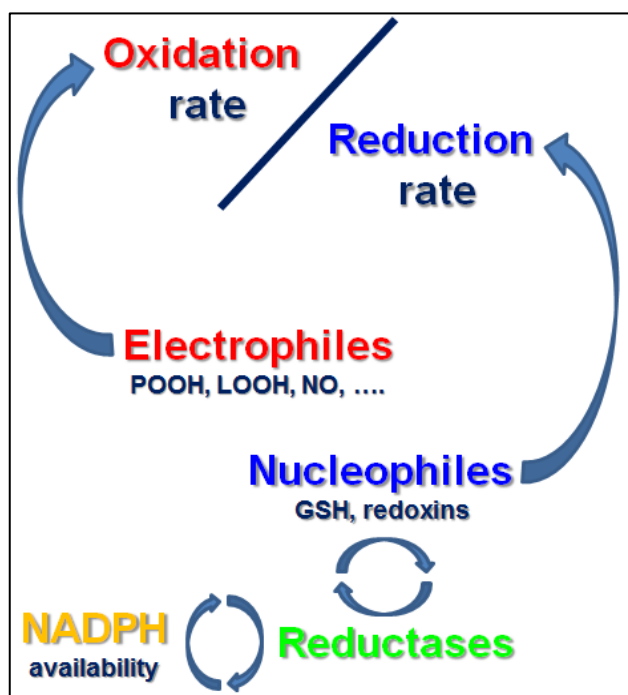


Fig. 2.d Schematic representation of the main contributors to the dynamic oxidation/reduction rate inside the cell.

Nucleophiles group includes enzymes of the cellular antioxidant defense system while reductases are able to regenerate such enzymes using NADPH reducing equivalents. POOH = protein peroxides; LOOH = lipid peroxides, NO = nitric oxide; GSH = glutathione.

Moreover also the enzymatic switch off machinery is distributed inside the cell and so it is unlikely to act by turning off oxidative stimulus just locally. Definitely rather than thinking of a point-targeted specific modification of signal effectors or transducers we should better look at a more general dynamic equilibrium between oxidation and reduction rate inside the cell. A simplified view of the main actors of such mechanism is reported in Fig. 2.d while a more general view of the cellular systems taking part in the regulation of oxidation/reduction rate is reported from [Kobayashi et al., 2012] [Fig. 2.e].

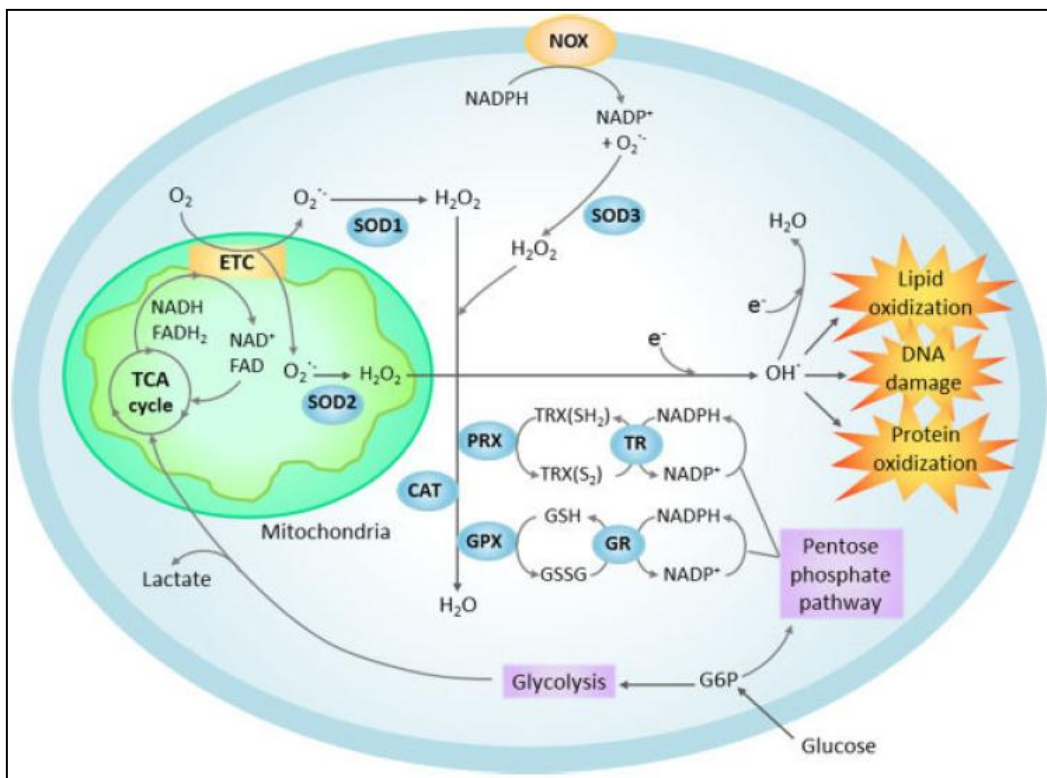


Fig. 2.e Schematic illustration of ROS generation and elimination pathways.

$O_2\cdot^-$ is generated mainly through the mitochondrial electron transport chain, and also by membrane bound NOX, and quickly converted into H_2O_2 by SOD. H_2O_2 is then neutralized by several enzymes and proteins such as CAT, PRX, and GPX in processes coupled to GSH and TRX(SH_2) oxidation. TRX(S_2) and GSSG are reduced by TR and GR, respectively, in an NADPH-dependent reaction. Highly reactive $OH\cdot$ is generated from H_2O_2 , leading to oxidation of macromolecules in the cell. [From Kobayashi et al., 2012]

The main concept behind redox equilibrium in the context of redox signalling is that we need to take into account the concomitant presence of both electrophiles and nucleophiles at the same time inside the cell: that is to say we have the simultaneous action of both oxidation and reduction at any time and the balance between these two tendencies definitely drives redox signalling. Another important aspect, which emerges from the consideration of dynamic oxidation/reduction equilibrium, is the possibility to simultaneously set up both electrophilic and nucleophilic signalling: in this view thioredoxin system

(nucleophiles) should reverse target thiols oxidized by electrophiles. The balance between oxidation and reduction rate is then determined by both thermodynamic and kinetic criteria, where kinetic mainly accounts for peroxidases activity on one side and thermodynamic constraints determine which thiols will be reversed by thioredoxins system and which will not.

This latter aspect is then finely regulated by the availability of reducing equivalents in the form of NADPH which will act on the reduction potential of the redox couple $\text{Trx}_{\text{reduced}}/\text{Trx}_{\text{oxidized}}$ and in turn on which thiols will be reduced back and which will be kept oxidized. The rate-limiting enzyme of the pentose phosphate pathway glucose-6-phosphate dehydrogenase could then be viewed as the main responsible for NADPH redox status [Fig. 2.f].

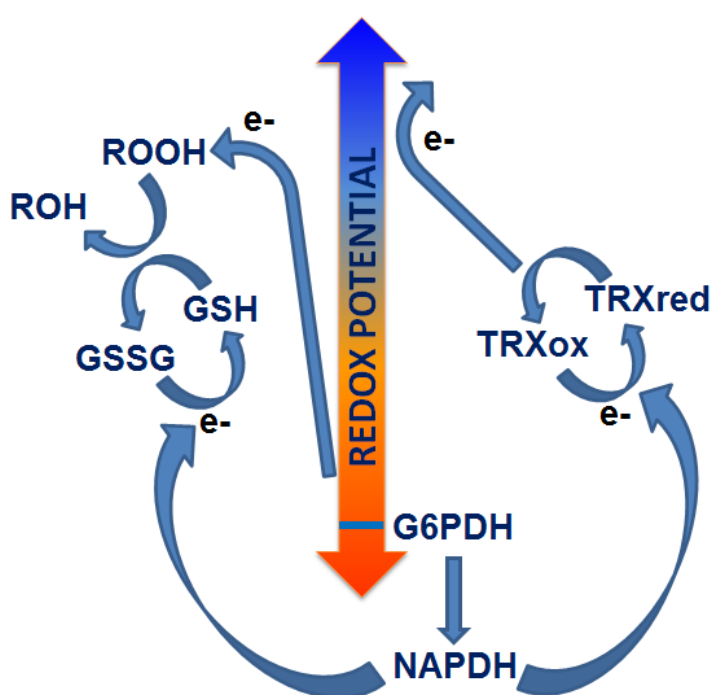


Fig. 2.f Interplay of kinetic and thermodynamic criteria in regulation of oxidation/reduction rate.

On the left side there are electrophiles (ROOH) with very high reduction potential pushing toward oxidation of protein cysteine-thiols characterized by lower reduction potential. Peroxidases and other scavenging systems in turn act kinetically by reducing electrophiles to ROH. Reduced to oxidized glutathione ratio (GSH/GSSG) on the other hand influences peroxidases activity. On the other side

there is the thioredoxin system (TRX) which can reduce back all protein cysteine-thiols having higher reduction potential than that of the redox couple $\text{TRX}_{\text{red}}/\text{TRX}_{\text{ox}}$. Both glutathione pool and thioredoxin reduction potential could be finely tuned acting on intracellular reducing equivalents in the form of NADPH. Simplified electron flows are represented by arrows and reductases systems (TRXR and GR) have been omitted.

2.2.1 Electrophiles and nucleophiles formation

In the previous section we have considered the rather complex system in which redox signalling should be viewed as the result of the interplay of “opposing tendencies” inside the cell: electrophiles on one side and nucleophiles on the other. Given a quite simplistic overview electrophiles could be defined as oxidants while nucleophiles act by favouring reduction rate inside the cell. The main reaction involved is nucleophilic substitution. In this section we will briefly consider the main sources of both these elements inside the cell.

Sources of biologically relevant ROS

According to Kobayashi [Kobayashi et al., 2012] the term *Reactive Oxygen Species* (ROS) could be defined as a collective term for oxygen species that are more reactive than free oxygen. Superoxide, hydrogen peroxide, hydroxyl radical, and singlet oxygen comprise the main ROS. But broadly speaking, ROS also encompasses nitric oxide. Another author [Gupta et al., 2012] distinguishes ROS into two main types: the free oxygen radical and the non-radical. While free oxygen radical ROS contain one or more unpaired electron in their outer molecular orbital, the non-radical ROS lack unpaired electrons but are chemically reactive and can be converted to radical ROS. The sources of ROS are both extracellular and intracellular. Extracellular ROS can be found as pollutants, tobacco smoke, drugs, xenobiotics, or radiation. Inside the cell ROS are produced through multiple mechanisms: mitochondria, peroxisomes, endoplasmic reticulum and the NADPH oxidase complexes (NOX) in cell membranes [Fig. 2.g].

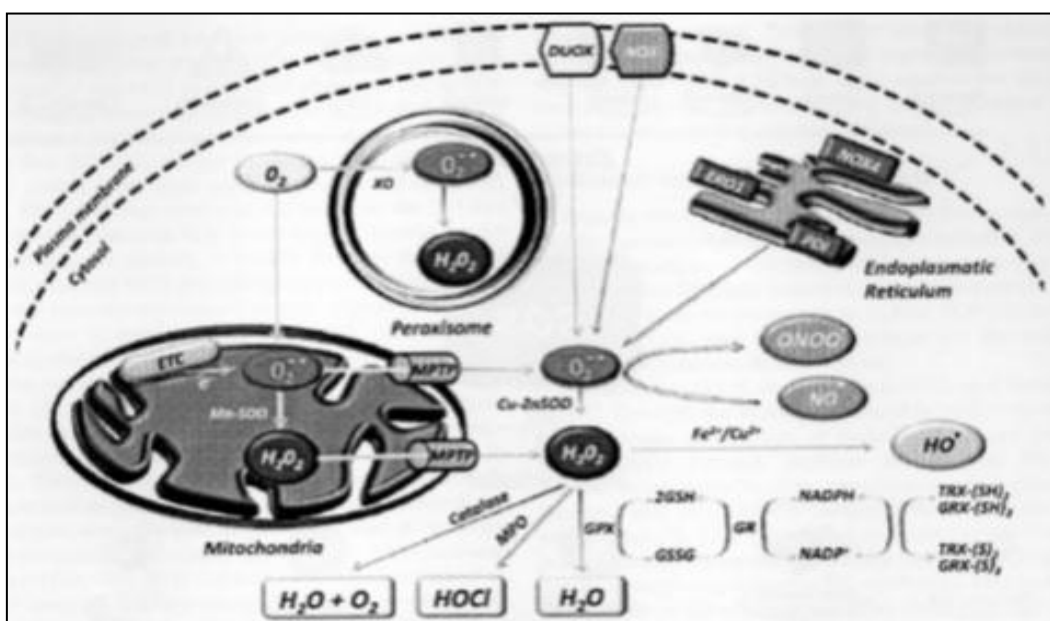


Fig. 2.g Major intracellular sources of ROS.

The main sources are mitochondria, peroxisomes, endoplasmic reticulum, and the NOX complex in cell membranes. DUOX = dual oxidase; ERO1 = endoplasmic reticulum oxidoreductin 1; ETC = electron transport chain; GPx = glutathione peroxidase; GR = glutathione reductase; GRX-(S)₂ = oxidized glutaredoxin; GRX-(SH)₂ = reduced glutaredoxin; GSH = glutathione; GSSG = glutathione oxidized; H₂O₂ = hydrogen peroxide; HO• = hydroxyl radical; HOCl = hypochlorous acid; MPO = myeloperoxidase; MPTP = mitochondrial permeability transition pore; NADP⁺ = nicotinamide adenine dinucleotide phosphate oxidized; NADPH = nicotinamide adenine dinucleotide phosphate reduced; NO• = nitric oxide; NOX = NADPH oxidase; O₂^{•-} = superoxide radical; ONOO⁻ = peroxynitrite; PDI = protein disulfide isomerase; SOD = superoxide dismutase; TRX-(S)₂ = oxidized thioredoxin; TRX-(SH)₂ = reduced thioredoxin; XO = xanthine oxidase. [From Gupta et al., 2012]

Mitochondria house the electron transport chain, which transfers to oxygen electrons from NADH and succinate during respiratory ATP synthesis. The leakage of electrons from the electron transport chain during such process results in the reduction of molecular oxygen to superoxide [Murphy, 2009]. The mitochondrial permeability transition pore in the outer membrane of mitochondria allows leakage of superoxide into the cytoplasm. Superoxide is then dismutated into hydrogen peroxide either in the mitochondrial matrix (by Mn-SOD) or in the cytosol (by Cu-ZnSOD). H_2O_2 , which is highly diffusible oxygen specie can be converted to water by catalase and peroxidases, or, in the presence of transition metals, it can be converted to highly reactive hydroxyl radicals. Moreover, superoxide can also react with the reactive nitric oxide ($NO\bullet$) to form peroxynitrite ($ONOO^-$). Another major source of ROS, in the form of superoxide or hydrogen peroxide, are NOX and its dual oxidase relatives (DUOX) [Lambeth, 2004], which are localized to various cellular membranes. NOX system consists of NOX1, NOX2, NOX4, NOX5, p22^{phox}, p47^{phox}, and the small G protein Rac1. ROS are also generated in the endoplasmic reticulum during the process of protein folding and disulphide bond formation. The glycoprotein endoplasmic reticulum oxidoreductin 1, the protein disulphide isomerase, and NOX4 are the major sources of ROS in the endoplasmic reticulum [Gupta et al., 2012].

Antioxidant defense mechanisms

Under normoxic conditions, intracellular levels of ROS are kept low to protect cells from damage. The formation of reactive oxygen and nitrogen species is balanced by the action of both enzymatic and non-enzymatic antioxidants. The most efficient enzymatic antioxidants involve superoxide dismutase, catalase and glutathione peroxidases. Instead non-enzymatic antioxidants encompass Vitamin C, Vitamin E, carotenoids, glutathione, lipoic acid, natural flavonoids, melatonin and other compounds [Valko et al., 2006 and references therein]. Moreover certain antioxidants are able to regenerate other antioxidants and thus restore their original function (antioxidant network). About the antioxidant network Bindoli et al. [Bindoli et al., 2008] talk out the concept of “cellular thiol redox state control by thioredoxin and glutathione system” which was first introduced to indicate the signalling action of the thioredoxin system on the thiol enzyme activity.

The cellular thiol redox state is controlled by two major systems, the thioredoxin and glutathione systems, which are in close communication with hydrogen peroxide through peroxiredoxins and glutathione peroxidases, respectively [Fig. 2.h]. They are present both in the cytosol and mitochondria and, in either systems, the reducing equivalents are fed by NADPH. Different pathways of $NADP^+$ reduction are operative in the cytosol and mitochondria. Whereas cytosolic $NADP^+$ is reduced in the pentose phosphate pathway, in mitochondria, electrons are delivered through the various dehydrogenases coupled to the energy-linked transhydrogenase that catalyzes the transfer of reducing equivalents from NADH

to NADP^+ . Furthermore, the mitochondrial glutamate and isocitrate dehydrogenases, in addition to NAD^+ , use NADP^+ for the oxidation of their respective substrates, providing a further source of NADPH . The thioredoxin system includes thioredoxin reductases (TrxR) and thioredoxins (Trx), which act sequentially in transferring electrons delivered by NADPH . Thioredoxins act as electron donors for a number of enzymes, such as ribonucleotide reductase, methionine sulfoxidereductase and peroxiredoxins which may be active as antioxidants by rapidly regulating the level of hydrogen peroxide [Bindoli et al., 2008 and references therein]. On the other hand, glutathione is the predominant non-protein thiol in cells where it plays essential roles as an enzyme substrate and a protecting agent against xenobiotics and oxidants.

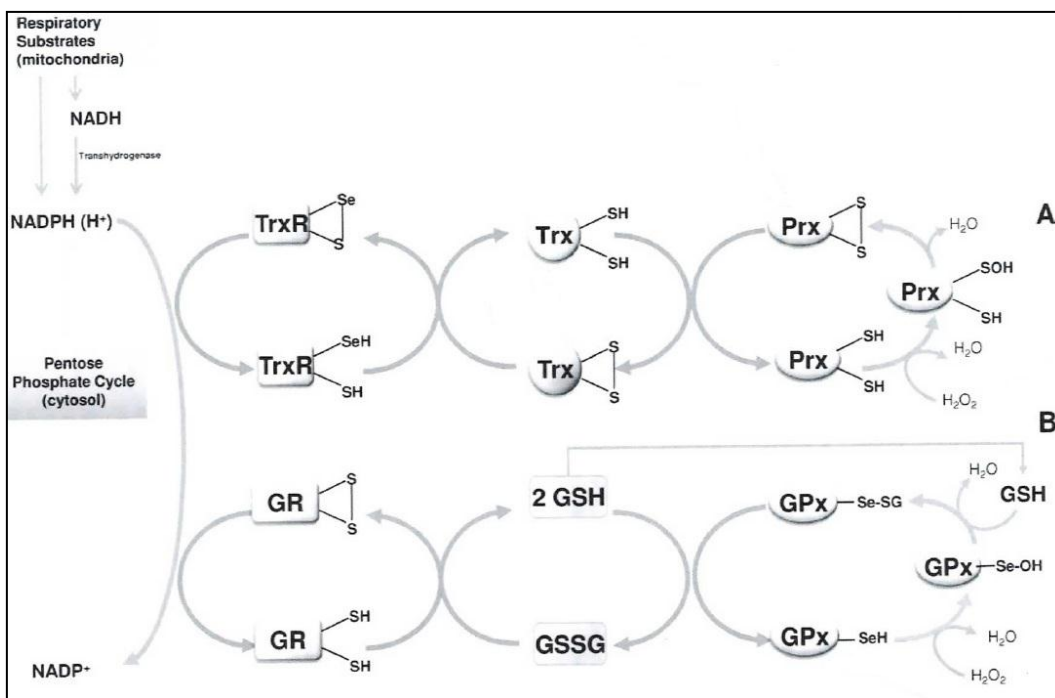


Fig. 2.h Reduction of hydrogen peroxide mediated by thioredoxin (A) and glutathione (B) pathways.

Electrons are delivered by NADPH maintained reduced by the pentose phosphate pathway in the cytosol, and by the respiratory substrates in mitochondria. The proton-translocating transhydrogenase transfers electrons from NADH to NADP^+ to form NADPH . Sulfenic and selenenic acid residues appear as key intermediates in the thioredoxin and glutathione pathways, respectively [From Bindoli et al., 2008]

Glutathione, maintained in the reduced state by glutathione reductase, is able to transfer its reducing equivalents to several enzymes, such as glutathione peroxidases (GPx), glutathione transferases (GSTs) and glutaredoxins. Although thioredoxin and glutathione systems are apparently similar in their cellular functions as they both maintain a reduced environment by using NADPH as source of reducing equivalents, a major difference is represented by the cell

concentrations of glutathione that are far larger than that of thioredoxin. Nevertheless, the two systems operate independently, fulfilling different roles within the cell [Trotter et al., 2003].

2.2.2 Nrf2-Keap1 feedback loop

Upon exposure of cells to oxidative stress or chemopreventive compounds, Nrf2 translocates to the nucleus, forms a heterodimer with its obligatory partner Maf, and binds to the antioxidant response element (ARE) sequence to activate transcription of several different genes. The Nrf2 downstream genes reported by Lau et al [Lau et al., 2008] can be grouped into several categories, including (1) intracellular redox-balancing proteins: glutamate cysteine ligase (GCL), glutathione peroxidase (GPx), thioredoxin (Trx), thioredoxin reductase (TrxR), peroxiredoxin (Prx), and heme oxygenase-1 (HMOX-1) (2) phase II detoxifying enzymes: glutathione-S-transferase (GST), NADPH quinone oxidoreductase-1 (NQO1), and UDP-glucuronosyltransferase (UGT), and (3) transporters: multidrug resistance-associated protein (MRP).

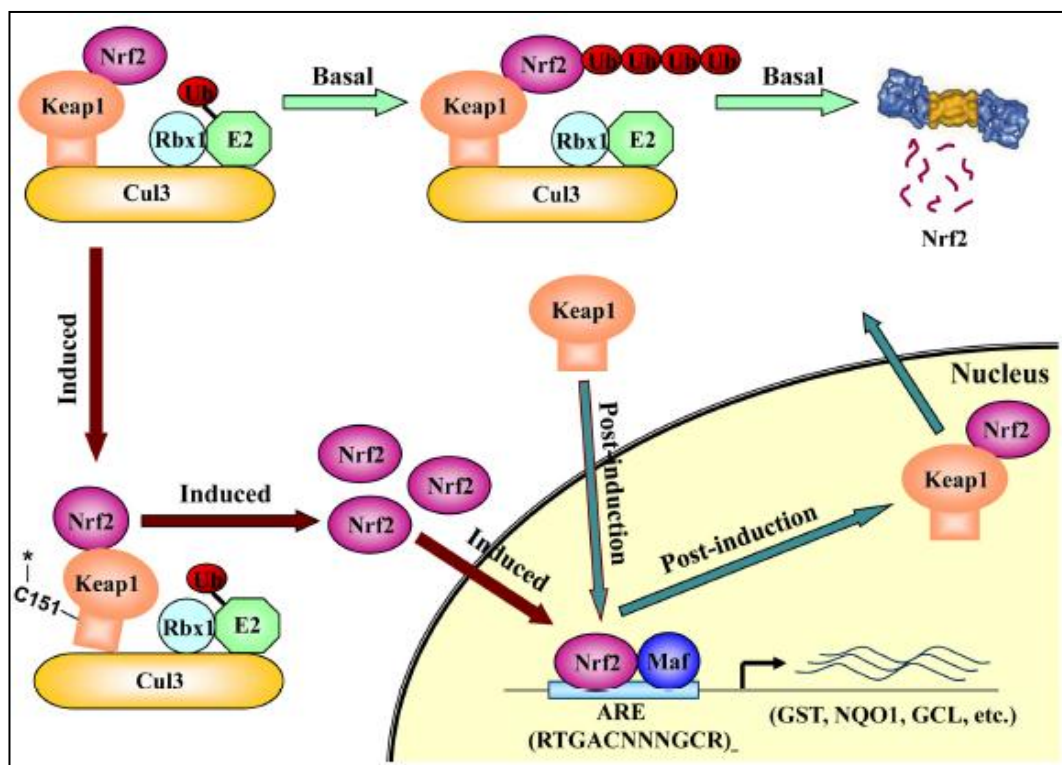


Fig. 2.i Schematic model of Nrf2 regulation by Keap1.

Keap1 is a key regulator of the Nrf2 signaling pathway and serves as a molecular switch to turn on and off the Nrf2-mediated antioxidant response. (I) The switch is in off position: under basal conditions, Keap1, functioning as an E3 ubiquitin ligase, constantly targets Nrf2 for ubiquitination and degradation. As a consequence, there are minimal levels of Nrf2. (II) The switch is turned on: oxidative stress or chemopreventive compounds inhibit activity of the Keap1-Cul3-Rbx1 E3 ubiquitin ligase, resulting in increased levels of Nrf2 and activation of its downstream target genes.

(III) The switch is turned off again: Upon recovery of cellular redox homeostasis, Keap1 travels into the nucleus to remove Nrf2 from the ARE. The Nrf2-Keap1 complex is then transported out of the nucleus by the nuclear export sequence (NES) in Keap1. In the cytosol, the Nrf2-Keap1 complex associates with the Cul3-Rbx1 core ubiquitin machinery, leading to degradation of Nrf2. For clarity, the constitutive cytoplasmic-nuclear shuttling of Nrf2, Keap1, and the complex is omitted. [From Lau et al., 2008]

The primary function of intracellular redox-balancing proteins is to maintain cellular glutathione and Trx levels and reduce levels of reactive oxygen species. Phase II enzymes function in two aspects: (I) metabolize xenobiotics into less toxic forms, or (II) catalyse conjugation reactions to increase the solubility of xenobiotics, thereby, facilitating their elimination. Lastly, the main function of transporters is to control uptake and efflux of endogenous substances and xenobiotics. The majority of genes downstream of Nrf2 contain an ARE sequence in their promoter. The activity of Nrf2 is negatively regulated by Kelch-like ECH-associated protein 1 (Keap1). It has been proposed that Keap1 acts as a molecular switch that is able to turn the Nrf2 signalling pathway on or off according to intracellular redox conditions. Serving as a molecular switch, Keap1 possesses dual functions: it is able to (I) “sense” changes in the redox homeostasis and (II) turn the Nrf2-mediated response on or off. Keap1 is rich in cysteine residues (27 cysteine residues in human Keap1), which encodes the sensor mechanism. Under basal conditions, when redox homeostasis is maintained in cells, the molecular switch of Keap1 is in an “off” position. This is achieved through constant Keap1-mediated degradation of Nrf2 by the ubiquitin-mediated proteasomal degradation system. Lau et al. propose a model of Keap1 functions in switching on/off the Nrf2 signaling pathway (Fig. 2.i). Under basal conditions, Keap1 switches the Nrf2 signalling pathway off and maintains low basal levels of Nrf2 by constantly targeting Nrf2 for ubiquitin-mediated protein degradation. When Keap1 senses an alteration in the redox balance, the cysteine residues in Keap1 are modified, resulting in a conformational change of the E3 ubiquitin ligase to a configuration not conducive for Nrf2 ubiquitination. Consequently, Nrf2 accumulates under oxidative conditions, which allows free Nrf2 to translocate to the nucleus and transcriptionally activate downstream genes by binding to the ARE sequences and switching the Nrf2 signalling pathway on. Upon recovery of the redox balance, Keap1 travels into the nucleus, where it causes dissociation of Nrf2 from the ARE sequence. Subsequently, Keap1 escorts Nrf2 out of the nucleus to the cytoplasmic Cul3-dependent E3 ubiquitin ligase machinery for degradation. Thus, a low level of Nrf2 is re-established, turning the Nrf2 signalling pathway off [Lau et al., 2008].

Nrf2 in cancer prevention and promotion: dual roles of Nrf2

In their work Lau et al. summarizes half a century of reports on the concept of chemoprevention through the use of dietary compounds or synthetic chemicals able to decrease or related to decrease of the incidence of cancer. Moreover, as

many of the compounds possessing chemopreventive activities are phytochemicals, many well studied chemopreventive compounds have been identified as Nrf2 inducers. Examples of potent Nrf2 inducers from plants include sulforaphane (cruciferous vegetables), curcumin (a widely used spice), epigallocatechin-3-gallate (EGCG) (green tea), resveratrol (grapes), caffeic acid phenethyl ester (conifer trees), wasabi (Japanese horseradish), cafestol and kahweol (coffee), cinnamonyl-based compounds (cinnamon), zerumbone (ginger), garlic organosulfur compounds (garlic), lycopene (tomato), carnosol (rosemary), and avicins (Bentham plant) [Lau et al., 2008 and references therein]. Definitely it has been reported that these compounds exert their chemopreventive activity by inducing the Nrf2-dependent adaptive response, including phase II detoxifying enzymes, antioxidants, and transporters that protect cells from carcinogenic insults.

Nevertheless, during the last years literature on Nrf2 has revealed new data supporting a “dark” side of Nrf2 since it seems that this transcription factor protects not only normal cells from malignant transformation, but could also promote the survival of cancer cells. The first evidence indicating the involvement of Nrf2 in cancer promotion came from the finding that Nrf2 and GSTP1 were up-regulated during development of hepatocellular carcinoma [Ikeda et al., 2004]. Many Keap1 mutations or loss of heterozygosity in the Keap1 locus have also been identified in lung cancer cell lines or cancer tissues. In both cases the result was inactivation of Keap1 or its reduced expression which consequently upregulated Nrf2 protein level and transactivation of its downstream genes, thus supporting a positive role of Nrf2 in tumorigenesis [Singh et al., 2006]. Another study from Kim et al. indicates that Nrf2 may be responsible for chemoresistance too. Indeed elevated expression of Nrf2 and its downstream genes, such as HMOX-1, Trx, Prx and GCL, have been associated to acquired resistance to tamoxifen in the breast cancer MCF-7 derived tamoxifen resistance cell line [Kim et al., 2008]. Moreover knockdown of Nrf2 with Nrf2-siRNA reversed tamoxifen resistance of this cell line. Investigating the molecular mechanism of acquired resistance to tamoxifen, many Nrf2 downstream genes have been shown to contribute to the observed Nrf2-dependent chemoresistance: those genes have the ability to function as antioxidants and detoxifying enzymes. Finally *in vitro* studies show that overexpression of Nrf2 can lead to the increased expression of several intracellular redox-balancing proteins, phase II detoxifying enzymes, and transporters, which can provide cancer cells with a growth advantage and cause resistance to chemotherapy.

2.3 Events related to malignancy are redox regulated

Because oxidants electrophiles influence the redox status, they can cause either cell proliferation or growth arrest and cell death [Valko et al., 2006]. According to numerous authors there are two main interpretations of the physiological role of

ROS in several aspects of intracellular signalling: while high concentrations of ROS cause cell death, the effects of ROS on cell proliferation occurred exclusively at low or transient concentrations of electrophiles. In fact low concentrations of superoxide radical and hydrogen peroxide stimulate proliferation and enhanced survival in a wide variety of cell types. On the other hand, excessive ROS production resulting in an overload of the thiol redox system causes the progressive inactivation of the anti-oxidant thiols containing proteins such that redox homeostasis becomes compromised. This represents an extreme situation, but according to Ralph et al. [Ralph et al., 2010] for H₂O₂ to serve as a signal by oxidative modifications to signalling proteins, by necessity it follows that ROS levels must be raised above a certain threshold steady-state level whereby the anti-oxidant cellular enzymes that otherwise counteract this build up become inhibited. Such a view is known as the “floodgate hypothesis”. Nevertheless redox signalling scenario is more complex as demonstrated by accumulating evidence over the past years from both *in vitro* and *in vivo* studies which indicated a role for ROS as a signalling mediator of angiogenesis and metastasis [Ushio-Fukai 2008/2010]. ROS has been shown to mediate these effects through induction of transcription factors and genes involved in angiogenesis and metastasis, two interrelated processes that represent the final, most devastating stage of malignancy. However, the role of ROS in modulating tumour cell metastasis and angiogenesis has seemed paradoxical: high ROS levels suppress tumour angiogenesis and metastasis by destroying cancer cells, whereas sub-optimal concentrations assist cancer cells in metastasizing. Also a variety of cytokines and growth factors that bind to receptors of different classes, such as receptor tyrosine kinases (RTKs), have been reported to generate ROS in nonphagocytic cells. The information is then transmitted via the activation of mitogen-activated protein kinases (MAPKs) signalling pathways. ROS production as a result of activated growth factor receptor signalling includes epidermal growth factor (EGF) receptor, platelet-derived growth factor (PDGF) receptor, vascular endothelial growth factor (VEGF) receptor, cytokine receptors (TNF- α and IFN- γ), and interleukin receptors (IL-1 β) [Valko et al., 2006 and references therein]. It is generally accepted that ROS generated by these ligand/receptor-initiated pathways can mediate important cellular functions such as proliferation and programmed cell death. Moreover, abnormalities in growth factor receptor functioning are closely associated with the development of many cancers.

It turns out that events related to malignancy are redox regulated in many ways: from malignant transformation onset, to cancer cells survival/proliferation and metastasis and even to cell death by apoptosis necrosis, or autophagy. Indeed localization, timing, chemical identity, and intensity of electrophilic pulse will determine different effects. Mechanisms underlying such regulation are still almost unknown and we would like to summarize here the reached consensus: while malignancy onset is probably favoured by severe oxidative unbalance leading to spread damage to various cellular structures (DNA, lipids, proteins),

tumour cells survival, metastasising processes and acquisition of chemoresistance are instead the result of a more finely tuned dynamic equilibrium between coexisting pro-oxidant (electrophiles) and anti-oxidant (nucleophiles) stimuli. This is why ROS seem to play a “dual role” for cancer, since they can prompt survival as well as death signalling pathways in cancer cells.

2.3.1 Oxidation

DNA and lipids

Pro-oxidant stimuli (electrophiles, see § 2.2.1) can affect various target biomolecules such as DNA, lipids or proteins. It has been estimated that one human cell is exposed to approximately $1.5 \cdot 10^5$ oxidative hits a day from hydroxyl radicals and other such reactive species. Permanent modification of genetic material resulting from this “oxidative damage” represents the first step involved in mutagenesis, carcinogenesis and ageing. Carcinogenesis is associated with arrest or induction of transcription, induction of signal transduction pathways, replication errors and genomic instability, all of which can be caused by DNA damage. The hydroxyl radical is able to add to double bonds of DNA bases at a second-order rate constant in the range of $3 \cdot 10^{10} \text{ M}^{-1} \text{ s}^{-1}$ and it abstracts an H-atom from the methyl group of thymine and each of the five carbon atoms of 2' deoxyribose at a rate constant of approximately $2 \cdot 10^9 \text{ M}^{-1} \text{ s}^{-1}$ [Valko et al., 2006 and references therein]. An example of oxidative damage of DNA is the formation of 8-hydroxyguanine (8-OH-G) the presence of which has first been reported in urine by Shigenaga et al. [Shigenaga et al., 1989]. Tobacco smoking, a carcinogenic source of ROS, increases the oxidative DNA damage rate by 35-50%, as estimated from the urinary excretion of 8-OH-G, and the level of 8-OH-G in leukocytes by 25-50% [Valko et al., 2006]. In addition to the extensive studies devoted to the role of oxidative nuclear DNA damage in neoplasia, evidence exists about the involvement of the mitochondrial oxidative DNA damage in the carcinogenesis. The mitochondrial genome in human cells is small (16596 base pairs (bp)) compared to the nuclear DNA although every mitochondrion contains between 2 and 20 copies of mitochondrial DNA (mtDNA) and the copy number of mitochondrial genomes per cell ranges from several hundreds to more than 10000 depending on the cell type (typically around 1000 mitochondria per cell). Moreover different mtDNA content has been reported in cancer cells and the relationship of mtDNA copy number to oxidative stress and changes in ROS production taking place during the onset of malignancy has been outlined by Ralph and co-workers [Ralph et al., 2010]. Indeed it was proposed that mtDNA copy number was increased by a feedback mechanism that compensated for any defects in those mitochondria with mutated mtDNA and defective respiratory systems. Moreover the age-associated increased production of O_2^- and H_2O_2 in cells was one of the factors involved in this regulation process. In conclusion, as

observed with oxidative genomic DNA modification, oxidative damage and the induction of mutation in mtDNA may participate at multiple stages of the process of carcinogenesis, involving mitochondria-derived ROS and induction of mutations in mitochondrial genes.

It is known that metal-induced generation of oxygen radicals results in the attack of not only DNA in the cell nucleus, but also other cellular components involving polyunsaturated fatty acid residues of phospholipids which are extremely sensitive to oxidation [Valko et al., 2006 and references therein]. Several experimental models of iron overload *in vivo*, confirmed increased polyunsaturated fatty acids (PUFA) oxidation of hepatic mitochondria, as well as lysosomal fragility. The deleterious process of the peroxidation of lipids is also very important in arteriosclerosis, cancer and inflammation. The overall process of lipid peroxidation consists of three stages; initiation, propagation and termination. Its full discussion is outside the topics of this thesis and here it is sufficient to say that among final products of the peroxidation process there are aldehydes among which the most relevant is 4-hydroxy-2-nonenal (HNE). Malondialdehyde (MDA) is mutagenic in bacterial and mammalian cells and carcinogenic in rats. Hydroxynonenal is weakly mutagenic but appears to be the major toxic product of lipid peroxidation. In addition, HNE has powerful effects on signal transduction pathways, which in turn have a major effect on the phenotypic characteristics of cells.

Proteins

Mechanisms involved in the oxidation of proteins by ROS were elucidated by studies in which amino acids, simple peptides and proteins were exposed to ionising radiations under conditions where hydroxyl radicals or a mixture of hydroxyl/superoxide radicals are formed. The results of these studies demonstrated that reaction with hydroxyl radicals lead to abstraction of a hydrogen atom from the protein polypeptide backbone to form a carbon-centred radical, which under aerobic conditions reacts readily with dioxygen to form peroxy radicals. The peroxy radicals are then converted to the alkyl peroxides by reactions with the protonated form of superoxide HO_2^\bullet . In the absence of radiation, proteins are resistant to damage by H_2O_2 and by other simple oxidants unless transition metals are present. Indeed it is believed that the iron(II) binds both to high and low-affinity metal-binding sites on the protein. The Fe(II)-protein complex reacts with H_2O_2 via the Fenton reaction to yield an active oxygen species at the site. While it has been proposed by many authors that the hydroxyl radical represents the major species responsible for the oxidation of proteins, clear experimental evidence is still missing.

Besides radicals initiated reactions and transition metals “assisted” oxidative damage of proteins we have seen above that there are many proteins bearing so-called redox switches: such redox sensitive cysteine-residue thiols should be

considered the preferred target for reversible oxidative modifications underlying redox signalling. The ability to “sense” even humble variations in electrophilic tone and to readily react with mild-oxidizing non-specific molecules like H₂O₂ made such proteins ideal players as signal sensors, transducers and effectors as well. Indeed low concentrations of hydrogen peroxide can regulate cytosolic calcium concentration, protein phosphorylation and transcription factors activation leading to different cell fates (survival, proliferation, death).

Non receptor tyrosine kinases (PTKs): Src

Several non-receptor protein kinases belonging to the Src family (src kinases) and Janus kinase (JAK) are also activated by ROS [Esposito et al., 2003]. For example H₂O₂ and O₂[•] induce tyrosine phosphorylation of several PTKs in different cell types, including fibroblasts, T and B lymphocytes, macrophages and myeloid cells. Activated Src binds to cell membranes by myristilation and initiates MAPK, NF-κB and phosphoinositide 3-kinase (PI3K) signalling pathways [Valko et al., 2006]. Moreover it has been demonstrated [Zhang et al., 2012] that Src could be activated by cigarette smokes extracts in human non-small cell lung carcinoma cell line (H358) by redox modification. Activated Src (increased Tyr418 phosphorylation) initiates in turn the epithelial-mesenchymal transition, a well characterized process implicated in the pathogenesis of lung fibrosis and cancer metastasis.

Rat Sarcoma genes product (Ras) and the Raf/MEK/ERK pathway

Ras gene products are membrane-bound G proteins whose main function is to regulate cell growth and oppose apoptotic effects. Ras is activated by ROS as well as by UV radiation (which is also known to start ROS production through radical formation), by metals and mitogenic stimuli [Valko et al., 2006]. Inactive Ras could be induced to exchange GDP for GTP undergoing a conformational change and becoming active. The GTP bound active Ras can then recruit Raf to cell membrane. Activated Raf could in turn regulate Mitogen-activated protein kinase/ERK kinase (MEK1) activation via phosphorylation of its S residue on catalytic domain. The main target of MEK is then extracellular-signal-regulated kinases (ERK) the activity of which is positively regulated by MEK mediated phosphorylation. Activated ERK could directly phosphorylate many transcription factors including c-Jun and c-Myc. Moreover, through an indirect mechanism, ERK can lead to activation of the nuclear factor immunoglobulin κ chain enhancer-B cell (Nf-κB) transcription factor. From a wider point of view the Ras/Raf/MEK/ERK pathway is responsible for coupling signals from cell surface to transcription factors and can definitely lead to an anti-apoptotic response via phosphorylation of the anti-apoptotic protein Mcl-1 and the pro-apoptotic protein Bim which becomes ubiquitinated and targeted to proteasome. However

phosphorylation of Bim by another MAPK, c-jun-NH₂-terminal kinase (JNK) can instead result in apoptosis due to stimulation of the pro-apoptotic protein Bax:Bax interaction. Thus ROS can influence Ras/Raf/MEK/ERK pathway in many ways, one we have seen is the activation of Ras, but ROS could as well activate receptors like EGFR and PDGF receptor by a ligand independent mechanism [McCubrey et al., 2009]. On the same way ROS seems to activate the JNK pathway through the apoptosis signal related kinase 1 (ASK1): reduced thioredoxin binds to the N-terminal of ASK1 inhibiting its activity, upon oxidative stress thioredoxin becomes oxidized and disassociates from ASK1 which in turn oligomerize, auto-phosphorylate, and become activated [Saitoh et al., 1998].

PI3K/AKT pathway and protein tyrosine phosphatases: PTP1B and PTEN

The family of phosphoinositide 3'-kinases (PI3K) consists of several structurally related enzymes catalyzing the phosphorylation of inositol phospholipids in the 3'-position, thus generating phosphatidylinositol-3'-phosphate (PIP), phosphatidylinositol-3',4'-bisphosphate (PIP₂) and phosphatidylinositol-3',4',5'-trisphosphate (PIP₃) [Foster et al., 2003]. The classical (class Ia) PI3K is made of heterodimers consisting of a catalytical (p110) and a regulatory (p85 or p55) subunit, that are typically activated via receptor tyrosine kinases (RTK) after stimulation of cells with growth factors. Generation of 3'-phosphoinositides results in recruitment of the 3'-phosphoinositide-dependent kinases (PDK1 and the putative PDK2) to the cell membrane and consecutive activation of the serine-/threonine kinase Akt (protein kinase B, PKB) by phosphorylation at Thr308 and Ser473. Akt can be regarded as a master switch of the cell integrating incoming signals on cell growth, apoptosis and metabolism. For example, activation of Akt results in a direct phosphorylation and consecutive inhibition of the pro-apoptotic factor Bad [Franke et al., 1997]. The anti-apoptotic effects of Akt may also be mediated via activation of the transcription factor NF-κB by an interaction of Akt with IκB kinase (IKK). Activation of this kinase by Akt stimulates degradation of IκBα, a potent repressor of NF-κB [Romashkova et al., 1999]. Moreover PI3K-dependent inactivation of FoxO1, a member of the FoxO-family of Akt directly targeted transcription factors, results in cell cycle progression. An important antagonist of PI3K is phosphatase and tensin homolog deleted on chromosome 10 (PTEN), a lipid phosphatase that cleaves off the 3'-phosphate from PIP, PIP₂ and PIP₃, thereby inactivating the lipid products of PI3K [Barthel et al., 2007]. The PI3K/Akt cascade is modulated also by the PTP-ases like phosphatase PTP1B, which is able to reverse receptor tyrosine kinases tyr-phosphorylation thereby avoiding PI3K activation. From a wider point of view, PI3K/Akt pathway definitely leads to cell proliferation and prevention of apoptosis and is regulated positively by Ras (see above) and negatively by PTEN and PTP1B [Chang et al., 2003; Gao et al., 2009].

Protein tyrosine phosphatases are probably the best-characterised direct target of ROS. It has been shown that inhibition of PTPs by ROS may directly trigger PTKs and we have seen that PTPs and PTKs act in conjunction to control cell cycle and signal transduction by regulating levels of protein tyrosine phosphorylation in response to cellular signals. The effects of ROS occur through targeting the cysteine residues of the active sites of tyrosine phosphatases as demonstrated by Barrett [Barrett et al., 1999]. Protein tyrosine phosphatase 1B (PTP1B) Cys215 has indeed been demonstrated to form both sulfenic acid derivative and mixed disulfide with glutathione. Active site Cys215 residue glutathionylation (by treatment with diamide and reduced glutathione or with only glutathione disulfide) inactivates PTP1B while dithiothreitol or glutaredoxin (a glutathione-specific dethiolase enzyme thioltransferase) are able to recover phosphatase activity. It is then clear how ROS could interconnect at various level both Raf/MEK/ERK pathway and PI3K/AKT pathway leading to different cell fate like proliferation or cell death.

2.3.2 Reduction

As seen above (see § 2.3) the role of oxidation/reduction rate on intracellular signalling is performed by both unspecific signals (e.g. – electrophiles) and specific signal transducers/effectors bearing redox switches (e.g. – phosphatases, kinases, transcription factors). Thus the concomitant action of cellular scavenging systems (e.g. – nucleophile tone: peroxidases, glutathione, reductase) and electrophile tone (e.g. – mitochondrial electron transport chain (ETC) and NOX superoxide production) defines an equilibrium in which both pro-oxidant and anti-oxidant signals coexist. Indeed in addition to their role in promoting cellular proliferation or inhibiting apoptosis (see above Raf/MEK/ERK and PI3K/AKT pathways) ROS have many functions also in tumour cell death and negative transcription factors regulation [Gupta et al., 2012]. One of the chief characteristics of cancer cells is their inherent capacity to survive and it has been demonstrated that ROS have effects on apoptosis [Ozben, 2007]. Apoptosis is a tightly controlled form of cell death and can be initiated by death receptors (extrinsic pathway) or through mitochondria (intrinsic pathways). ROS control both extrinsic and intrinsic pathway. In the extrinsic pathway ROS are generated by Fas ligand as an upstream event for Fas activation. In turn, ROS are required for Fas phosphorylation, which is a signal for subsequent recruitment of Fas-associated protein with death domain and caspase 8 and for apoptosis induction [Denning et al., 1992]. In contrast the intrinsic pathway of apoptosis is characterized by the opening of the permeability transition pore complex on the mitochondrial membrane, which results in cytochrome *c* release, apoptosome formation, and caspase activation. ROS function to open the pore by both activating pore-destabilizing proteins (Bcl-2 associated X protein, Bcl-2 homologous antagonist/killer) and inhibiting pore-stabilizing proteins (Bcl-2 and

Bcl-xL) [Martindale et al., 2002]. In his review on the “dual role of ROS for cancer” Gupta also quote many sources of examples of apoptosis induction by exogenous administration of H₂O₂ in lymphoma cells, bladder cancer cells, hepatoma cells, leukemia cells, osteosarcoma, breast and lung cancer cells [Gupta et al., 2012 and references therein]. Numerous agents have been shown to induce ROS and apoptosis in various cancer types. The most common signalling molecules modulated by ROS in these cell models are kinases, pro-inflammatory transcription factors such as NF-κB, caspases, cell survival proteins, pro-apoptotic proteins, and phosphatases like the already mentioned PTEN. Many authors still share the floodgate-like hypothesis (see above) by virtue of which the survival/proliferation/death fate of the cell is dependent mainly on the intensity and duration of pro-oxidant stimulus: here we would like to sustain the possibility of a dynamic equilibrium in the context of which specific targets could be kept oxidized while maintaining an overall nucleophile tone thus conferring to the cell both advantages of pro-survival signals and death-escape signals. As an example, the transcription factor activator protein-1 (AP-1) is induced by treatment of cells with H₂O₂, but its activity is directly regulated by redox in the opposite manner. Indeed, the activity of AP-1 has been revealed to be regulated through the conserved cysteine residues that are located in the DNA-binding domain of each of its two dimer subunits (oncongene products Jun/Fos or Jun/Jun): modification of these residues by a sulphydryl modifying agent, such as N-ethylmaleimide (NEM) or diamide, reduce its activity, whereas treatment with reductants, such as dithiothreitol (DTT), enhance DNA binding. Similarly the DNA-binding activity of NF-κB, which induces immune response, stress response, cell growth and cell survival gene expression, is inactivated by treatment with NEM and diamide while DTT and β-mercaptoethanol enhance its DNA binding. Finally it has been discovered that also the tumour suppressor gene p53 receives more complicated redox regulation through many cysteine residues: indeed also in this case treatment with diamide or NEM disrupts wild-type p53 conformation and inhibits its DNA-binding activity [Kamata et al., 1999 and references therein].

ROS mediated activation of Src has also been associated to activation of EGFR via ligand-independent phosphorylation. Redox-dependent activation of EGFR in turn activates both extracellular signal-regulated protein kinase and Akt downstream signalling pathways, culminating in degradation of the pro-apoptotic protein Bim. These results highlighted a fundamental role of ROS in ensuring protection from the apoptotic process induced by the loss of integrin-mediated cell-extra cellular matrix (ECM) contact. Proper attachment to the ECM is essential for cell survival and such ECM-contact induced apoptotic process has been called *anoikis* [Giannoni et al., 2008].

2.3.3 Localization

GSH/GSSG redox potential in cellular compartments

We have already seen (§ 2.2.1) two main intracellular sources of pro-oxidant species: mitochondrial ETC and membrane NOX. On the other hand the compartmentalization of peroxide-metabolizing systems within peroxisomes has long been recognized to provide a means to utilize hydrogen peroxide as a metabolic reagent while at the same time protect redox-sensitive cell components in other cell compartments from oxidative damage. Moreover unique redox characteristics have evolved with each of the major compartments in mammalian cells. Mitochondria are the most redox-active compartment of mammalian cells, accounting for more than 90% of electron transfer to O_2 as the terminal electron acceptor and ROS such as $O_2^{\cdot-}$ and its dismutation product H_2O_2 are derived from several sources in mitochondria. Indeed complexes I and III within the ETC are the main sites of electron transfer to O_2 to produce $O_2^{\cdot-}$. In addition to the electron transport chain, mitochondrial ROS may also be generated by pyruvate, α -ketoglutarate dehydrogenase, glycerol-3-phosphate dehydrogenase, and monoamine oxidase. The redox potential of mitochondrial GSH/GSSG, is about -280 mV. This value is more reduced than cytoplasmic values (-200 mV) indicating that the mitochondrial GSH/GSSG redox status is more reduced than total cellular GSH/GSSH [Go et al., 2008 and references therein]. The GSH/GSSG redox potential in mitochondria is in turn dependent upon concentrations of GSH and GSSG. Thus because mitochondrial GSH is not synthesized in mitochondria, it must rely on synthesis in the cytoplasm and subsequent transport into mitochondria. Finally, in apoptosis, oxidation of mitochondrial GSH/GSSG stimulates cytochrome *c* release, and GSH depletion resulted in increased ROS which was generated from complex III, suggesting a role for GSH in controlling mitochondrial ROS generation. We have seen so far that ROS serve as messengers in cell signalling but also cause oxidative damage to macromolecules, including DNA damage. Sequestration of DNA within nuclei protects the genome from reactive chemicals generated in other parts of the cells; however H_2O_2 and organic hydroperoxides, can diffuse across membranes, thus posing a potential damage from normal signalling events. Nevertheless, similar to other organelles, nuclei also contain two major antioxidant systems dependent upon GSH and Trx1. Data reported by Go et al. [Go et al., 2008] show that the GSH/GSSG redox potential is likely to be more reduced in nuclei than in cytoplasm and that protein S-glutathionylation is independently controlled in the cytoplasmic and nuclear compartment. As for the redox status of cytoplasm it has been measured using cytosolic Trx1 and GSH/GSSG. The total cellular GSH/GSSG couple largely represents the cytoplasmic GSH/GSSG pool, even if some misleading contribution from more negative organelles has been already reported. Nevertheless the standard redox potential E_{red}^{θ} for the active site

dithiol/disulfide couple of Trx1 was estimated to be -230 mV [Watson et al., 2003]. Using this value and measuring the percentage reduction with a redox western blot [Watson et al., 2003], cellular Trx1 has a E_{red} of -280 mV. Moreover, in a study on the increase of ROS which accompanies EGF binding to its receptor, it has been shown [Halvey et al., 2005] that nuclear Trx1, mitochondrial Trx2, and cellular GSH did not show any significant oxidation following EGF stimulation while cytoplasmic Trx1 was oxidized. These findings demonstrated that physiologic stimulation at the plasma membrane can cause the oxidation of specific redox couples in the cytoplasm without affecting other subcellular compartments. Thus as far we could generalize mitochondria as a compartment utilizing oxidations for energy conversion, and the endoplasmic reticulum (ER) in different cell types is specialized with different oxidative functions. In addition to these more specialized oxidative functions, the ER has a more general oxidative function to introduce structural disulfides in protein folding for membranal and exported proteins: central redox proteins for these functions include the endoplasmic reticulum oxidase-1 (Ero-1) and protein disulfideisomerase (PDI). The GSH/GSSG ratio in the ER varies between 3/1 and 1/1 and is considerably more oxidized than cytoplasmic GSH/GSSG ratio (30/1 to 100/1). Based upon these values the ER redox potential has been estimated to be -189 mV, which is relatively oxidizing compared to other cellular compartments. Indeed a significant amount of GSH in the ER was detected as protein mixed disulfides, and regulates the activity of redox-active thiol containing proteins [Cuozzo et al., 1999].

Redox regulation of cell migration and adhesion

In a recent work Hurd and co-workers pointed out another interesting aspect of redox driven cell-signalling: the regulation of migrating cell movement and non-migrating cell matrix and cell-cell interactions. Movement and migration are crucial during organism developmental phases but they also play important roles in pathological processes such as cancer metastatization. Indeed, developmental migratory programs can be inappropriately reactivated in metastatic cancer. In both cases gradients of attractive and repulsive cues are used to direct cell migration. Those extracellular signals are first received by receptors on the surface of migrating cells, and intracellular transduction of such signal direct migration by changing cellular cytoskeletal and adhesive properties for example. It has been reported that H_2O_2 could be used to relay signals from activated cell surface receptors to direct changes necessary for cell movement thus “intrinsically” promoting movement [Hurd et al., 2012]. Upon binding of growth factors and chemoattractants to cell surface receptors, NOXs produce superoxide or hydrogen peroxide in the extracellular or luminal space, and for ROS to transduce signals they must first be internalized into the cytoplasm of the cell. Once inside the cell, NOX generated hydrogen peroxide can act as a redox signal by reversibly modifying the activity of specific proteins, as we have seen above

often by oxidizing responsive thiols on cysteine residues. Moreover if proteins such as Prx are used to relay redox signals from NOX to target proteins, specificity can be obtained through protein-protein interactions between the relaying protein and its target. But given the abundance of enzymes such as Prx, which is able to terminate the signal as well, H₂O₂ accumulation turns out to be a critical issue. Evidences suggest that localized inactivation of antioxidant enzymes, such as Prx1, allows for transient accumulation of hydrogen peroxide around membranes, where signalling components are concentrated [Woo et al., 2010]. Indeed, treatment of different cell types with ROS degrading enzymes is able to suppress their migration towards growth factors and chemoattractants. Definitely, due to their diffusibility, their short-lived nature, and the abundance of ROS-degrading enzymes, localized production of ROS by NOXs is probably necessary for efficient signal transduction.

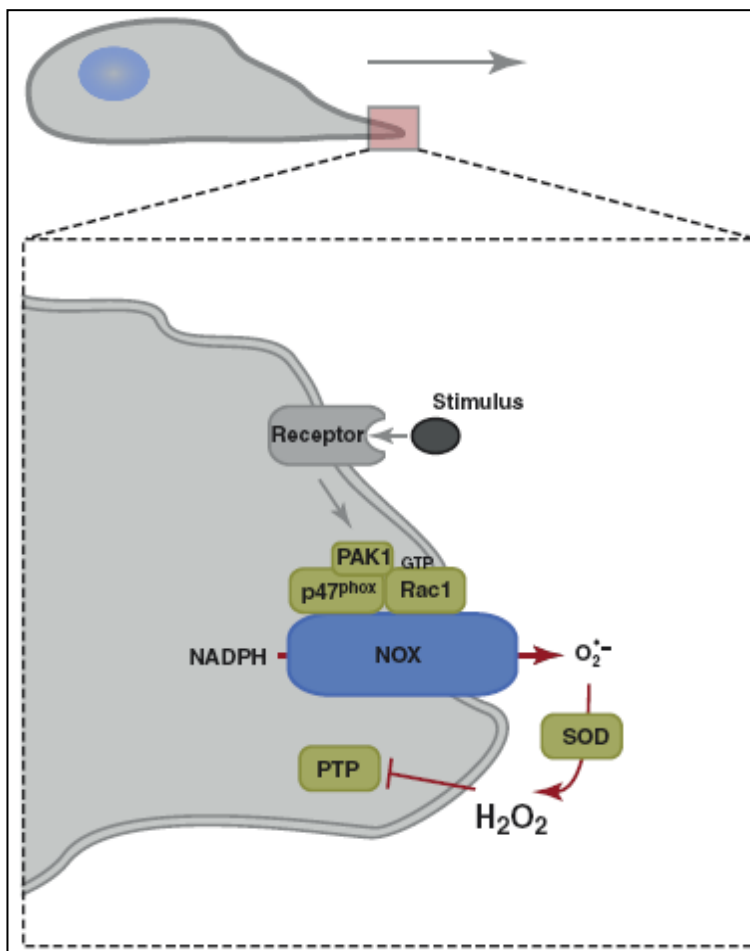


Fig. 2.1 The mechanism by which ROS are generated and act within endothelial-derived cells to promote migration.

During cell migration, NOX2, p47^{phox} and probably other NADPH oxidase subunits are targeted to the leading edge of the cell, where they generate superoxide in a Rac1- and PAK1-dependent manner. Superoxide is produced into the extracellular or luminal space, where it is converted to hydrogen peroxide by SOD and enters into the cytoplasm of the cell. Intracellular hydrogen peroxide then oxidizes proteins such as PTPs (possibly directly or through other thiol proteins) to promote migration. [From Hurd et al., 2012]

Thus it is clear that localized inactivation of cellular signal-switch off mechanisms is required in order to allow pro-oxidant molecules to act in redox signalling. Nevertheless localized production of hydrogen peroxide seems to be another mechanism to transduce signals only in specific cellular compartments. Indeed *in vivo* studies have suggested that NOX2 derived ROS also play an important role

in cell migration during the formation of new blood vessels after tissue ischemia [Hurd et al., 2012] and *in vitro* studies show that production of ROS in migrating endothelial-derived cells is probably spatially and functionally coordinated at the leading edge to promote directional cell migration (fig. 2.1). On the other hand, PTPs negatively regulate cell migration by dephosphorylating and inactivating proteins that promote migration. We have seen that PTPs have an active-site cysteine with suitable characteristics to act as a redox switch (H_2O_2 oxidation-dependent reversible enzyme inhibition), but it is also known that PTPs reaction rate with hydrogen peroxide makes it unlikely that these enzymes can compete for H_2O_2 *in vivo*. So both co-localization of PTPs with NOXs and indirect PTPs oxidation *via* another thiol protein such as Prx, might facilitate PTP oxidative inactivation, thus favouring migration.

Moreover, in addition to their role in regulating migration in migrating-cells, ROS seem able also to mediate changes in non-migrating cells. This is the case of those cells which permits motile cells to bind and penetrate tissues, like vascular mammalian endothelial cells and leukocyte shuttling between the bloodstream and interstitial tissues. ROS were first suggested to play a role in this process when it was noted that treatment of endothelial cell cultures with moderate to high (100 μ M to 5mM) concentrations of hydrogen peroxide induced cell surface expression of the adhesion molecule 1 (ICAM-1) and P-selectin and increased the binding of polymorphonuclear leukocytes (PMNs) to endothelial cells [Patel et al., 1991]. It was also demonstrated that various cytokines (TNF- α , TNF-related activation-induced cytokine TRANCE and visfatin) increase cell surface expression of adhesion molecules through a transient increase in ROS levels in endothelial cells. Furthermore, inhibition of NOX attenuated this increase in ROS levels, thus sustaining the hypothesis of NOX-mediated redox signalling transduction. The mechanism of adhesion molecule promotion by ROS is not yet clear, but some authors reported in Hurd [Hurd et al., 2012] proposed that this could be achieved through activation of the transcription factor NF- κ B. Finally, in addition to influencing cell-cell adhesion through adherens junctions, Hurd reports a role for ROS also in cell-matrix interactions. Indeed ROS seem to affect cell-cell and cell-matrix adhesion by altering the cell surface expression of integrins and cell adhesion molecules such as vascular cell adhesion molecule 1 (VCAM-1), and decreasing adherens junction components.

2.4 Methodological approach: traditional and innovative methods for disulfide bonds assessment

Referring to the steps traditionally involved in disulfide bonds determination they are: (1) fragmentation of the non-reduced protein of interest into disulfide-linked peptides with cleavages between all half-cystine residues, if possible, and under conditions that avoid rearrangement (interchange) of disulfide bonds; (2) separation of disulfide-linked peptides from one another; (3)

location/identification of disulfide-linked peptides in various separated fractions; (4) fragmentation of the disulfide linked peptides at the disulfide bond; and (5) isolation and characterization of the half-cystinyl products of the disulfide cleavage reaction. These early studies also provided insights into the experimental conditions required for disulfide bond determination. Indeed, it was observed that disulfide bond rearrangement could be promoted by strong acids, by the presence of thiols at neutral pH, and by thiols produced by hydrolytic cleavage of disulfide bonds at neutral and alkaline pH (Disulfide interchange was in fact noted under the conditions of enzymatic cleavage at slightly alkaline pH) [Gorman et al. 2002 and references therein]. Consequently, chemical and enzymatic protein cleavage methods like dilute acids and/or cyanogen bromide or pepsin are preferred. Moreover also downstream analytical technologies that require disulfide-linked fragments to be isolated for defining linkages (e.g. - amino acid analysis or Edman degradation) are highly dependent on purification strategies. As reviewed by Gorman et al. cation-exchange HPLC has been used to isolate disulfide-linked peptides due to the greater retention on cation-exchange media than single-chain peptides due to relative differences in cationic properties of these classes of peptides at acidic pH. Another elegant method for identification of disulfide-linked peptides and isolation of the component half-cystinyl peptides for analysis involved diagonal peptide mapping by paper electrophoresis. This technique involved: (1) cleavage of the non-reduced protein with pepsin; (2) separation of the disulfide-linked peptides by one dimension of paper electrophoresis at acid pH; (3) exposure of the original electrophoretogram to performic acid vapor; and (4) a second dimension of separation by paper electrophoresis at right angles to the initial direction of separation. Performic acid cleaves disulfide bonds, and converts the half-cystine residues into highly negatively charged cysteic acids (ie – sulphonic acid RSO_3H). Thus, peptides not affected by performic acid migrated in a diagonal fashion after the combined electrophoretic steps, and peptides with disulfides prior to performic acid oxidation migrated off the diagonal. Peptides that were paired by inter-chain disulfide linkages prior to oxidative cleavage migrated with a vertical orientation to each other. All approaches mentioned so far are quite complex and time consuming anyway and today they are progressively substituted by modern mass spectrometry (MS) based technology. The potential for MS to facilitate the determination of disulfide bond linkages in proteins was realized with the advent of reliable methods for ionization of peptides and proteins (fast atom bombardment FAB, laser desorption ionization LDI, electrospray ionization ESI) together with the development of instruments suitable for analysis of relatively small quantities of proteins and peptides with good resolution and accuracy in a reasonable mass range. With respect to traditional methods, in case of MS approach to disulfide bonds identification separation and analysis are done simultaneously in the mass spectrometer. When a protein potentially containing one (or more) disulfide bonds is in its oxidized form, proteolysis produces either single fragments containing the disulfide as intra-chain linkage or multiple

fragments still linked to each other by the disulfide bond. In both cases a new peptide with a mass 2 a.m.u. (atomic mass units) lower than the mass of either the reduced peptide or the sum of two peptides suggests an identification that could be validated by MS/MS (tandem mass spectrometry) sequencing [Mauri et al. 2010]. Of course the issue of disulfide reshuffling during sample preparation, i.e. especially during proteolytic digestion is still pressing and this is really true if we consider trypsin as the most specific and standardized endoprotease used in proteomics, both because of the reproducibility of its digestion pattern (arginine and lysine residues are commonly always present in a reasonable amount in almost any protein) and because of the advantage got from ionization of peptides containing basic residues at their carboxyl-terminal ends. Indeed trypsin works best at alkaline pH, where dissociated cys-thiols (thiolates) could account for disulfide reshuffling by means of a nucleophilic attack of thiolate on disulfide.

2.4.1 Disulfide proteome of complex samples

Thus, given interest in the identification of proteins with redox-active cysteines, in the past decade proteomic approaches that aimed at large-scale identification of proteins with modified cysteines have provided tools for unraveling new redox-regulated processes. Such studies have often been pointed out as searches for the “redoxome” or more restrictively “disulfide proteome”. The term disulfide proteome might be used in the strict sense as a set of proteins containing disulfide bonds. However, it is often understood implicitly that the disulfide subproteome of interest consists of those proteins containing disulfides, which are susceptible to reduction by oxido-reductases (so not the structural ones). Otherwise disulfide proteomes have also been widely defined as sets of proteins that contain cysteines, which exhibit any kind of change in their redox state or “reactive cysteine proteome”. The reactive nature of cysteine thiols is an experimental challenge when determining the oxidation status of cysteines in proteins. Indeed in samples from tissues or cell cultures, post-lysis thiol-disulfide exchange between proteins may lead to misinterpretation of data and, if molecular oxygen is present in the buffers together with transition metals, oxidation of thiols may also occur during isolation. Hence, one of the critical steps when working in redox biochemistry is to trap the thiol-disulfide status in the sample. This is usually achieved by either acidification followed by alkylation or by direct alkylation of free thiols both during cell lysis and immediately after. Generally speaking, different approaches share the common principle of “differential thiols probing”, namely after the first trapping with a first labeling reagent, oxidized thiols (e.g. disulfides not reacted with the probe) are subsequently reduced and then blocked by a second labeling reagent. Of course the two probes should be different and somehow distinguishable from each other: some often used compounds are N-ethylmaleimide (NEM), iodoacetamide (IAM), iodoacetic acid (IA) possibly joined to reagents allowing for fluorescence, radioactivity, or differential mass

tags detection (fluorophores or isotopes). On the other hand di-thiothreitol (DTT), β -Mercaptoethanol or Tris-Carboxy-ethyl-phosphine (TCEP) are often used as reducing agents. Probes with some specificity for Cys-SOH exist too, like dimedone or even bi-functional probes potentially able to react with both Cys involved in a disulfide, like dibromomaleimides. Probes could also be divided summarily into reversible tags or irreversible tags and could even be joined to functional groups like biotin molecule allowing for affinity enrichment or fishing of protein thiols of interest. Other known techniques aimed at the enrichment in proteins containing reactive cysteine thiols are the activated thiols sepharose (ATS) or Trx affinity chromatography. As for detection methods, the two main fields we would like to consider here are the gel based non-reducing/reducing diagonal electrophoresis and 2D-redox-DIGE (two dimensional redox differential gel electrophoresis) and the mass spectrometry (MS)-based detection of proteins with reactive disulfides. The latter approach is greatly affected by difficulties in analyzing disulfide peptides by tandem mass spectrometry (MS/MS) especially when complex samples are to be analyzed. Strong development of software tools might then facilitate the interpretation of MS/MS spectra of disulfide linked peptides. On the other hand, if we consider MS based method in the more comprehensive context of differential labeling approach, it is possible to outline labeling methodologies like cleavable isotope coded affinity tagging (cICAT) in its forward and reverse approach and also the so called oxidative ICAT (oxICAT).

3. MATERIALS AND METHODS

3.1 Cell cultures

Ras-transformed MCF10A-T1k cells (hereafter named M2) - an isogenic derivative of the human mammary MCF10A cell line - were kindly provided as a model of tumor progression from Prof. Stefano Piccolo's laboratory. Precisely M2 cells overexpressing a constitutive active point mutant of the Hippo transducer TAZ, TAZ(S89A) were provided as "case sample" (hereafter M2T) while M2 cells were used as "control sample" in this study. Thorough experimental evidence already attested a role for TAZ in endowing M2 cells with CSCs like properties and particularly demonstrated TAZ relationship with EMT (Piccolo et. al., 2011). Both M2 and M2T cells were incubated at 37 °C in moisture added air-CO₂ (95 - 5 %) blend into DMEM/F12 medium (Gibco) freshly supplemented with: 5 % heat inactivated horse serum (Gibco), 2 mM glutamine (Gibco), 10 ug/mL Insulin (I9278 SIGMA), 20 nGr/mL rH-EGF (AF-100-15, Peprotech), 8.5 nGr/mL Cholera toxin (C8052, SIGMA), 500 nGr/mL hydrocortisone (H0369, SIGMA), 100 U/mL penicillin and 100 ug/mL streptomycin. Cells were cultured on 75 cm² flasks and spread at 1:4 to 1:6 ratio when reaching sub-confluence.

Two days before each experiment cells were seeded at a density of 30 - 35,000 cells/cm² into 15 mL of complete culture medium without antibiotics. One day before each experiment medium was freshly renewed and the day of each experiment cells were harvested by trypsinization and counted. On average 7 - 8 * 10⁶ cells/flask were gathered with > 98 % vitality at trypan blue assay (T8154, SIGMA). Culture medium was further maintained at 37 °C for 3 - 5 more days to assess absence of contaminations.

3.2 Sub-cellular fraction enrichment

For each experiment about 15*10⁶ cells for both M2 and M2T cell lines were disrupted on ice by Dounce homogenization in 1 ml of 0.1 M PBS pH 7.4, 0.25M sucrose, 1 mM EDTA and protease inhibitor cocktail (0.1 mg/mL Phenylmethylsulfonyl fluoride PMSF, 0.7 mg/mL pepstatin, 0.5 mg/mL leupeptin). Homogenates were centrifuged 10' at 1000*gat 4°C in order to separate particulate fraction containing nuclei and cell debris (*pellet I*). Isolated supernatant was then further centrifuged 60' at 105,000*g at 4°C to separate cytosol from other cellular organelles (*pellet II*). Supernatant from this latter centrifugation step has been provided freshly for each experiment.

3.2.1 Protein assay

Protein content was measured according to Lowry as modified by Bensadoun et al., (Bensadoun et al., 1976) taking advantage of previous TCA precipitation. Each sample to be measured was first diluted to 3 mL final volume with water. A minimal volume of diluted DOC detergent was then added to a final concentration of 0.02% (w/v) followed by 1 mL of diluted TCA to a final concentration of 6.25%. Sample was left to incubate 10' at ambient temperature before spinning it down at 3800*g 30' at 4°C. Supernatant containing soluble contaminants was then discarded carefully. A solution of Na₂CO₃ 2% (w/v), NaOH 0.1 N and a solution of CuSO₄ 0.5% (w/v), KNaTartrate 1% (w/v) were mixed together to a ratio of 50:1 prior to use and each precipitated sample pellet was dissolved into 1 mL of the resulting solution and incubated for 30' at ambient temperature in the dark. After incubation 0.1 mL of freshly 1:1 water diluted Folin's reagent (SIGMA) was added to each sample and left to incubate for another 30' at ambient temperature in the dark. At the end of incubation each sample absorbance was recorded at 750 nM with a Multiskan microplate reader (ThermScientific). Sample concentration was then calculated with reference to a standard curve ranging from 3 to 30 ug of BSA prepared in the same way of protein samples to be measured.

3.2.2 DTNB assay

DTNB 10 mM solution was prepared freshly into TrisHCl 0.1 M, EDTA 1 mM pH 8.3 and diluted to DTNB 140 µM into TrisHCl 50 mM, NaCl 150 mM pH 7.5. Up to 200 µL of sample volume or sample buffer as blank were added to each 1 mL aliquot of diluted DTNB solution. This aromatic disulfide reacts with aliphatic thiol groups to form a mixed disulfide of the protein and one mole of 2-nitro-5-thiobenzoate per mole of protein sulfhydryl group. DTNB has little if any absorbance, but when it reacts with thiol groups under mild alkaline conditions, the 2-nitro-5-thiobenzoate anion gives an intense yellow color at 412 nm. Whole soluble reduced thiols were read almost immediately, since they readily react with DTNB, while protein thiols detection needs preventive incubation at room temperature for 30'. Samples were kept into quartz cuvette for measurement. Scan mode acquisition with the DU70 Spectrophotometer (Beckman Coulter) was then performed between 380 and 480 nm, at 300 nm/min scan rate. Calibration was done against H₂O₂ and blank absorbance was registered as background. Sample absorbance values at $\lambda = 412$ nm were used to calculate thiols concentration given the molar extinction coefficient $13.6 \text{ mM}^{-1} \text{ cm}^{-1}$ at 412 nm. Finally thiol groups concentration per milligrams of protein were calculated dividing such values by protein content.

3.3 Differential “redox” labelling

A methodological constraint to fulfil the aim of this project is to identify and quantify proteins which could be possibly distinguished with respect to their thiols oxidation status among different samples to compare. In order to achieve such goal we combined a differential labelling protocol to extract proteins of interest from the sample and mass spectrometry analysis joined to informatics data handling to identify and quantify those proteins (fig. 3.a).

All subsequent protocol steps were carried out at the same time for both M2 and M2T samples.

Alkylation of free thiols

First, 1mM NEM was added during cell lysis and then fraction enrichment to avoid unwanted thiol oxidation. 180 to 200 ugr of proteins from cytosol fraction were then subjected to buffer exchange against 0.1 M sodium-phosphate pH 8.0 1 mM EDTA on NAP-5 columns (GE Healthcare) to remove unreacted NEM.

Reduction of oxidized thiols

Eluted samples were reduced with 1mM DTT (SIGMA) for 1h at ambient temperature. This is intended to release reversibly oxidized protein thiol groups for subsequent reaction with HPDP probe. Again excess DTT was removed by means of buffer exchange on NAP-10 columns (GE Healthcare) against the same buffer.

HPDP Labelling

Eluted samples were then treated with EZ-Link HPDP-Biotin probe (Thermo Scientific) at ambient temperature for 1h. 1:1 protein thiol groups to probe ratio was calculated from DTNB data on protein thiol and reaction was carried out at pH 8. Moreover, reaction of EZ-Link HPDP-Biotin probe with protein free thiols was monitored as reported (§ 3.3.1). Unreacted EZ-Link HPDP-Biotin was removed from the sample by means of another step of buffer exchange on PD-10 column against PBS pH 7.0.

Enrichment of labelled proteins

Labeled proteins were then “fished out” on homemade affinity Neutravidin columns: 125 ugr of High Capacity NeutrAvidin Agarose Resin (Thermo Scientific) were first packed and washed extensively with PBS EDTA 1mM pH 7.4 into empty Micro Bio-Spin Columns (2 cm working bed height, 0.8 mL bed volume, BioRad). Whole sample was then loaded into the column by adding

subsequently 200 μL aliquots and letting each of them flow through the column by gravity. Flow through was recovered and loaded again for two more times. Bounded sample was instead washed three times with binding buffer (PBS EDTA 1 mM pH 7.4) and three times with TrisHCl 0.1 M EDTA 1 mM pH 8.3. Elution was achieved by reducing back disulfides between EZ-Link Biotin-HPDP and protein thiols with the same buffer containing DTT 5 mM. This was intended to avoid harsh conditions normally required to disrupt biotin-neutr/avidin interaction and allowed the obtainment of suitable conditions for subsequent MS analysis. Elution time was critical to achieve good experimental reproducibility and five elution steps with 1 mL of elution buffer were performed letting the elution buffer to incubate with resin exactly 2' at ambient temperature each time before collecting the sample by gravity.

Alkylation of formerly oxidized thiols

Eluted samples contained reduced thiols at pH 8.3 and further alkylation was needed to avoid disulphide reshuffling and/or random oxidation. Therefore samples were incubated 1h at ambient temperature with 1 mM IAM and excess reactant was blocked by adding DTT to the reaction at a final concentration of 2 mM.

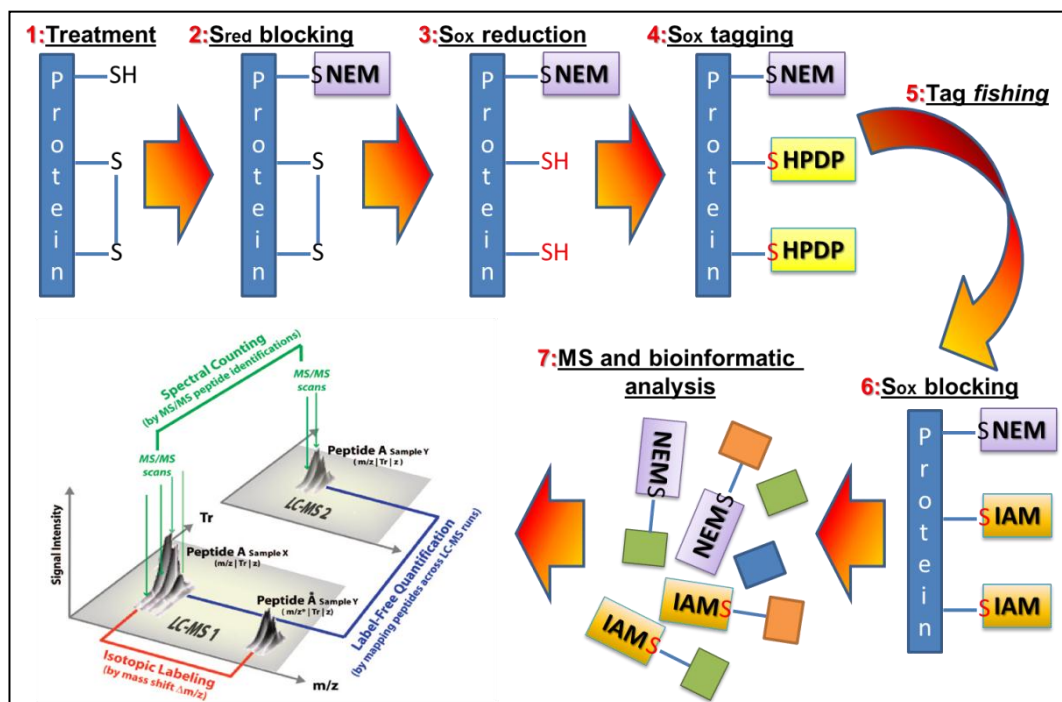


Fig. 3.a Differential labelling approach

Schematic representation in figure summarizes the main steps of the methodology developed in this work: (1) first samples are “treated” that, in the case of the M2 and M2T breast cancer cellular model, indicates different cell strains engineered in order to express a constitutive active mutant of TAZ; (2) right during cell lysis accessible thiol-groups are blocked with NEM to avoid unwanted

oxidation which would otherwise compromise results interpretation; (3) thiol-groups which were oxidized in the starting sample, and so which did not react with NEM, are reduced with DTT and let free to react for further labelling; (4) formerly oxidized thiol-groups are then marked with HPDP which contains a biotin function allowing us to affinity purify tagged (i.e. *redox-sensitive*) proteins on neutravidin resins (5); given the use of reducing agents for elution from neutravidin the next step is to block newly-reduced thiol-groups with IAM (6). Finally, samples enriched with redox-sensitive proteins fished out of starting samples, are digested in order to proceed with MS analysis and label free quantification.

3.3.1 HPDP assay

The reaction of Biotin-HPDP to sulfhydryl groups results in displacement of a pyridine-2-thione group, the concentration of which may be determined by measuring the absorbance at 343 nm. 60 and 180 μ g of proteins, corresponding respectively to 8 and 24 μ M thiols, were incubated with 10 and 30 μ M EZ-Link-Biotin-HPDP in sodium phosphate 0.1 M pH 8.0 for up to 1h at ambient temperature. Reaction was followed on a DU70 Spectrophotometer (Beckman Coulter) reading absorbance at 343 nm to confirm reaction extent.

3.3.2 Electrophoresis

Samples were analyzed also by means of SDS-PAGE and Wb. For SDS-PAGE samples were diluted into suitable quantity of sample buffer (62.5 mM TrisHCl pH 6.8, 2.5% SDS, 10% glycerol, 0.004% pyronin in H₂O mQ) and reduced/denatured by heating to 95°C for 5' with 1 M β -mercapto-ethanol before run. Gels were casted at a final acrylamide concentration of T = 3.9% (w/v) for the stacking gel and T = 14% (w/v) for the separating gel using suitable amounts of APS (Sigma) and TEMED (Sigma) as catalyst for polymerization. SDS-PAGE Molecular Weight Standards (BioRad) in sample buffer was used as molecular weight marker. Separation was performed at constant current and running buffer was prepared freshly each time (25 mM TrisHCl pH 8.6, 0.19 M glycine, 0.01% SDS in H₂O mQ). Occasionally also 12% Bis-Tris Criterion XT pre-cast gels (BioRad) were used with XT MOPS running buffer and Precision Plus Protein Standard Unstained (BioRad) as MW marker. Gels were stained overnight with colloidal coomassie (1 mM Coomassie Brilliant Blue G-250, 34% (v/v) methanol, 1.3 M ammonium sulphate, 3% (v/v) phosphoric acid in H₂O mQ) and destained with H₂O mQ water.

3.3.3 Western blotting

In order to evaluate oxidation status and quantity of G6PDH protein in M2 and M2T samples we performed Wb analysis on 20 μ g of total protein previously separated by SDS-PAGE (see above) with and without the addition of reducing

agent. Gel-separated samples were electro-transferred on nitrocellulose membrane at 180 mA constant current overnight into blotting buffer (25 mM ethanolamine, 25 mM glycine and 20% v/v methanol pH 9.5) and the success of transfer was verified by Ponceau red staining (0.2% (w/v) in 3% (v/v) TCA aqueous solution). Immunological detection was then performed using rabbit polyclonal antibody against human G6PD (sc-67165, Santa Cruz Biotechnology) and mouse monoclonal antibody against human GAPDH for loading control (mAbcam 9484) as primary antibodies and HRP-conjugated anti-rabbit and anti-mouse secondary antibodies for detection. Detection was done with freshly prepared luminol solution (1.1 mM luminol, 1 mM 4-iodophenol, 0.12% BSA, 1.4 M H₂O₂, 0.025 mM Tris-HCl pH 9.25) and densitometric analysis of immunoblots was obtained by the Image Station 440 (KODAK). All washes were done with PBS 0.1% Tween-20, saturation with PBS, 0.1% Tween-20, 0.9% NaCl and 3% BSA and antibodies were diluted with PBS, 1% BSA.

3.4 Sample preparation for MS analysis

In order to identify proteins present into enriched fractions from § 3.4, samples must be digested and analysed by MS. To remove excess DTT and IAM each sample was concentrated by means of TCA precipitation: each sample was first diluted to 3 mL final volume with water. A minimal volume of diluted DOC detergent was then added to a final concentration of 0.02% (w/v) followed by 1 mL of TCA to a final concentration of 8 %. Sample was left to incubate 10' at ambient temperature before spinning it down at 3800*g 30' at 4°C. Supernatant containing soluble contaminants was then discarded carefully and pellet was washed with 1 mL of cold ethanol by vortex and spinning at 3800*g 20' at 4°C. Again supernatant was discarded and each precipitated sample pellet was dissolved into 100 µL of NH₄HCO₃ 40 mM ACN 10% containing 10 nGrTrypsin Gold Mass Spectrometry Grade (SIGMA). Digestion was performed overnight into a 37 °C water bath and arrested by adding formic acid (FA - SIGMA) lowering pH to 3 – 4. Trypsinized samples were then dried by vacuum centrifugation and re-suspended into 20 µL of FA 0.1% milliQ grade water solution prior to analysis.

3.5 Q-TOF analysis

Each peptide mixture from M2 and M2T samples was analysed in triplicate. Specifically: 6 µL of sample per technical replica were injected and each time samples runs followed this order: M2replica1_M2Treplica1; M2replica2_M2Treplica2; M2replica3_M2Treplica3. Samples were resolved by means of reversed-phase chromatography on a nano-fluidic HPLC-Chip apparatus coupled with a quadrupole ion trap and time of flight mass spectrometer, using the

6520 Accurate-Mass Q-TOF LC/MS system (Agilent Technologies, Santa Clara, CA, USA) equipped with MassHunter Workstation Software Qualitative Analysis B.02.00 as graphical interface for data handling. A 1200 Rapid Resolution system (Agilent Technologies, Santa Clara, CA, USA) containing a binary pump and degasser and a well-plate autosampler with thermostat were associated to the HPLC-Chip interface directly connected to a nanoESI ionization source thus providing a rugged technology suitable for sample identification analysis. Loaded samples were enriched on a 160 nL enrichment column and separated with an acetonitrile gradient (50% ACN in 60', 80% ACN in 80' and re-equilibration to 6% ACN in 120') on a 75 μm x 150 mm separation column packed with Zorbax 300SB-C18 5 μm material at a flow rate of 0.36 $\mu\text{L}/\text{min}$. Source parameters were: gas temperature 325 $^{\circ}\text{C}$ and drying gas 5 L/min while voltage values for fragmentor, skimmer and octapole were respectively 175 V, 65 V and 750 V. Counts threshold for storage were 200 for MS data and 5 for MS/MS data *or* 0.01% relative to base peak intensity in both cases. MS data were acquired in the range between 350 and 2400 m/z and MS/MS data were acquired in the range between 59 and 3000 m/z . Scan rate was 4 spectra/second for MS and 3 spectra/second (2378 transient spectrum) for MS/MS (3213 transient spectrum). Data dependent MS/MS analysis were then carried on the 3th most intense peaks from each MS scan using collision induced dissociation fragmentation (3.6 V/100 Da with - 4.8 V offset). Only precursors above 1000 counts *or* $\geq 0.01\%$ with reference to base peak intensity were used for fragmentation with an isolation width of 4 Da. Dynamic exclusion for MS/MS analysis (exclusion after 2 spectra and release after 0.5') was applied in order to enhance sequencing of less abundant species too. The use of dynamic exclusion during MS/MS data acquisition was made possible since we adopted a *label free* quantification method relying on MS/MS data only for species identification, while actual abundance values were obtained from MS feature.

3.6 G6PDH enzymatic activity measurement

Assays were performed at ambient temperature. Sample was diluted into reaction mixture: 0.1 M TrisHCl pH 7.4, 0.15 M KCl, 5 mM EDTA, 0.1% (v/v) Triton X-100 and 1.25mM glucose-6-phosphate disodium salt according to Scott (Scott, 1971). The reaction was initiated by the addition of 0.25mM NADP and was followed at 340 nm for 23 min with a DU70 Spectrophotometer (Beckman). Activities are reported in nmol of NADPH formed per min per mgr of proteins using extinction coefficient for $\text{NADPH}_{\lambda 340} = 6.22 \text{ M}^{-1} \text{ cm}^{-1}$.

For inhibition experiments, M2 and M2T samples devoid of NEM were pre-treated with 1mM DTT in a minimal volume of 0.1 M sodium-phosphate pH 8.0, 1 mM EDTA. Activity was then measured with or without removing DTT by means of buffer exchange. In order to block reduced protein thiol-groups, samples

were also treated with 1mM NEM right after 1mM DTT reduction and activity was measured after removal of both DTT and NEM by means of buffer exchange.

3.7 Data analysis

Two of the main applications of mass spectrometry are today identification and quantitation of compounds. Although a variety of software tools exists for those tasks, they are often monolithic and difficult to adapt to rapidly evolving demand. Since many different quantitation protocols exist, it is desirable to have smaller algorithmic components that can be readily combined into more complex workflows or tools. OpenMS, a free software package (available under the Lesser GNU Public License LGPL from the project website at <http://www.openms.de>) aims at providing exactly this functionality and is therefore more flexible than almost all current commercial tools and most of the openly available libraries. I took advantage of the essential collaboration of computer engineer Dr. Marco Falda in order to improve and finely tune OpenMS to perform desired analysis on our data. Briefly speaking, OpenMS tools have been designed following a bottom-up philosophy: from the code library, to the command line tools, to a high level visual block workflow. Each layer simplifies the management, but also restricts the flexibility, since it constrains the user to follow “*a priori*” well defined behaviours. We then decided to work at the intermediate level represented by the command line tools, since the most abstract level had some inconveniences; for instance, they do not cache intermediate results nor provide any sort of flow distribution and concurrency. Computational Proteomics tasks require complex and long operations, such as identifying sequences or characterizing features in terms of wavelets. For this reason the workflow has been designed distributed over a cluster of computers supervised using a so-called “*job manager*”, namely the Sun Grid Engine 6.2u5 (SGE). The caching of the results and the concurrency of independent tasks has been obtained using the SCons build system. Scons has been preferred over more traditional tools like make or CMake for its ease of customization. It can be programmed in the Python programming language and all the repertoire of this language, such as functions, list comprehensions and dynamic types are readily available. It has also a built-in scheduler able to queue the jobs concurrently. These jobs are distributed among the cluster workstations by delegating them to the SGE. The cluster is composed by 3 Dell™ PowerEdge™ R410 workstations equipped with 4 Intel® Xeon® quad-core CPUs at 2.3GHz and 32 GB RAM; the storage unit is an Dell™ EqualLogic™ PS4000. Refer to Fig. 4.f for an overview of the reported analytical workflow.

3.7.1 Input data

Input data required by OpenMS are mzML files, a specific kind of XML files (others are mzData or mzXML). Nevertheless raw data from Agilent Accurate Mass Q-TOF LC/MS 6520 are stored by default into a multi-folder format (.d) which can be processed by proprietary software Agilent Mass Hunter Qualitative Analysis only (we used version B.02.00 Build 2.0.197.0) and exported into .mzData file format. In order to best keep unbiased and unfiltered raw data to be processed by OpenMS, raw data from each experiment have been exported into corresponding .mzData file format without applying any filter at this level beside the required deisotopic function (peptides model) at centroid level. No further baseline subtraction or spectra smoothing have been applied before going ahead with analysis workflow.

3.7.2 Identification

Input mzML files are first processed by three different search engines: X!Tandem, OMSSA and Mascot. We used a licensed in house server version of Mascot (ver. 2.3) on the cluster which has been implemented with Mascot search engine, while X!Tandem and OMSSA referred to their own executables installed on the same cluster. All search engines have been used with reference to SwissProt database dated February 2012, taxonomically limited to *Homo sapiens* and enriched with both potential contaminant proteins from the *common Repository of Adventitious Protein* “cRAP” (www.thegpm.org/crap/index.html) and decoy proteins obtained by inverting all the former sequences. Decoy proteins are used to distinguish random sequence matches and compute *false discovery rate* (FDR) values. Different identification scores from search engines are equalized and merged by means of their *posterior error probability* (PEP) value, computed from FDR value (Käll et al., 2008). So resulting matches (identifications) are gathered and merged through the IDMerger and ConsensusIDblocks and before being passed to FDR block peptides are also assigned to matched proteins and flagged as belonging to the decoy database or not (depending on the fact that they match or don't match to reversed proteins in decoy database) by the PeptideIndexer block. The parameters we set for each analysis step are shown below (please refer to http://ftp.mi.fu-berlin.de/OpenMS/doc-1.9-official/html/TOPP_documentation.html for a complete description):

MascotAdapterOnline:

- database = SwissProt_H_Decoy
- enzyme = none
- instrument = ESI-QUAD-TOF
- missed_cleavages = 0
- precursor_mass_tolerance = 5

- precursor_error_units = ppm
- fragment_mass_tolerance = 0.05
- fragment_error_units = Da
- charges = 2,3,4
- taxonomy = Homo sapiens
- fixed_modifications = []
- variable_modifications = [Carbamidomethyl (C), Nethylmleimide (C)]
- mass_type = monoisotopic
- number_of_hits = 0 (i.e. auto)
- skip_spectrum_charges = FALSE

OMSSAAdapter:

- database = SwissProt_HUMAN_decoy_crap_2012_02.fasta (together with the corresponding *psq* generated through command *makeblastdb*)
- precursor_mass_tolerance = 5
- precursor_mass_tolerance_unit_ppm = TRUE
- fragment_mass_tolerance = 0.05
- min_precursor_charge = 2
- max_precursor_charge = 4
- fixed_modification = []
- variable_modification = [Carbamidomethyl (C), Nethylmleimide (C)]
- v = 1
- e = 17
- hl = 1
- he = 1

X!TandemAdapter:

- database = SwissProt_HUMAN_decoy_crap_2012_02.fasta
- missed_cleavage = 1
- precursor_mass_tolerance = 5
- precursor_error_units = ppm
- fragment_mass_tolerance = 0.05
- min_precursor_charge = 2
- max_precursor_charge = 4
- fixed_modifications = []
- variable_modifications = [Carbamidomethyl (C), Nethylmleimide (C)]
- minimum_fragment_mz = 150
- cleavage_site = [X][X]
- max_valid_expect = 0.1
- no_refinement = FALSE
- no_semi_cleavage = FALSE

IDPosteriorErrorProbability:

- split_charge = TRUE
- top_hits_only = TRUE
- ignore_bad_data = TRUE

ConsensusID:

- rt_delta = 0.1
- mz_delta = 5
- min_lenght = 6
- use_all_hits = FALSE
- algorithm = PEP_Matrix

PeptideIndexer:

- decoy_string = _rev
- write_protein_sequence = TRUE
- keep_unreferenced_proteins = FALSE
- allow_unmatched = TRUE
- aaa_max = 4

FalseDiscoveryRate:

- proteins_only = FALSE
- peptides_only = FALSE

3.7.3 Quantification

Once that identification maps have been obtained as couples of coordinates <<mz, Rt>, peptide>, such identifications can be correlated to the so called *features* through the IDMapper block. A feature is a group of spectra generated from a peptide and recognised by the FeatureFinderCentroided block among the complex three dimensional raw data map which is characterized by the whole mz, RT and intensity values from an entire LC-MS experiment (such data are given in input with the mzML file quoted above §3.7.1). At this point M2 and M2T samples are coupled together combining them into all nine possible ways and features are joined between them obtaining nine *consensus* maps. Features correctly mapped to identified peptides (by IDMapper) are finally quantified by means of the ProteinQuantifier block. The parameters we set for each analysis step are shown below (please refer to http://ftp.mi.fu-berlin.de/OpenMS/doc-1.9-official/html/TOPP_documentation.html for a complete description):

FeatureFinderCentroided:

- intensity:bins = 10

- mass_trace:mz_tolerance = 0.02
- isotopic_pattern:mz_tolerance = 0.04
- isotopic_pattern:charge_low = 2
- algorithm = left at default values

IDMapper:

- rt_tolerance = 15
- mz_tolerance = 10
- mz_measure = ppm
- mz_reference = precursor
- ignore_charge = FALSE
- use_centroid_rt = FALSE
- use_centroid_mz = TRUE

FeatureLinkerUnlabeledQT:

- use_identifications = TRUE
- ignore_charge = FALSE

ProteinQuantifier:

- top = 3
- average = MEDIAN
- include_all = TRUE
- filter_charge = FALSE
- normalize = FALSE
- fix_peptides = FALSE

3.7.4 Results filtering and score ranking

The last component of the OpensMS analytical workflow, ProteinQuantifier, ultimately produces two data tables containing respectively quantified peptides values and values of proteins quantified starting from such peptides. Two Python scripts allow gathering of both proteins and peptides among all the combinations of experimental technical repetitions while another Python script create simple to handle Excel sheets containing peptides and proteins identified during each step of the analysis. In order to obtain reliable quantitative data strengthened by six biological replica, we called for cut off criteria driving us in the classification of non-differential, more oxidized and less oxidized proteins/reduced (with reference to M2T to M2 ratio): so given the M2T/M2ratio threshold of ≤ 0.6 for reduced ≥ 1.4 for oxidized groups (i.e. at least 40% relative difference), we made the following categorisation:

Over oxidized: ≥ 1.4 for ≥ 3 experiments AND ≤ 0.6 for ≤ 2 experiments

Reduced: ≤ 0.6 for ≥ 3 experiments AND ≥ 1.4 for ≤ 2 experiments

Non differential: ≥ 0.6 AND ≤ 1.4 for ≥ 3 experiments AND ≤ 0.6 for ≤ 2 experiments AND ≥ 1.4 for ≤ 2 experiments

All those quantified proteins not belonging to any of the former groups have then been classified as too variable to be characterized as oxidized/reduced in M2T over M2 samples. This could be due of course to the fact that such proteins are not abundant enough or too variables due to intrinsic biological variability to be reproducibly classified. Moreover results obtained this way have been further on ranked depending on both the number of experiments in which they have been observed and the number of identified peptides matching the protein: globally those parameters have been integrated into the so called *f-measure*. F-measure has been calculated this way for each protein in the former groups:

Given: mean of identified peptides/max identified peptides = P

Given: n. ° of experiments confirming identification/max n. ° of experiments = B

We calculated harmonic mean of ratios as:

$$\frac{(2 * P * B)}{(P + B)}$$

Such harmonic mean has then been corrected with a factor X to compensate for the different numerosity of experiments and identified peptides:

$$\frac{(2 * P * B)}{(P + B)} + X$$

Where X is equal to:

given: max n. ° of experiments / 2 = H

$B > H$	AND $P = 1$	$X = 2$
$B > H$	AND $P > 1$	$X = 4$
$B > H - 1$	AND $P = 1$	$X = 3$
$B > 1$	AND $P > 3$	$X = 2$

4. RESULTS

4.1 Development of label free methodology to characterize and differentially quantify oxidatively modified proteins in complex sample

The aim of this project was to identify both the proteins and the cysteine residues differentially oxidized in the samples and also to quantify the difference. We then sought to develop a methodology allowing us both to label reversibly modified residues and to purify proteins containing them in order to analyse a sample devoid of “background” (unlabelled) proteins. Critical steps are reported.

4.1.1 Differential redox labelling

For our project we choose to rely neither on isotope labelling techniques nor on electrophoretic fractionation which could be troublesome with respect to reproducibility. So we choose to use simple alkylating agents like NEM and IAM to mark reduced and oxidized cysteines in the sample and the biotinilated HPDP probe for affinity purifying modified proteins. So main steps are:

- (1) Trapping of native redox state of the thiol proteome to avoid artifactual modification during protein isolation and labelling (with NEM).
- (2) Reduction of the reversibly oxidized cysteine residues in the sample (with DTT)
- (3) Labelling of formerly oxidized cysteine residues (with biotin-HPDP)
- (4) Affinity purification of modified proteins (with Neutravidin)
- (5) Elution of affinity purified proteins (with DTT)
- (6) Labelling of formerly modified cysteine residues (with IAM)

4.1.1.1 *Trapping of the native redox state of thiols*

Given that many cysteine residues are relatively labile since thiols are prone to artifactual modification during protein isolation we needed to trap thiols in their native state as soon as we started to process M2 and M2T cell samples. DTNB assay on residual protein free thiols demonstrated the need for at least 1:2 [SH]:NEM ratio and incubation time of no less than 90' Fig. 4.a. Thus we managed to use 2x[SH] NEM already into the buffer used for cell lysis and cytosolic fraction enrichment.

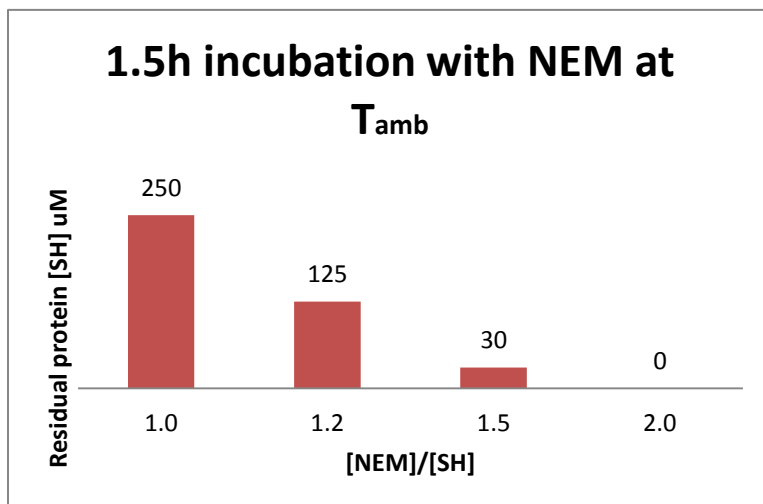


Fig. 4.a

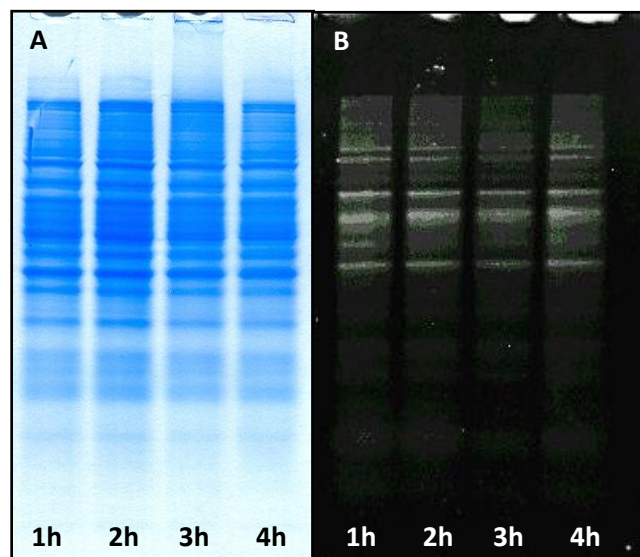
We checked protein free thiols with DTNB assay after incubation with NEM aimed at trapping free thiols in native sample. [SH]:[NEM] ratio of 1:2 was demonstrated to be enough to reach the goal.

4.1.1.2 Reduction of oxidized thiols

We aimed at identifying and quantifying proteins containing reversible oxidative modifications. Of course the number and typology of reversible oxidative modifications which could occur inside the cell is remarkable and not all of them could be addressed by a single methodology at the same time. So we decided to focus on cysteine reversible oxidation products like low redox potential - solvent accessible intra/inter-protein disulfides, sulfenic acid groups, glutathionylation and cysteinilation products as they have been recognized as possible forms of redox modifications entailed in signal transduction inside the cell. DTT is a common reducing agent suitable for reducing back all the above mentioned oxidation products and we demonstrated that 60' incubation at ambient temperature with 1 mM DTT is enough to free our target thiol groups on proteins Fig. 4.b.

Fig. 4.b

7.5 ugr of cytosolic proteins were reduced with 1 mM DTT at pH 8 for up to 4h. Samples were checked after SDS-PAGE separation with CCB staining (A) and reduced thiols were revealed by labelling with 5-IAF and detecting at 518 nm (B).



4.1.1.3 Labelling reaction

Proteins containing thiols reduced at § 4.1.1.2 were our target and thus we wanted to isolate them out of the whole protein sample. Instead of using isotope labelling approaches to mark reduced cysteine-residues and quantify those proteins together with all the others (representing potential troublesome background) we sought an affinity purification approach by means of the labelling reagent biotin-HPDP. The biotin function on this probe allowed fishing marked proteins on neutravidin resin while the pyridine-2-thione leaving group allowed reversible disulphide binding of the probe to target thiol groups in the sample. Thus the pyridine-2-thione group displaced by HPDP reaction with free thiol groups was quantified by measuring its absorbance at 343 nm. In preliminary experiments 280 ugr of proteins, corresponding to roughly 30 uM [SH] were incubated with 40 uM HPDP at Tamb for 1h, final reaction volume 1 mL. Given molar extinction coefficient for pyridine-2-thione at 343 nm = $8.08 \cdot 10^3 \text{ M}^{-1} \text{ cm}^{-1}$ and $\Delta(A_{60} - A_0)_{\lambda 343} = 0.24$ measured for the reaction, we estimated biotinylation of about 29.37 nmol/mL [SH] therefore nearly completion. We also evaluated HPDP labelling of NEM treated/untreated M2 and M2T samples Fig. 4.c.

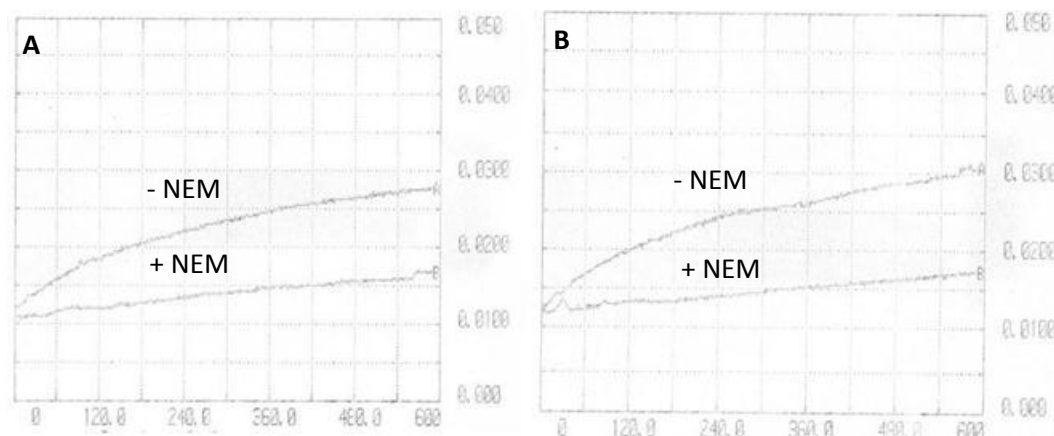


Fig. 4.c Monitoring of HPHP labelling reaction

60 ugr of total proteins of M2 (A) and M2T (B) samples were incubated with 10 uM HPDP for 10 minutes (horizontal axe) and reaction was followed monitoring absorbance at 343 nm (vertical axe). We confirmed remarkable difference between +/- NEM samples in both M2 and M2T samples, confirming the efficacy of the trapping of natively reduced thiols (§4.2.1.1). It is noteworthy also the higher protein thiols labelled into M2T with respect to M2 cell line as will be confirmed also by DTNB assay hereafter.

4.1.1.4 Critical aspects of elution

We assembled Neutravidin columns suitable for the affinity purification of HPDP-labelled samples. Among different parameters pertaining to binding and washing steps the most important step which was tuned in order to obtain good

reproducibility was the elution step. Specifically we wanted to obtain affinity purified sample suitable for subsequent MS analysis without introducing artifactual quantitative modifications between samples to be compared. Thus we choose to elute proteins by reducing back HPDP-protein disulfides rather than by breaking biotin-neutravidin bound. Accurate incubation time and extensive elution steps at pH 8.0 were critical in order to obtain reproducibly enriched samples Fig. 4.d. Thus elution was performed with five sequential steps and rigid incubation time for each experiment.

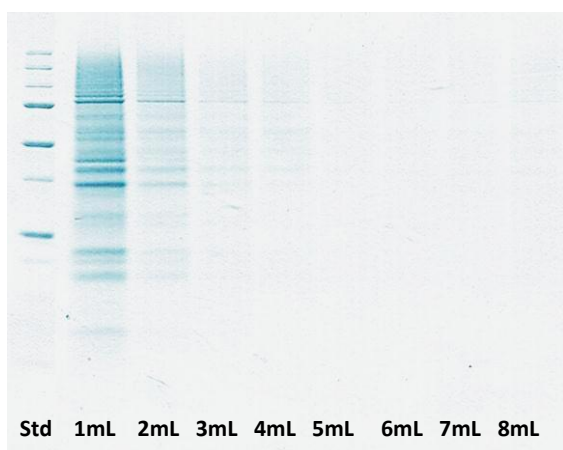


Fig. 4.d

180 uGr of proteins were eluted from 250 uL of neutravidin resin with 8 aliquots of 1 mL of 0.1 M Na_2HPO_4 / NaH_2PO_4 1 mM EDTA 5 mM DTT pH 8.3. Each time the sample was incubated for 2' with elution buffer before collecting it by gravity.

4.1.2 Quantification of extracted proteins

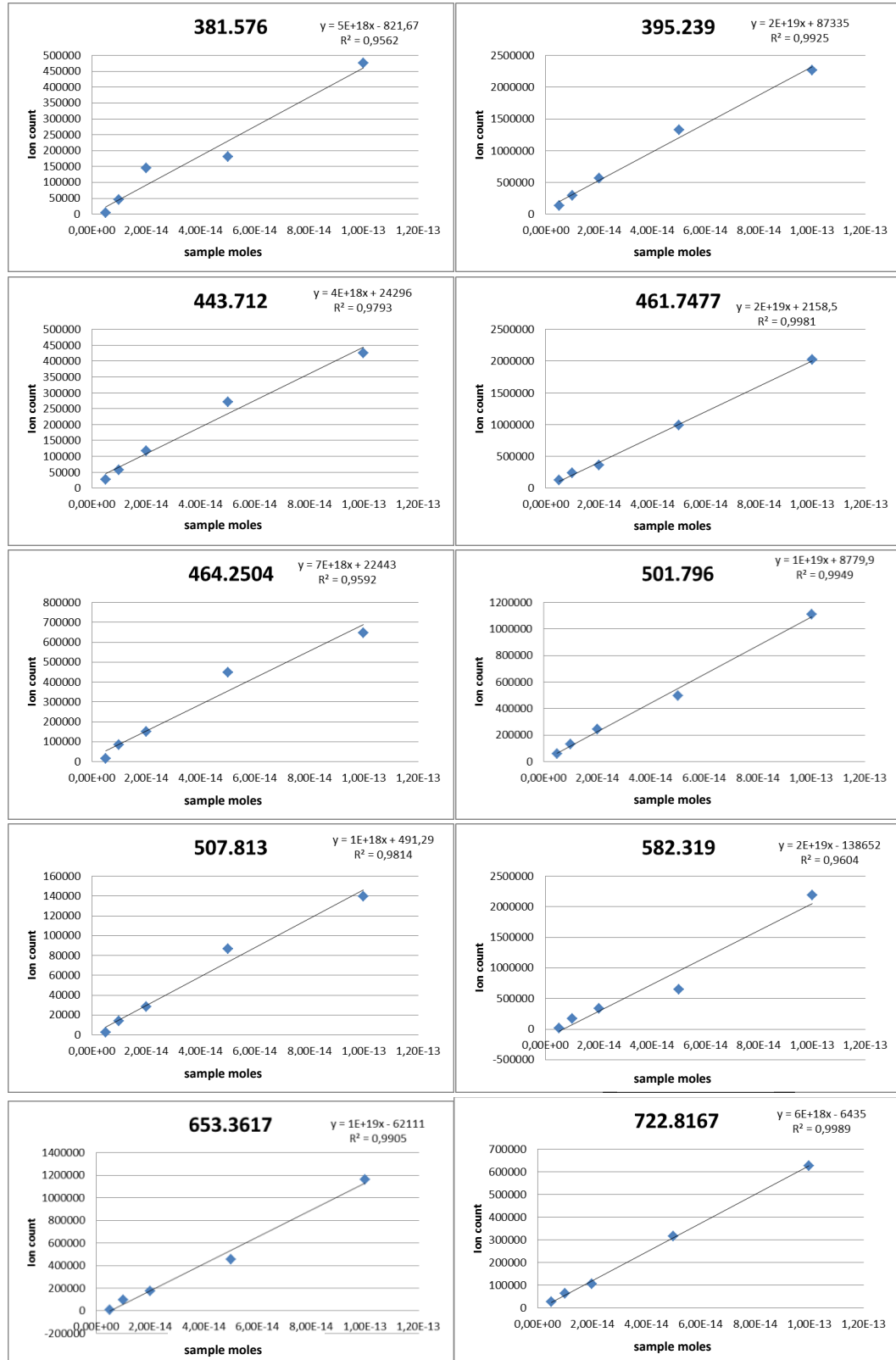
After developing aforementioned methodology to enrich samples to be compared with reversibly oxidatively modified proteins we faced another challenge that was both to identify and quantify our targets. Indeed the choice to use a label free quantification approach forced us to develop also suitable analytical and computational methodology in order to shed light on overwhelming data quantity. Instead of relying on more diffused and hardware burdensome 2D-LC-ESI/MS coupled to *spectral counting* approach we managed to apply dynamic exclusion lists and reiterated runs in order to resolve and identify peptides. This implied focusing on MS profile for quantification issues and on MS/MS data for identification.

4.1.2.1 Ion abundance linearity

First of all we checked the linearity of ion abundance signals on ESI-Q-TOF MS with respect to the quantity of sample injected. We used a standard carboxymethylated tryptic digest of BSA as reference and calculated the area under ten of the most abundant peaks detected to evaluate linearity from 5 up to 100 fmol of protein Tab. 4.a and Fig. 4.e. For each analysis peptides were resolved by means of RPC as described. Good linear correlation between peaks

area and sample injected support the reliability of the MS profile quantification approach reported hereafter.

Fig. 4.e Linear regression plot for observed peptides



Tab. 4.a Intensities are reported as peaks integration area

	fmols of sample injected (6 uL total volume)					reg. coeff.
	5	10	20	50	100	
Observed m/z						
381.576	3137	44876	145689	179997	475411	0.956
395.239	130732	293483	562201	1325979	2266845	0.992
443.712	26329	56938	117438	271292	424358	0.979
461.7477	120714	238528	354387	983791	2023372	0.998
464.2504	16851	84178	150706	447619	647709	0.959
501.796	60713	132563	242626	497663	1111577	0.994
507.813	2737	13932	28412	86788	139944	0.981
582.319	19388	169967	332614	652934	2189001	0.96
653.3617	5669	93390	172697	456795	1162787	0.99
722.8167	26564	63753	106679	317231	625577	0.998

4.1.2.2 Workflow development: from identification to quantification

As stated above the target of our analysis was to identify and quantify proteins in our enriched samples using MS. Therefore we needed to step from experimental *input* data consisting of MS and MS/MS peaks with their m/z, Rt and intensity coordinates to desired *output* which was a list of the most representative proteins in the biological sample. In order to do so we selected OpenMS among open source tools because of its flexibility and efficiency: our workflow was then built up at command line level with the help of Dr. Marco Falda who managed also to implement flow distribution over a cluster of computers as well as the caching of results and concurrency of independent tasks. Thus given an experimental framework encompassing multiple experiments performed over time (biological replicates) the workflow we developed encapsulated (1) identification of peptides (2) mapping of peptides to features and linking of features among samples (3) quantification Fig. 4.f.Part (B) of the workflow described in fig. 4.f joins together information obtained from both identification (A) and *feature finding* fig. 4.g.

A feature is the signal caused by a chemical entity detected in an HPLC-MS experiment (peptide in the present study) and *finding a feature* means to group spectra related to such chemical entity (characterized by m/z, Rt and intensity values) and model them in order to define m/z and Rt constraints for each peptide found in a raw data map. This is achieved by the feature finder block which is integrated into the third part of the workflow: quantitation (fig. 4.h). In order to obtain reproducible quantification we needed to define also raw data exporting criteria. Since the lack of standardization among proprietary data formats we choose not to apply any filter at the exported raw data: the only operation preliminary to workflow processing was to extract centroid instead of profile data for raw maps. Therefore feature finding relied on interpretation of isotopic and multi-charged pattern of centroid data.

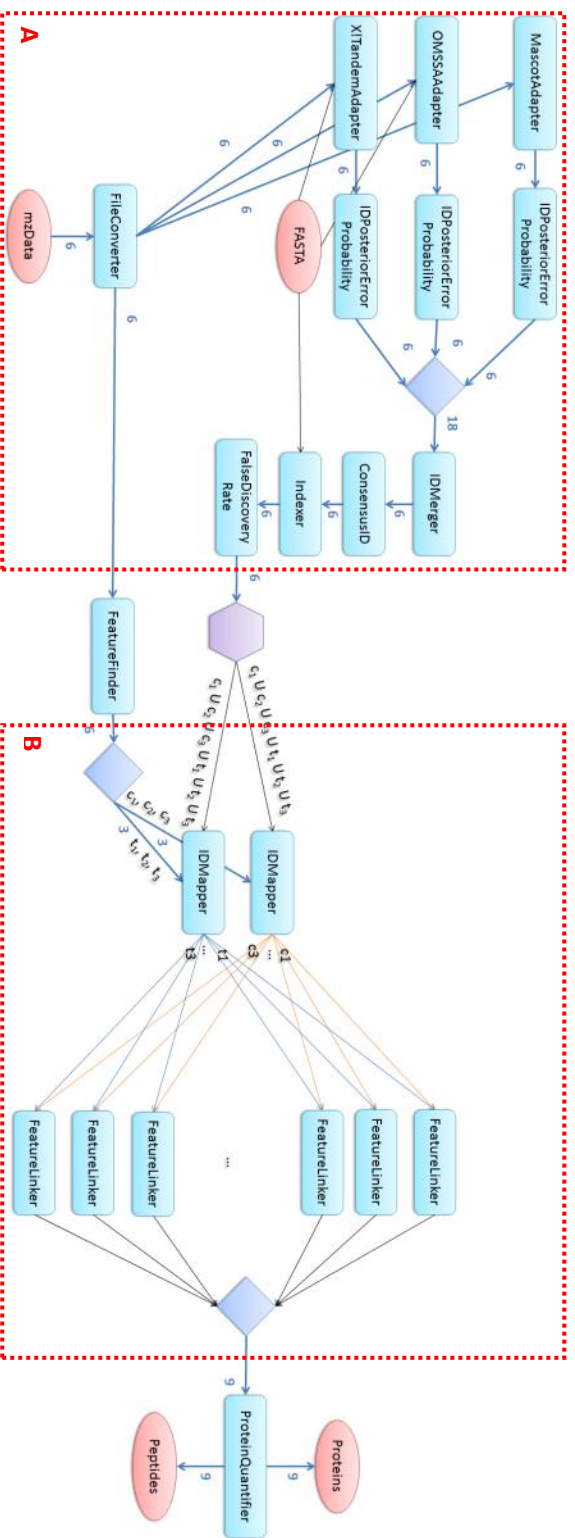


Fig. 4.f Data analysis workflow

Figure represents a visual summary of the OpenMS workflow. The number above connector arrows represents set of files to be processed: for each experiment input were 3 M2 samples and 3 M2T samples. Specifically: mzData exported raw data maps (see § 3 for details) were used in input for both the identification of peptides relying on MS/MS data (A) and the mapping and linking of features (B). Multiple search engines matched MS/MS fragments data to protein databanks scoring peptide to spectrum matches (PSM). Heterogeneous scoring algorithm results from all the search engines were then combined by means of the posterior error probability (PEP) function and the IDmerger block. Consensus identification from peptide identifications of several identification engines was obtained by the ConsensusID block and protein reference for each peptide (comprising matching to decoy-DB) was refreshed by the Indexer block. False discovery rate was estimated from matching to decoy-DB with respect to overall matches and matches to decoy-DB were removed by the False Discovery Rate block. In the second part of the workflow (B) identifications coming from all replicates of a given biological sample are merged together and mapped on the 6 files whose features has been characterized. From these 6 files 9 possible combinations between control and treated samples are linked.

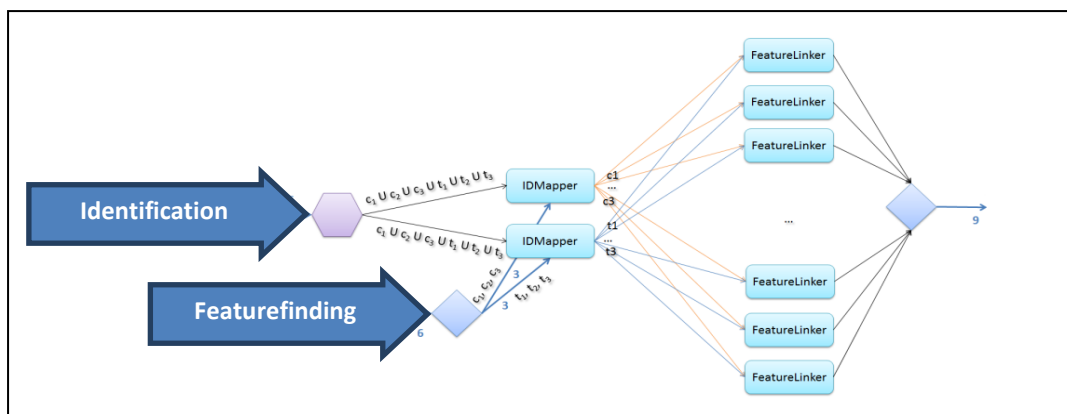


Fig. 4.g Feature relative quantification is based on both MS and MS/MS data Mapping and linking block of the workflow (fig. 4.f B) joins information from both identification (derived from MS/MS data) and feature finding (derived from MS data)

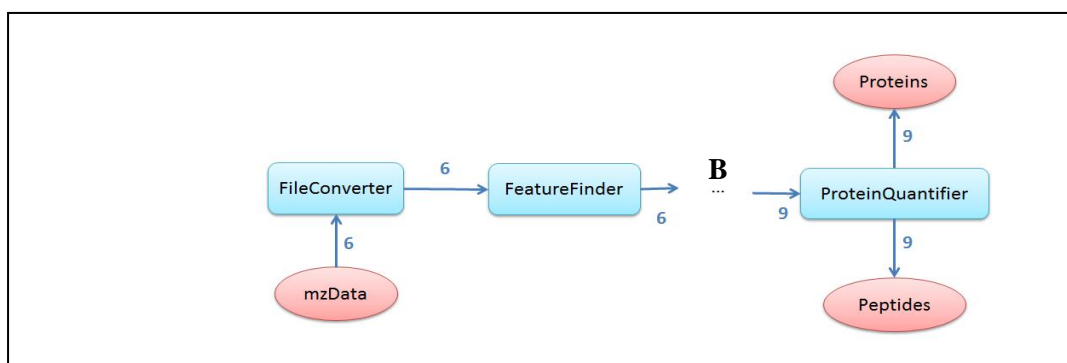


Fig. 4.h Quantification branch of the workflow Quantitation block find features to give as input to the merging block (B). From mapped and linked features the quantitation block finally extracts and quantifies peptides and proteins relying on features intensity.

4.1.2.3 Workflow validation

The aim to identify and quantify redox active proteins implies that we built aforementioned data analysis workflow in the context of an explorative experiment. Therefore we did not take advantage of any “fixed point” in our samples for validation. Instead we performed two empirical checks of the correctness of this methodology by considering both the quality of the consensus features identified (see below) and the application of the entire workflow on a simple benchmark experiment. After Feature Finder identified features in each of the samples to be compared, features were mapped (i.e. identified by means of MS/MS data association) and linked among M2 and M2T sample: the result of feature linking is the so called *consensus feature map*. So consensus features are those features contextualized in the linked map and possibly used for subsequent quantification. We then evaluated the distance in terms of m/z and Rt values of

identified consensus features with respect to the constituent mapped features Fig. 4.i.

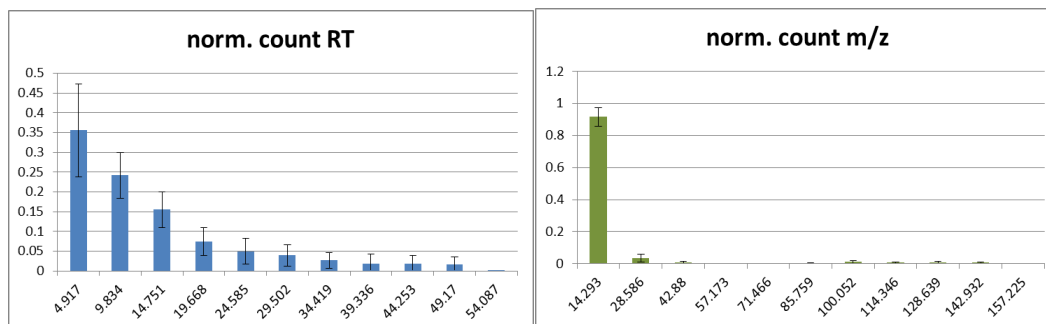


Fig. 4.i Consensus feature alignment

Rt distance in seconds (left) and m/z distance in mTh (right) of consensus feature with respect to constituent mapped features are grouped into categories and plotted against the number of events (consensus feature) into each category. Hyperbolic trend of both plots confirm that mapped features are well aligned and that their distance with respect to consensus features used for quantification in terms of Rt and m/z is between 5 sec and 0.014 Da.

In order to evaluate the reliability of our quantification workflow it was also applied to a benchmark dataset obtained from a mixture of 13 proteins in known quantity. Similarly to our experimental framework benchmark dataset encompassed multiple biological and technical replicates: 3 pairs of samples to compare (biological replicates) and each of them was measured 3 times (technical replicates). We managed to correctly evaluate the under/over expression of 13/13 benchmark proteins and for 5/13 real values were within estimated interquartile distance. We also identified 6 “false positives” comprising Trypsin which was present indeed. Results of benchmark dataset analysis are reported into Fig. 4.1.

4.1.2.4 Decision-making criteria

The final output of OpenMS workflow provides quantitation ratios for peptides and proteins in the sample based on features intensity. Further processing was then required to compute the median values among technical replicates for each biological replicate and to compute median among biological replicates as well. Finally we needed to align such ratios and count them applying a criterion to filter the proteins. The last step was then to rank obtained results.

First of all we checked instrumental variability by comparing measured peptide intensity ratios among technical replicates Fig. 4.m. Based on estimated instrumental variability we then choose to set threshold for under/over represented proteins at $\pm 40\%$. Based on such threshold we were able to reliably quantify out of 331 identified proteins: 17 proteins over expressed into M2T over M2 samples and 29 under expressed proteins with respect to the same ratio. Other 45 proteins resulted otherwise not differential between M2T over M2 sample.

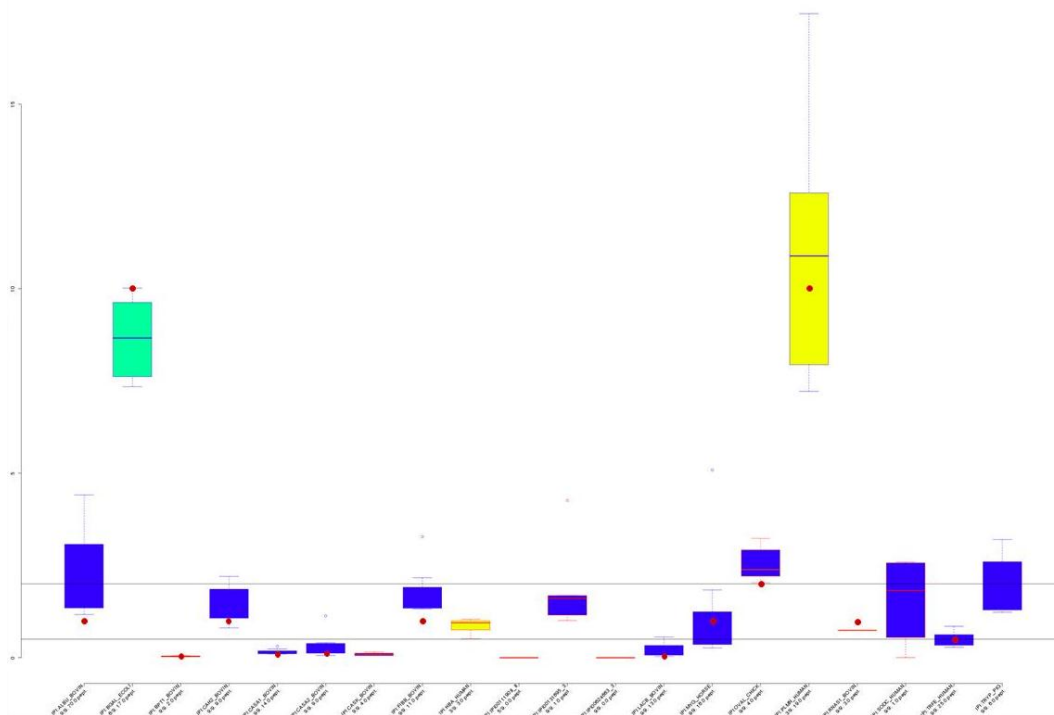


Fig. 4.1 Analysis of benchmark dataset

The boxplot reports actual and measured quantitative ratios for proteins in the benchmark dataset. Horizontal lines represent the threshold of under/over expression (we considered at least $\pm 50\%$ variation) and the boxes represent the interquartile estimates for the proteins. Red dots are the true quantities which lie often within measured values boxes. 13/13 proteins boxes obtained with our analytical workflow are good estimate of real under/over expression. Protein mix has been obtained from the work of Jaffe et al. [Jaffe et al., 2006] and is made of two samples (α and β) containing different quantities of the same proteins. Values estimated by our analytical workflow (boxes in the plot) are given as $\beta:\alpha$ ratios. Proteins and respective $\alpha:\beta$ ratio are: BPT1_BOVIN = 100:5; RNAS1_BOVIN = 100:100; MYG_HORSE = 100:100; LACB_BOVIN = 50:1; CASA2_BOVIN = 100:10; CASA1_BOVIN = 100:10; CAH2_BOVIN = 100:100; OVAL_CHICK = 5:10; FIBB_BOVIN = 25:25; ALBU_BOVIN = 10:200; TRFE_HUMAN = 2.5:5; BGAL_ECOLI = 1:10. We also correctly identified trypsin used for sample digestion, which correctly resulted non-differential among the two samples.

Nevertheless once we obtained aforementioned lists of proteins we needed to rank them too in order to evaluate the robustness of each result. We then choose to rely on the number of peptides used to identify a protein and on the percentage of biological replicates in which the protein was correctly identified. To combine those two criteria we adopted the harmonic mean function (from now on called “f-measure”) modified with a “step” parameter as reported at § 3.7.4. This was intended to award proteins identified with more than 2 peptides or reproducibly identified in more than half of the biological replicates. Modification of f-measure scoring of the results reported hereafter is plotted for clarity in Fig. 4.n

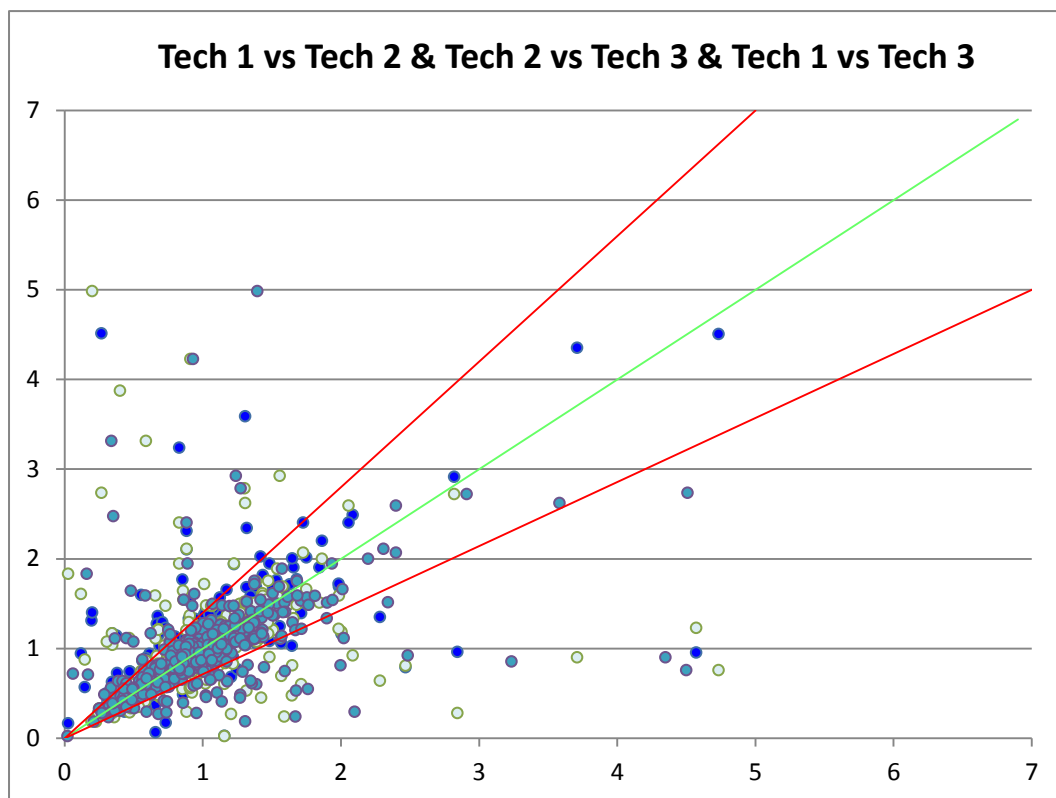


Fig. 4.m Peptides intensity ratios among technical replicates

Scatter plot reports correspondence of measured intensity ratio of identified peptides between couples of technical replicates. Tech 1 vs Tech 2 = dark blue, Tech 2 vs Tech 3 = blue, Tech 2 vs Tech 2 = light blue. Green line indicates ratio = 1 that is to say no instrumental variability at all while red lines represents +/- 40% with respect to measured ratio among technical couples. Between 86 and 90 % of measured peptides lie inside the two red lines and so we choose to set an arbitrary threshold for differentially expressed proteins of at least +/- 40% variability.

Data reported here were obtained from a single biological replicate and are exemplificative of the whole experiment.

4.2 Differences in M2 and M2T redoxome

We fished out of M2T and M2 sample proteins containing reversibly oxidatively modified cysteines and we identified and quantified them. We also determined M2T/M2 quantity ratio for each of those proteins. In this context the term “over-expressed” means that a protein was found as *more oxidized* into M2T with respect to M2 sample. On the other hand “under-expressed” means that a protein was more reduced into M2T with respect to M2 sample. Of course “non-differential” means that we found the same quantity for a specific protein in both samples to be compared. Remaining identified proteins were instead classified as neither under/over-expressed nor non-differential because we detected such variability among biological replicates that we couldn’t give reasonable estimate for their abundance ratio. Identifying and quantifying are indeed actually different tasks to achieve. Nevertheless by this approach we were able to stress some reproducible differences of the oxidation status of relevant proteins into MCF10A

M2T and M2 cell lines. Such differences are also sustained by experimental data on free thiol concentration on both cell lines.

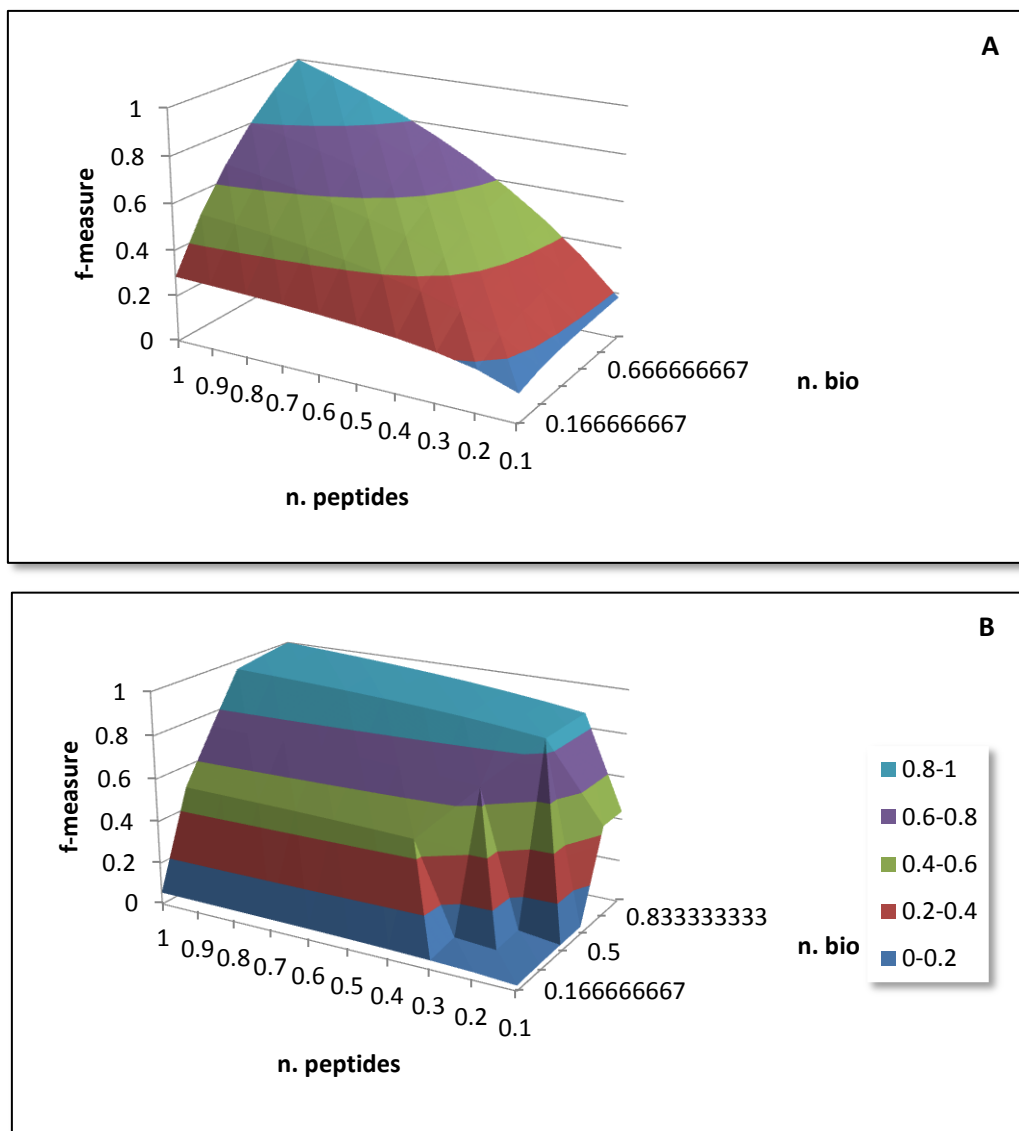


Fig. 4.n Criteria for ranking differentially oxidized protein lists

Surface plot reports trend of a canonical harmonic function (A) and of our modified f-measure (B). Steps are intended to award proteins identified with more than 2 peptides or identified reproducibly into more than 50% of the biological replicates.

4.2.1 Differential protein list

Hereafter are reported tables containing identified and quantified proteins Tab. 4.b/c/d. All “ratio” values are given as means of absolute intensity ratio for each protein over all the considered biological replicates.

Tab. 4.b Proteins more oxidized into M2T over M2 sample

Description	Ratio	f-measure
Mucin-16	1.8	4.1
Glucose-6-phosphate 1-dehydrogenase	15.2	2.2
S-adenosylmethionine synthase isoform type-2	1.8	0.1
Serine/threonine-protein kinase LMTK3	25.0	0.1
Hemicentin-2	1.8	0.1
Trophinin	1.6	0.1
Uncharacterizedprotein KIAA1109	4.8	0.1
Dyneinheavychain7, axonemal	3.0	0.1
Chondroitinsulfateproteoglycan4	1.6	0.1
Short transient receptorpotential channel 6	1.7	0.1
Usherin	27.4	0.1
Fibrousheath-interactingprotein2	27.4	0.1
Unconventionalmyosin-XV	27.4	0.1
Short transient receptor potential channel 6	27.4	0.1
PHD finger protein3	4.0	0.1
Spermatogenesis-associatedprotein25	5.5	0.1
NudC domain-containingprotein2	27.4	0.1

Tab. 4.c Proteins more reduced into M2T over M2 sample

Description	Ratio	f-measure
Glutathione S-transferase P	0.5	4.3
Peroxiredoxin-1	0.5	4.3
Transcriptionintermediaryfactor 1-beta	0.5	4.2
Heat shock cognate 71 kDa protein	0.6	4.2
GTP-binding nuclear protein Ran	0.5	4.2
Heat shock protein 75 kDa, mitochondrial	0.5	4.1
Probable E3 ubiquitin-proteinligase C12orf51	0.1	4.1
Thioredoxin	0.1	0.1
Low-density lipoprotein receptor-related protein 2	0.5	0.1
Mucin-19	0.3	0.1
Prolow-density lipoprotein receptor-related protein 1	0.5	0.1
E3 ubiquitin-proteinligase HERC2	0.2	0.1
Proteinbassoon	0.1	0.1
Mucin-17	0.3	0.1
Tubulin beta-4B chain	0.5	0.1
ProbableXaa-Pro aminopeptidase3	0.5	0.1
Protein FAM75D1	0.4	0.1
Peroxisome proliferator-activated receptor gamma coactivator-related protein 1	0.4	0.1
Vinculin	0.1	0.1
Probablemethyltransferase TARBP1	0.1	0.1
E3 ubiquitin-proteinligase SHPRH	0.1	0.1
Kinesin-likeprotein KIF16B	0.1	0.1

Erythroid membrane-associated protein	0.1	0.1
Vacuolar protein sorting-associated protein 16 homolog	0.1	0.1
Dynein heavy chain 17, axonemal	0.1	0.1
Protein PRRC2C	0.1	0.1
F-box/LRR-repeat protein 12	0.4	0.1
AMP deaminase 2	0.1	0.1
von Willebrand factor A domain-containing protein 5B2	0.1	0.1

Tab. 4.d Proteins with unchanged oxidative status into M2T over M2 sample

Description	Ratio	f-measure
Keratin, type II cytoskeletal 1	1.1	4.6
Pyruvate kinase isozymes M1/M2	0.9	4.6
Filamin-B	1.1	4.4
Alpha-enolase	0.9	4.4
Oleoyl-[acyl-carrier-protein] hydrolase	0.8	4.4
Filamin-A	1.3	4.3
Glyceraldehyde-3-phosphate dehydrogenase	1.1	4.3
Trypsin	0.8	4.3
T-complex protein 1 subunit theta	0.7	4.3
Transitional endoplasmic reticulum ATPase	1.4	4.2
Heat shock protein HSP 90-alpha	1.0	4.2
T-complex protein 1 subunit eta	1.0	4.2
Keratin, type II cytoskeletal 5	0.9	4.2
LIM and SH3 domain protein 1	0.9	4.2
Formyltetrahydrofolate synthetase	0.8	4.2
T-complex protein 1 subunit zeta	0.8	4.2
Heat shock protein HSP 90-beta	0.7	4.2
Peroxiredoxin-2	0.7	4.2
Protein arginine N-methyltransferase 1	0.9	4.1
40S ribosomal protein S12	0.8	4.1
Hornerin	0.8	4.1
Glycogen phosphorylase, brain form	0.7	4.1
Phosphoribosylglycinamide formyltransferase	0.7	4.1
Elongation factor 2	0.6	4.0
Cellular nucleic acid-binding protein	1.1	3.2
Glucose-6-phosphate isomerase	1.1	3.2
T-complex protein 1 subunit delta	1.0	3.2
Cofilin-1	0.8	3.2
Stress-induced phosphoprotein 1	0.8	3.2
Elongation factor 1-gamma	0.8	3.2
40S ribosomal protein S3	0.8	3.2
T-complex protein 1 subunit alpha	0.6	3.0
Profilin-1	0.6	3.0
Deoxyuridine 5'-triphosphate nucleotidohydrolase, mitochondrial	1.2	0.1
Ryanodine receptor 3	1.1	0.1

T-complex protein 1 subunit beta	1.0	0.1
Nucleophosmin	1.0	0.1
Voltage-dependent L-type calcium channel subunit alpha-1C	0.9	0.1
Isocitrate dehydrogenase [NADP] cytoplasmic	0.9	0.1
Toll-like receptor 9	0.9	0.1
FH1/FH2 domain-containing protein 1	0.9	0.1
Proliferating cell nuclear antigen	0.8	0.1
Carbonyl reductase [NADPH] 1	0.8	0.1
26S proteasome regulatory subunit 4	0.8	0.1
Cysteine and glycine-rich protein 1	0.7	0.1

4.2.2 Differential proteins characterization

Given the limited number of differentially oxidized proteins we identified it has been impossible to apply significant function enrichment analysis. So we manually retrieved function information from the Uniprot protein-databank for each protein: this way we were able to cluster some of them into functional groups. Among redox sensitive unchanged proteins Transitional endoplasmic reticulum ATPase (valosin containing protein, VCP), Heat shock protein HSP 90-alpha, Stress-induced-phosphoprotein 1, Heat shock protein HSP 90-beta, Heat shock cognate 71 kDa and six subunits of the T-complex protein 1 belong to the unfolded-protein response branch of the Nrf2/Keap1 pathway, while Glucose-6-phosphate isomerase, Glyceraldehyde-3-phosphate dehydrogenase, Isocitrate dehydrogenase [NADP cytoplasmic], Alpha-nolase and Pyruvate kinase isozymes M1/M2 share their role into cellular energy metabolism (both glycolysis and citric-acid cycle). Among proteins more reduced into M2T in respect to M2 cells we then have: Peroxiredoxin-1, Glutathione S-transferase P and Thioredoxin which belong to the antioxidant response branch of the same Nrf2/Keap1 pathway; while GTP-binding nuclear protein Ran, Tubulin beta-4B chain, Vinculin, Kinesin-like protein KIF16B, Vacuolar protein sorting-associated protein 1 and Dynein heavy chain 17 axonemal protein share a common role as components of the cytoskeleton and movement proteins. Another group of proteins more reduced into M2T in respect to M2 cells is that encompassing three members of the ubiquitination complex: F-box/LRR-repeat protein 12, E3 ubiquitin-protein ligase SHPRH and the probable E3 ubiquitin-protein ligase HECTD4. Finally, among proteins identified as more oxidized into the more malignant M2T cells in respect to their M2 counterpart, we were able to group up Usherin, Mucin-16, Chondroitin sulphate proteoglycan, Hemicentin and Trophinin as proteins involved at various levels into cellular adhesion and extra-cellular matrix (ECM) interaction. Particular interest was attracted by the pentose phosphate pathway rate limiting enzyme glucose-6-phosphate dehydrogenase, the main source of reducing equivalents in the form of NADPH (see after herein).

4.2.3 “Totally reduced” controls

Since our approach is aimed at the quantification of oxidatively modified proteins in the samples to be compared (M2 and M2T), the methodology we developed relies on the enrichment of those proteins bearing EZ-Link HPDP biotin label that is to say proteins bearing cysteine-residues with reversibly oxidized thiol groups in the original sample.

Protein	Standard approach ratio	Fully reduced control ratio
sp P11413 G6PD_HUMAN	↑ 15,2	↑ 1,9
sp Q8WXI7 MUC16_HUMAN	↑ 1,8	● 0,6
sp P31153 METK2_HUMAN	↑ 1,8	↑ 2,8
sp Q8NDA2 HMCN2_HUMAN	↑ 1,8	● 0,9
sp P21333 FLNA_HUMAN	● 1,3	↑ 1,7
sp O75369 FLNB_HUMAN	● 1,1	● 0,7
sp P04406 G3P_HUMAN	● 1,1	● 1,2
sp P07900 HS90A_HUMAN	● 1,0	● 0,8
sp P06748 NPM_HUMAN	● 1,0	● 0,9
sp P06733 ENOA_HUMAN	● 0,9	↑ 1,7
sp P14618 KP YM_HUMAN	● 0,9	● 1,4
sp P49327 FAS_HUMAN	● 0,8	● 1,2
sp P23528 COF1_HUMAN	● 0,8	● 0,9
sp P62191 PRS4_HUMAN	● 0,8	● 0,8
sp P11586 C1TC_HUMAN	● 0,8	● 1,3
sp P31948 STIP1_HUMAN	● 0,8	● 1,0
sp P26641 EF1G_HUMAN	● 0,8	● 0,8
sp P40227 TCPZ_HUMAN	● 0,8	● 0,7
sp P23396 RS3_HUMAN	● 0,8	↓ 0,6
sp P11216 PYGB_HUMAN	● 0,7	● 0,6
sp P22102 PUR2_HUMAN	● 0,7	● 0,8
sp P08238 HS90B_HUMAN	● 0,7	● 0,7
sp P32119 PRDX2_HUMAN	● 0,7	● 0,6
sp P50990 TCPQ_HUMAN	● 0,7	● 0,9
sp P11142 HSP7C_HUMAN	● 0,6	● 0,9
sp P17987 TCPA_HUMAN	● 0,6	↓ 0,4
sp P13639 EF2_HUMAN	↓ 0,6	● 0,8
sp Q06830 PRDX1_HUMAN	↓ 0,5	● 0,9
sp P62826 RAN_HUMAN	↓ 0,5	● 0,9
sp Q13263 TIF1B_HUMAN	↓ 0,5	● 1,1
sp P09211 GSTP1_HUMAN	↓ 0,5	↓ 0,6
sp P68371 TBB4B_HUMAN	↓ 0,5	↑ 2,0
sp P10599 THIO_HUMAN	↓ 0,1	● 0,8

Tab. 4.e

Proteins ratio into M2T over M2 sample for the extracted oxidized protein form (Standard approach) and for the total protein content (Fully reduced control).

Thus, in order to extend the quantification approach to both the initially reduced *and* oxidized forms of specific proteins in both samples (M2 and M2T), for three biological replicates we tried parallel experiments in which both samples have not been treated with NEM (i.e. no free thiol blocking), but, directly reduced and labelled with EZ-Link HPDP biotin. This approach was aimed at quantifying ideally all the accessible-cysteine-containing proteins in the sample in order to give some information on total protein quantity for those proteins already being quantified in respect to their redox status.

It has not been possible to obtain information for all of the proteins reported at § 4.2.1, mainly because in the “totally reduced” controls the sample contains much more proteins than in the standard approach so that protein-protein interactions may have partially altered sample behaviour during purification and because data in this case are gathered from only three biological replicates in respect to the full six experiments set of the standard approach. Anyway preliminary results from this approach are reported in Tab. 4.e.

4.2.4 Mapping of specific modifications

The issue of quantifying oxidized proteins in a complex sample and to precisely map the amino-acidic residues involved into such modification are usually two different tasks and different approaches are required to pursue them. Indeed mapping of specific modifications along protein sequence requires a complex and not computer-assisted analysis of thousands of mass data from MS/MS spectra: moreover such analysis often requires highly purified and abundant sample in order to get better results. Nevertheless, in our experimental approach, the use of different labels in sequence made us able to distinguish cysteine-residue thiols which were in the reduced or oxidized status in the original sample: thus by considering Cys residue monoisotopic mass (103.00919) and possible delta-mass for this residue from NEM-adduct (+125.047679) or IAM-adduct (+57.021464) we could highlight formerly reduced or oxidized Cysteine residues in identified proteins. Of course the “ideal” situation would require considering the possible concomitant presence of other modifications on different residues along Cys-containing identified peptides, like Methionine or Proline oxidation, NEM hydrolysis products, and many others. But it is not so feasible to simultaneously search thousands of fragmentation mass data in a combinatorial manner for multiple modifications since this would both incredibly raise the computational load and lower the statistical significance of matched values. Thus we choose to limit the number of considered modifications to those introduced by us (NEM/IAM) plus the known and frequent oxidation of methionine (reference to www.unimod.org: accession #108, #4 and #35 specificity definition 8). Moreover we pursued an approach in which a complex sample has been digested without pre-emptive denaturation, thus it is understandable that we could not reach extensive modification coverage for all of the identified proteins.

Mapped modifications for the enzyme glucose-6-phosphate dehydrogenase are reported as an example in Tab. 4.f. We also identified oxidized cysteine-residues (C₂₂₁₁₄ and C₂₂₁₁₇) in the big protein Mucin-16 and mapped them next to the small intracellular domain spanning from residue 22118 to residue 22152: the intracellular domain enclose also the C-terminus of MUC16 which is known to be phosphorylated in order to induce proteolytic cleavage and liberation of the extracellular domain. Many reversible oxidations have also been mapped to the extracellular domain of the protein Usherin: C₅₇₂ C₅₇₄ C₅₇₆ C₆₉₄ C₆₉₆ C₇₀₈ C₇₁₅ C₇₁₇ C₇₂₆ C₇₂₉ C₈₄₄ C₈₄₇ C₈₄₉ C₁₀₅₀. Usherin is known to contain many laminin EGF-like domains in this region, required for interaction with collagen IV and fibronectin (information have been retrieved from protein database Uniprot a www.uniprot.org).

Tab. 4.f Sequence of glucose-6-phosphate dehydrogenase is reported in (A): peptides identified by MS/MS are reported in red and two peptides containing cysteine-residues with thiol group oxidized in M2T sample are highlighted in yellow. Table with all identified peptides, retention time (Rt) in seconds, mass to charge ratio (m/z) and charges (z) characteristics is reported in (B).

(A)

MAEQVALSRT QV**C**GILREEL FQGDAFHQSD THIFIIMGAS GDLAKKKIYP TIWWLFRDGL
 LPENTFIVGY ARSRLTVADI RKQSEPFKA TPEEK**L**KLED FFARNSYVAG QYDDAASYQR
 LNSHMNALHL GSQANRLFYL ALPPTVY**E**AV TKNIHES**C**MS QIGWNR**I**IVE KPFGRLQSS
 DRLSNHIS**S**L FREDQIYRID HYL**G**KEMVQ**N** LMVLR**F**ANRI FGPIWNR**D**NI ACVIL**T**FK**E**P
 FGTEGRGGYF DEF**G**IIRDVM QNHLLQ**M**LCL VAMEKPASTN SDDVRDEKVK VLK**C**ISEVQA
 NN**V**VLGQYVG NPDGEGEATK GY**L**DDPTVPR GSTTATFAAV VLYVENERWD GVPFILR**C**GK
 ALNERKAEVR LQ**F**H**D**VAGDI FH**Q**Q**C**KRNEL VIRVQPNEAV YTKMMTK**K**PG MFFN**P**EESEL
 DLTYGNRYKN VK**L**PDAYERL IL**D**V**F**CGSQM HFVRSDELRE AWRIFTPLH QIELEKPKPI
 PYYIGSR**G**PT EA**D**ELMKRVG FQYEGTYKWV NPHKL

(B)

Peptide	Rt	m/z	Z
LQFHVDVAGDIFHQQC(Carbamidomethyl)K	1994,52	486,488	4
LKLEDFAR	2294,46	380,211	3
KPGMFFNPEESELDTYGNR	2286,24	782,036	3
GYLDDPTVPR	1602,36	566,787	2
DNIAC(Carbamidomethyl)VILTFK	2679,6	647,344	2
LFYLALPPTVYEA V TK	2977,02	913,012	2
DGLLPENTFIVGYAR	2412,9	832,939	2
(Acetyl)AEQVALSR	1697,82	458,246	2
GGYFDEFGIIR	2467,8	637,316	2
LPDAYER	1223,4	432,217	2
VQPNEAVYTK	1440,6	574,8	2
GPTEADELMK	1421,88	545,76	2
LSNHISLFR	1869,42	391,884	3
EMVQNLMLVLR	2273,88	616,828	2

IIVEKPFGR	1559,04	529,823	2
QSEPFCK	1595,7	441,722	2
KRNELVIRVQPN	2654,58	367,222	4
LNSHMNALHLGSQANR	1436,28	441,476	4

4.3 Redox environment of M2 and M2T cell lines

Beside the quantification of differentially modified proteins we also measured the global redox environment of M2 and M2T sample: DTNB assay on total lysate samples allow to measure *total* SH content, that is to say free thiol-groups from both proteins and soluble molecules like glutathione. Reduced thiol content has been measured on six independent samples set obtaining 212.38 ± 9.38 nmol [SH]/mGr [proteins] and 232.21 ± 10.21 nmol [SH]/mGr [proteins] respectively for M2 and M2T total thiol content. Similarly we obtained 106.56 ± 13.78 nmol [SH]/mGr [proteins] and 138.42 ± 13.41 nmol [SH]/mGr [proteins] respectively for M2 and M2T protein-thiol content. Those data describe a redox environment slightly more reduced into the more malignant M2T cell line in respect to M2 counterpart (Fig. 4.o).

4.4 G6PDH activity

After identification of glucose-6-phosphate dehydrogenase between the group of proteins more oxidized into M2T over M2 cells and given its known role as main intracellular source of reducing equivalents in the form of NADPH, we evaluated its enzymatic activity in our samples (Fig. 4.p). Mean specific activity for M2 is 126.13 ± 23.79 and M2T mean specific activity is 352.27 ± 83.13 . So a near three-fold difference is appreciable in favour of the more malignant cells. Anyway specific activity doesn't tells us if the enzyme is more active or just more expressed into M2T cells, but looking at both "totally reduced controls" (§ 4.2.3) and western blot results hereafter (§ 4.4.2) it is reasonable to consider that there is a contribution to the higher activity from both oxidized status *and* enzyme abundance.

4.4.1 G6PDH activity is affected by redox status

Since we found a ratio (M2T/M2) for oxidized G6PDH highly favourable to M2T cells and a corresponding higher activity in the same cells, we tested the effect of reduction on enzymatic activity (Fig. 4.q): at a concentration of 1mM DTT is able to reduce G6PDH specific activity to nearly 50-60% of the original activity in both M2 and M2T samples.

Moreover, to evaluate if this inhibitory effect was due to reversible reduction of protein thiol groups switching from oxidized to reduced status, we reduced the enzyme with 1mM DTT and then removed the reducing agent before measuring

activity: G6PDH activity was restored to nearly 65-70% of its original value. So it turns out that keeping G6PDH reduced lower its activity more than reducing the enzyme and leaving it without reducing agent (less than 3 minutes). This could mean that involved thiol groups are quite reactive and re-oxidize very fast, so good candidates as redox switches (Fig. 4.r).

Finally, given the above hypothesis, we also reduced the enzyme and blocked it with 1mM NEM right after reduction. Measured activity in this case drops to as low as 25-30% of original activity, despite DTT and NEM removal from the sample. Clearly this is suggestive of the fact that preventing the re-oxidation of specific cysteine residues in G6PDH decreases enzymatic activity (Fig. 4.r).

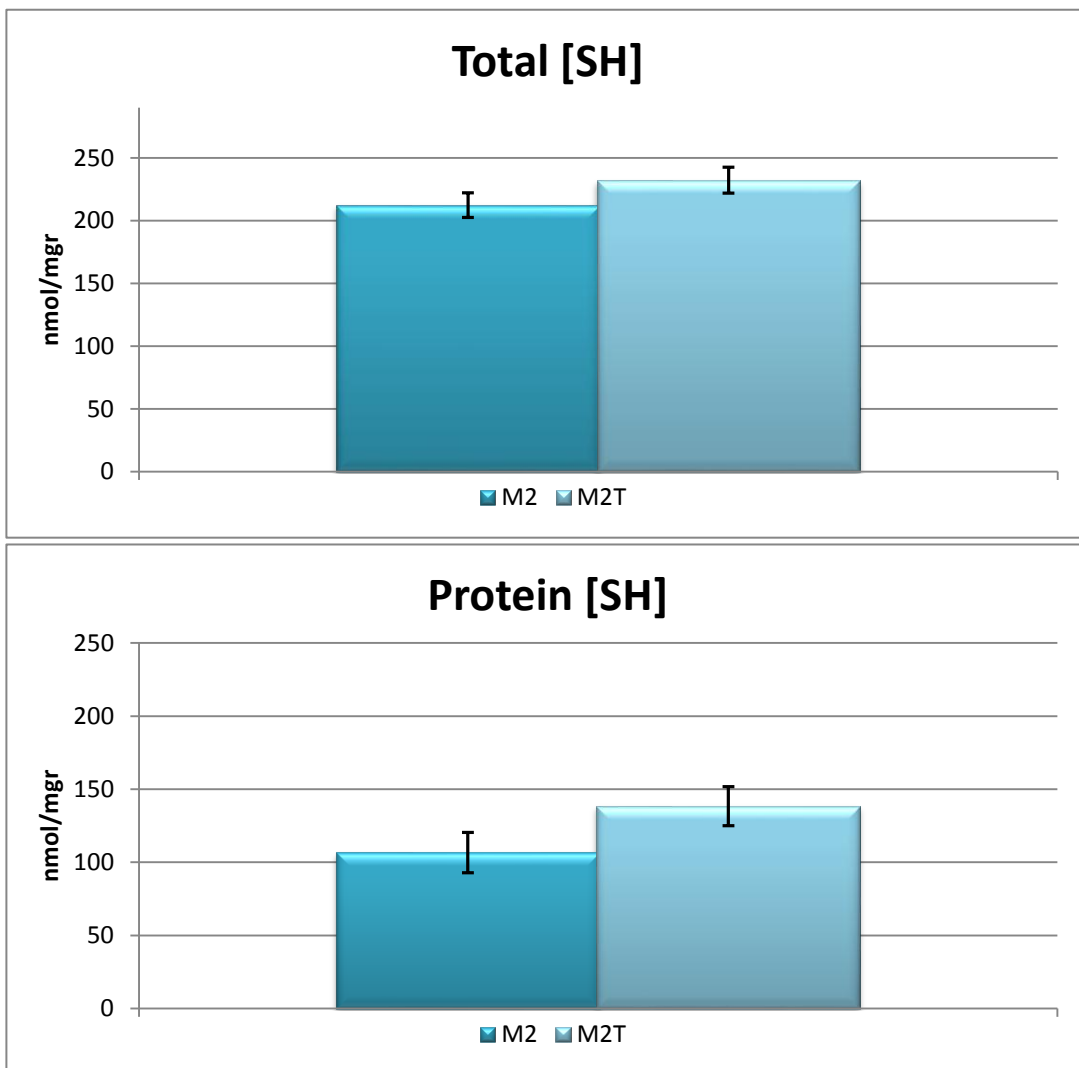


Fig. 4.o Soluble and protein free thiol content of M2T and M2 cells

Histograms summarizing measured total (protein + soluble): upper plot and protein: lower plot, thiol content of cellular lysates from M2 and M2T samples. Observed difference is more marked looking at the protein-thiol content and even if not so big it stresses a slightly more reduced intracellular environment for the more malignant M2T cell line.

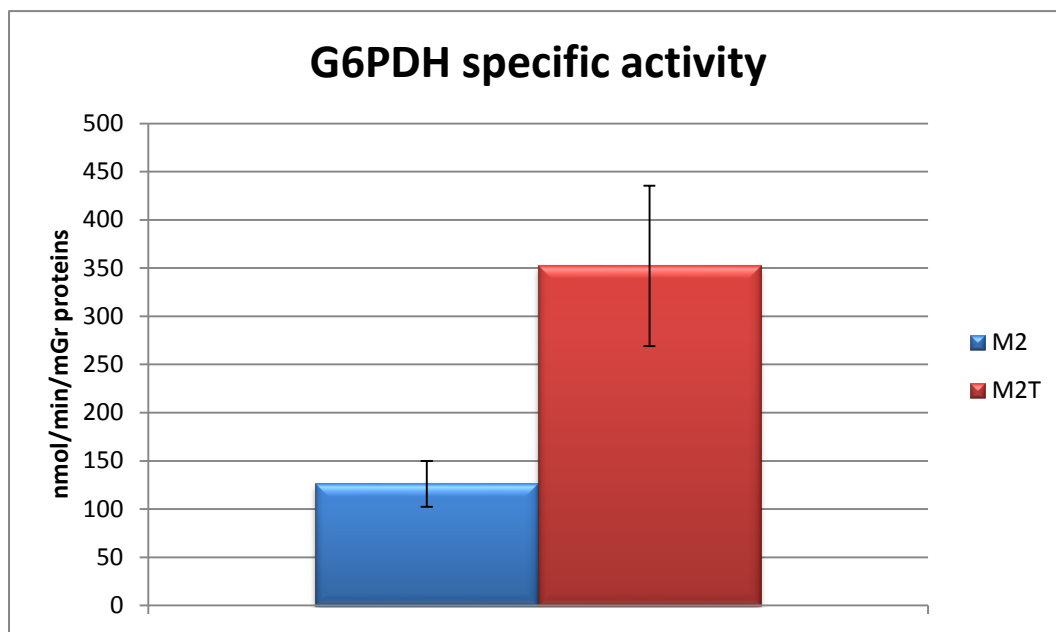


Fig. 4.p G6PDH enzymatic activity

Histograms summarize four independent measurements of G6PDH activity performed as reported in material and methods. It is noticeable a near three-fold greater specific activity of the enzyme in the more malignant M2T cells. M2 mean specific activity = 126.13 ± 23.79 nmol/min/mGr; M2T mean specific activity = 352.27 ± 83.13 nmol/min/mGr.

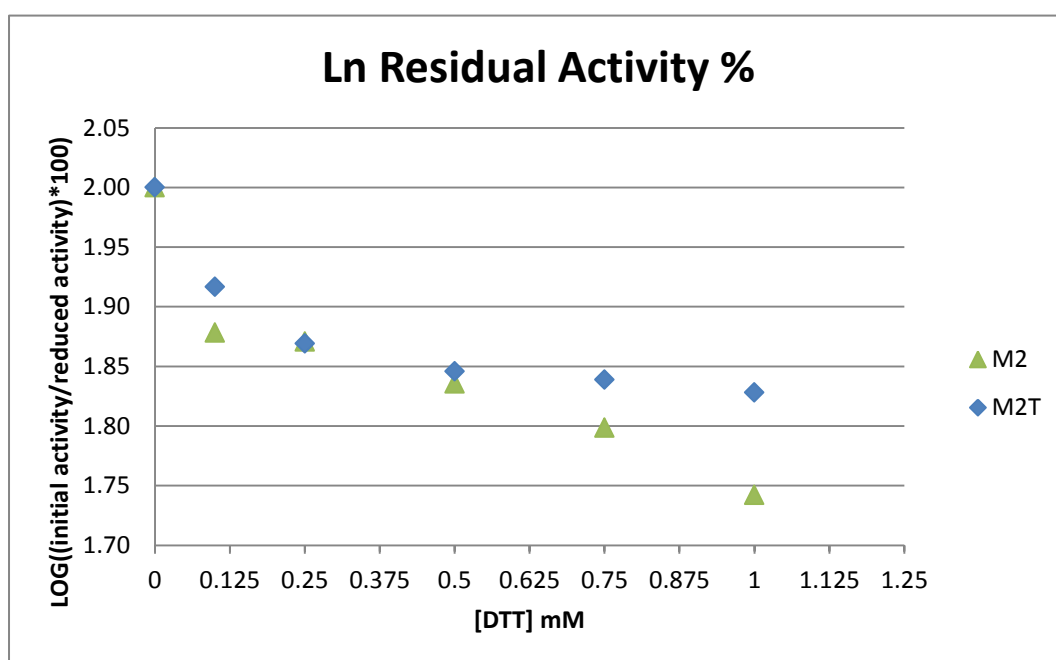


Fig. 4.q G6PDH enzymatic activity: decrease with DTT

Inhibitory effect of DTT on G6PDH activity. The effect of reduction is immediate, starting at 100 μ M DTT and the maximum effect is reached at 1 mM DTT. At this concentration activity is reduced to 55% and 67% of original activity respectively in M2 and M2T samples.

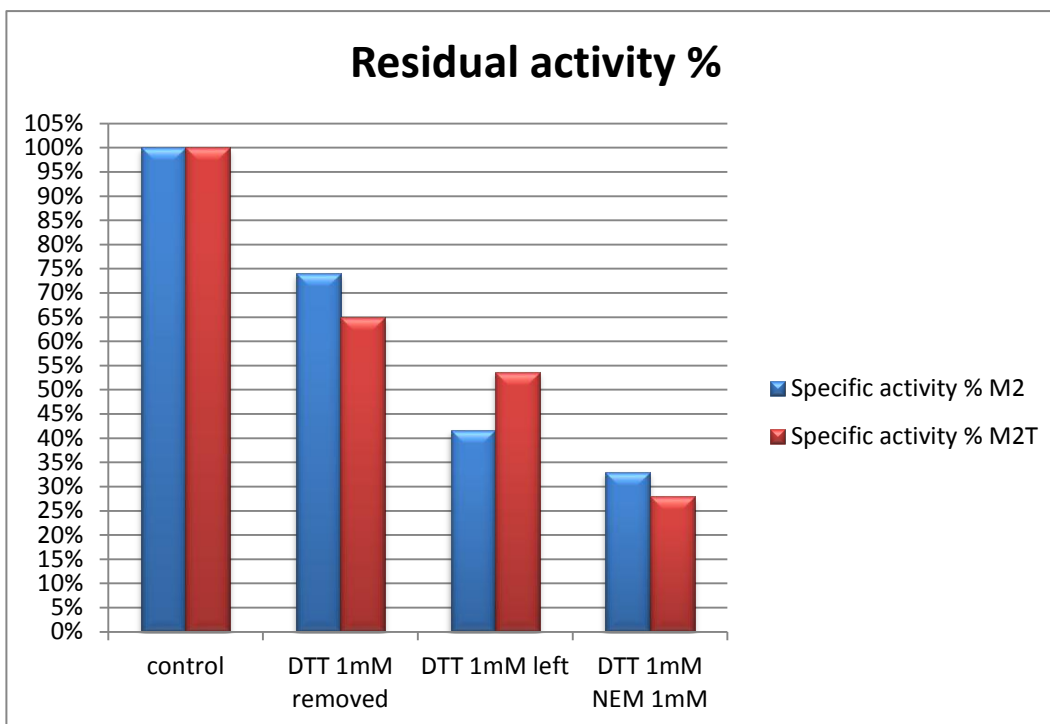


Fig. 4.r G6PDH enzymatic activity: decrease with DTT and NEM

Histograms summarize the effects of inhibition with 1mM DTT on G6PDH activity. All specific activities have been normalized to their own *starting* activity as percent values (M2 = 87.43 nmol/min/mGr proteins and M2T = 285.70 nmol/min/mGr proteins). In “DTT 1mM removed” the reducing agent has been removed immediately before measuring activity giving 74% and 65% residual activity respectively for M2 and M2T. In “DTT 1mM left” the sample has been kept reduced throughout the test, giving 42% and 54% residual activity for M2 and M2T samples respectively. Finally, in “DTT 1mM NEM 1mM” samples have been blocked with NEM right after reduction with DTT and after removal of residual DTT and NEM activity assay demonstrated as low as 33% and 28% residual activity for M2 and M2T samples respectively.

4.4.2 G6PDH reduced and oxidized forms

Given the observations on the different degree of oxidized G6PDH between M2T and M2 samples and the effect of reduction and reduction/alkylation on enzymatic activity, we then evaluated the presence of different forms of the enzyme by means of western blot in reducing and non-reducing conditions (Fig. 4.s).

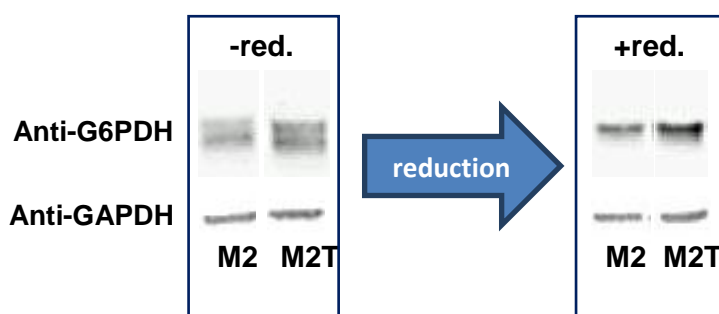


Fig. 4.s G6PDH oxidized/reduced isoforms

20 µg of total proteins from M2 and M2T cells lysates have been separated at constant current into 4 – 12 % SDS-PAGE and electro-blotted overnight at constant current. G6PDH rabbit polyclonal antibody has been used as primary antibody and anti-rabbit IgG horse-radish peroxidase conjugated secondary antibody has been used for detection with luminol. Same procedure was followed for the loading-control by using anti-GAPDH primary antibody. It is noticeable how reduction determine the collapse of lower MW G6PDH band observable into the left box (- red) into only one upper MW band (+ red, right box) for both M2 and M2T sample. This is suggestive of the presence of different oxidation-status forms of the enzyme in those cells. Moreover G6PDH band intensity analysis in +red (right box) revealed a ratio of about 1:1.6 for M2:M2T samples, thus confirming the data obtained for “totally reduced” controls (see text). Also GAPDH bands ratio (≈ 1) here confirms data from both differential redox approach (M2T/M2 = 1.1) and “totally reduced” controls (M2T/M2 = 1.2) for the same enzyme (see Tab. 4.d G3P)

Preliminary results point at the presence of at least two different forms of the enzyme, presumably distinguished by the oxidation status of redox-active thiol-disulfide cysteine-residues. Nevertheless it has not yet been possible to separately analyse the two forms by MS, which we are going to do soon.

4.5 Nrf2 pathway gene expression data

Finally, preliminary gene expression results from Prof.Cordenonsi laboratory, confirmed us that genes under the control of Nrf2 are mostly insensible to TAZ. Instead Nrf2 gene itself (NFE2L2) is down-regulated into M2T cells (Tab 4.g). Since it is known that Nrf2/Keap1 pathway could have a role in cancer survival and chemoresistance [Lau et al., 2004; Kim et al., 2008], further experiments are needed to specifically evaluate the activation status of this pathway in this cellular model of breast cancer.

Tab. 4.g – Table of preliminary gene-expression results from Prof.Cordenonsi laboratory: Nrf2 regulated genes are mostly insensible (black) to regulation by TAZ. Up (red) and down (blue) regulated genes are instead quite spread among both antioxidant and detoxification branches of the pathway. So it is not yet clear whether Nrf2 pathway is activated or not into M2T (active-TAZ expressing) cells, but NFE2L2 gene itself (bright yellow), which is the one coding for the Nrf2 protein, appears to be down-regulated into M2T cells. All genes are obtained through NCBI Gene bank (<http://www.ncbi.nlm.nih.gov/gene>).

Nrf2 controlled genes		
TAZ up-regulated	TAZ down-regulated	TAZ insensible
AOX1	NFE2L2	ABCC1
ATF4	CAT	AKR1B1
DNAJB1	FKBP5	AKR7A2
GSR	GPX2	CBR1
GSTK1	HMOX1	CCT7
	NQO1	CLPP
		EPHX1
		ERP29
		FMO1
		FOLH1

		FOLH1B FTH1 FTL GCLC HERPUD1 HIP2 HSP90AA1 HSPB8 HSPB8 PIIB PIIG PRDX1 PTPLAD1 SCARB1 SH2B1 SLC35A2 SOD1 SQSTM1 STIP1 TXN TXNRD1 UBB USP14 VCP
--	--	---

5. DISCUSSION

5.1 Redox proteomics: a technical challenge

Modification of cysteine residues has emerged as a significant mechanism for alteration of the structure and function of many proteins: indeed a broad range of reactions that occur to the protein cysteine thiol groups plays key signalling roles in a range of physiological and pathological processes (see chapter 1 for some examples). Additionally, some of these cysteine modifications are reversible through thioredoxin and glutathione systems [Bindoli et al., 2008]. Reversible thiol modifications include glutathionylation, mixed disulfide formation with low molecular weight thiols, sulfenic acid formation, S-nitrosation/nitrosylation, S-acylation, sulfenylamide formation and the generation of intra/inter-protein disulfides [Chouchani et al., 2011 and references therein]. Moreover, proteins affected by such modifications in a signalling context are reasonably only a small fraction of the whole cellular proteome, thus rising concentration dynamic-range issues.

During the last decade technological development bolstered the efforts in the field of redox proteomics, that is to say, in the search for reliable methods to identify both the proteins and residues affected by redox modifications, to determine the nature of the modification to the cysteine residue and to quantify the extent of the modification during redox signalling.

5.1.1 General strategies to screen for protein thiol modifications

Many thiol modifications on cysteine residues are relatively labile and thiols themselves are prone to artifactual modification during protein isolation and handling. Therefore an essential prerequisite for reliable screening for protein thiol modifications in biological samples is the efficient trapping of the native redox status of the thiol proteome. There are three general approaches used for the labelling of cysteine residues for proteomic studies (Fig. 5.a).

Loss of selective labelling due to thiol modification

Protein thiols are alkylated with a thiol specific probe that contains a reporting group that enables the labelled thiols to be detected: the loss of this signal is assessed as an indication of protein thiol modification. Control labelled protein samples can be separated by electrophoresis, or derived peptides are separated by LC-MS, and compared with related samples prepared under stressed or oxidant conditions: probe signal loss between conditions is indicative of both reversibly and irreversibly modified protein thiols [Chouchani et al., 2011]. This is a simple but limited strategy relying on measuring signal loss, instead of signal increase

over baseline and a significant limitation to the sensitivity of this approach came from the fact that most intracellular protein thiols are maintained in a reduced status by glutathione and thioredoxin systems. Nevertheless, this method can be adapted to detect only irreversible protein thiol modifications by the treatment of samples with a thiol-reductant before labelling: in this case any signal loss would be attributable to irreversibly oxidized thiols.

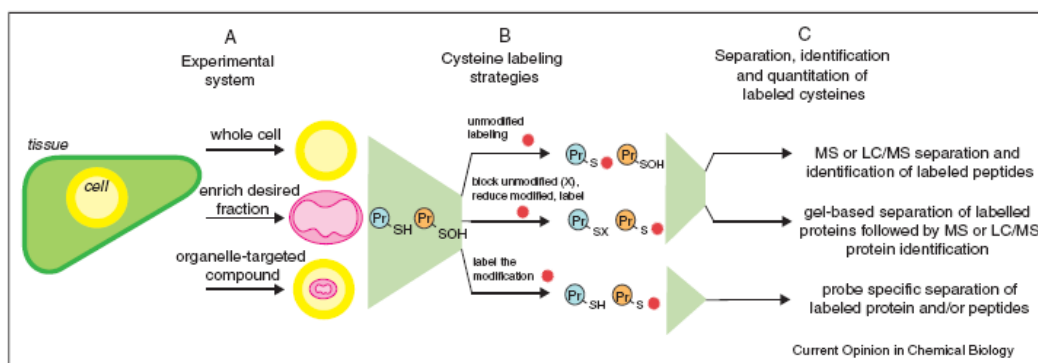


Fig. 5.a General strategies to screen for protein thiol modifications

General strategies for the identification of redox active cysteine residues. (a) The proteome can be assessed from the entire cell, or a particular subcellular fraction enriched before cysteine labeling. Alternatively, organelle-targeted compounds can be used to elicit an organelle specific effect. (b) Three general strategies are employed for the labeling of redox active cysteines (orange protein thiol): (Top) Unmodified cysteine residues are labeled with a detectable probe (red probe) while modified cysteines are not labeled. The decrease of labeling indicates the extent of modification. (Middle) To label reversibly modified cysteine residues, all unmodified cysteines are first blocked by reaction with a thiol reagent such as NEM. Then reversibly modified cysteines are selectively reduced and labeled with a detectable probe (red probe). (Bottom) To label a particular type of cysteine modification, such as a sulfenic acid, a chemoselective probe that reacts only with the modified cysteine is used (red probe). (c) Subsequent separation and identification of the proteins containing selectively labeled cysteine residues. (Top) LC/MS or LC/MS/MS methods to separate and identify labeled peptides. (Middle) Gel-based separation of proteins, often followed by LC/MS or LC/MS/MS methods to separate and identify labeled peptides. (Bottom) Methods to detect a chemo-specific probe. [From Chouchani et al., 2011]

Selective reduction of reversible protein thiol modifications

By this strategy, all unmodified thiols are derivatized with a thiol reagent such as NEM. This is followed by the selective reduction and labelling of all reversibly modified cysteine residues with a thiol probe: all redox-sensitive cysteine residues will be labelled and screened for, regardless of the nature of the reversible modification. Anyway, given the considerable interest in differentiating between different types of reversible cysteine modifications, some variations of this approach have been developed over time: the main differences in redox-modifications “selection” rely on the reduction step, right after blocking of natively unmodified thiols. As an example, the strategy for identification of S-nitrosated protein thiols involves the selective reduction of protein S-nitrosothiols

using either ascorbate or the combination of ascorbate and copper (II). Hogg group has demonstrated that the selective reduction of S-nitrosated proteins is best accomplished using a combination of ascorbate at low concentrations and copper (II) [Kettenhofen et al., 2008]. Vicinal dithiols, which are likely to form intra-protein disulfides because of their proximity, can be identified on the basis of a selective labelling and reduction strategy based on the use of the dithiol-specific reagent phenylarsine oxide (PAO) and NEM for differential blocking, followed by reduction by means of the PAO-specific reducing agent 2,3-dimercaptopropanesulfonic acid (DMPS) and final labelling with another alkylating probe. Similarly Lind et al. [Lind et al., 2002] used a mutant glutaredoxin from *E. coli* to selectively reduce glutathionylated proteins.

Selective reaction of particular protein thiol modifications

Although aforementioned methods make use of specific reduction of the cysteine modification of interest, others employ probes that react specifically with a particular modification thereby circumventing the requirement for reduction step. A number of examples are available for the identification of sulfenic acids using chemo-selective probes based on derivatives of 5,5-dimethyl-1,3-cyclohexadione (dimedone): conjugation of this sulfenic acid-specific probe to different reporter groups (fluorophores or biotin) has then allowed for proteomic screens of these conjugates. Moreover, Leonard et al. developed a membrane permeable propyl azide derivative of dimedone capable of labelling sulfenic acids in cells while allowing for downstream selective coupling with an alkyne or phosphine biotiny tag [Leonard et al., 2009]. Finally, an alternative strategy for the identification of glutathionylated proteins is based on metabolic labelling. Indeed Fratelli et al. metabolically labelled the glutathione pool of T-cells using [35S]-cysteine [Fratelli et al., 2002]. Additional treatment with the protein synthesis inhibitor cycloheximide allowed for labelled cysteine to be incorporated into the glutathione pool. Then [35S]-glutathionylated proteins were separated by two-dimensional electrophoresis and assessed by radio-fluorography. Nevertheless, by this approach proteins glutathionylated *before* labelling cannot be detected [Couchani et al., 2011].

5.1.2 The “biotin-switch” method

The method implemented in this work descends from a variant of the aforementioned selective reduction of reversible protein thiol modifications. In particular we refer to the so called “*biotin switch method*”. This approach basically relies on the selective reduction of DTT-reducible protein thiols following blocking of unmodified thiols with NEM. Labelling of reduced thiols is then achieved by means of HDPD-biotin probe, allowing for affinity purification of derivatized proteins. Adequate description of such methodology could be found

in the works on the yeast *Saccharomyces cerevisiae* redoxome by McDonagh et al. and LeMoan et al. [McDonagh et al., 2010; McDonagh et al., 2009, Le Moan et al., 2005] (Fig. 5.b).

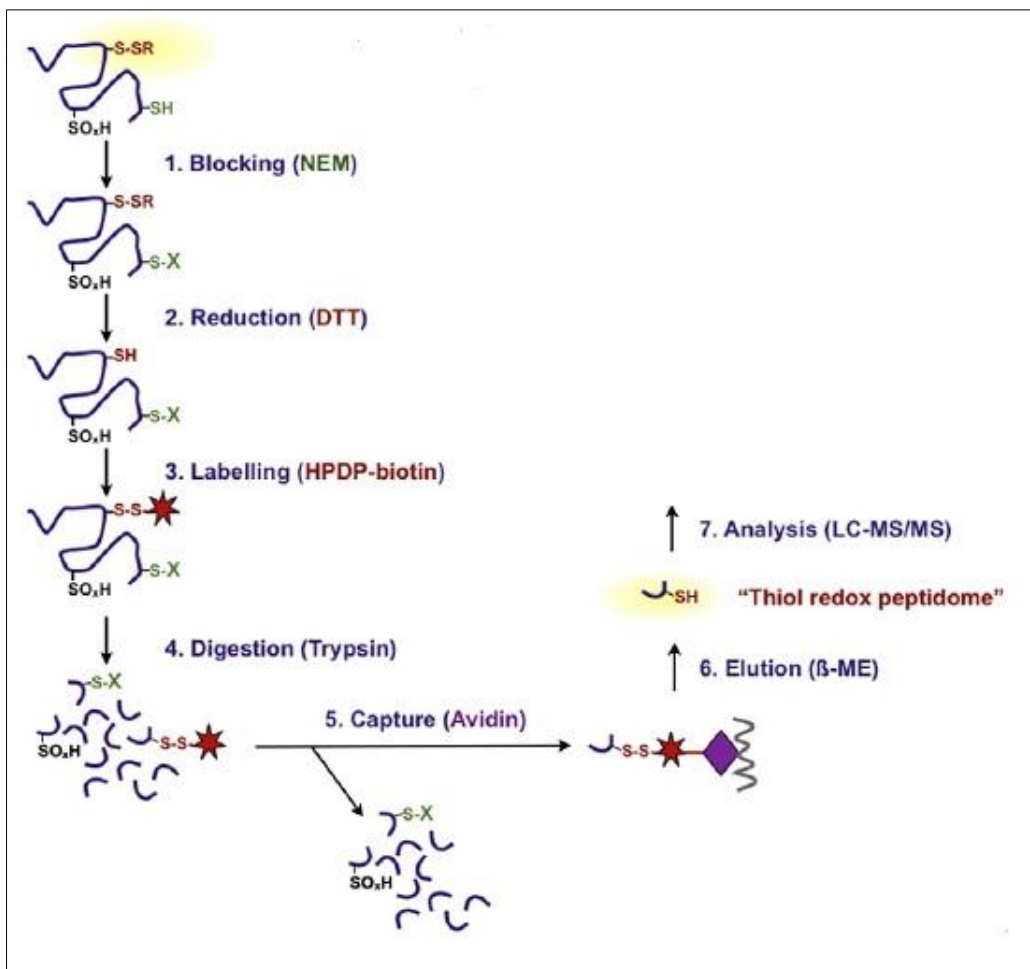


Fig. 5.b Schematic representation of the “biotin-switch” method

Figure is adapted from McDonagh et al. [McDonagh et al., 2011] and summarize the main steps of the biotin-switch method for redox proteome analysis. The crucial difference in respect our method rely on both the affinity chromatography performed on peptides rather than on intact proteins and on the denaturing conditions adopted through the whole procedure.

5.2 Innovative procedure for redox proteomics

In respect to other mentioned “fractional-reduction” / differential-labelling methods reported, our approach shares with the biotin-switch method the advantage of affinity-purification of modified-proteins of interest. Indeed, LC-MS analysis of complex samples would otherwise contain a significant background from non-cysteine and unlabelled cysteine containing proteins. Moreover the chemical labelling adopted here is undoubtedly cost-effective in respect to isotope-based labelling methods.

So the main differences in respect to “traditional” biotin-switch method reside in (1) differential labelling of the proteins is performed in *non-denaturing* conditions and (2) affinity purification by means of HPDP-biotin/Neutravidin interaction is done on intact proteins and not on peptides (i.e. tryptic digestion is performed *after* sample purification) (3) HPDP-labelled thiols are labelled after reductive-elution from neutravidin by means of IAM. Basically the use of non-denaturing conditions should allow for specific reduction of *solvent accessible* oxidized thiols: indeed it is commonly accepted that whether a modification takes place depends on a number of factors including the local environment of the cysteine residue, its proximity to the relevant reactive species, its pK_a , subcellular localization and solvent exposure [Chouchani et al., 2011 and references therein]. Moreover, the choice to purify modified thiols-containing proteins rather than redox-modified peptides is intended to allow further application of MS and MS/MS analysis in order to identify and *quantify* the extent of modification across samples to be compared. Instead the chromatographically less burdensome approach of redox “peptidome” [McDonagh et al., 2011] analysis is not compatible with our choice to implement further label-free computational analysis. Finally, the “double-labelling” step HPDP-IAM on redox-modified thiols proven valuable in order both to avoid further thiols artifactual (re)oxidation and to precisely map modified (IAM-labelled) and unmodified (NEM-labelled) thiols by MS/MS.

Unmodified thiols blocking

The status of protein thiols, as well as that of other redox pairs involved in their equilibrium, may be very different in distinct cellular compartments. Thus it is important to block the thiols status to try to detect the actual status of specific protein thiols, avoiding reactions that could affect them during extraction, either those due to the cross-contamination of different compartments or those involving oxidation due to sample handling (metal catalysed oxidation, contact with ambient air). One way of “freezing” the original status of thiols is by using TCA during the extraction to precipitate the protein samples [Izquierdo-Álvarez et al., 2011], alternatively, the blocking reagent can be added to the lysis buffer. This latter is the way we choose in reason of the required characterization of modified protein-thiols: indeed NEM-modified thiols (+125.047679) can be distinguished from IAM modified (+57.021464) (see above). Among the possible blocking agents, NEM is more efficient than IAM or IAA because it completely blocks free thiols at a lower concentration, in less time and is effective at pH values lower than 8 [Rogers et al., 2006]. Since we performed the lysis of our samples in pH 7.4 buffer, blocking of native-unmodified thiols with a [SH]:[NEM] ratio of 2 for 90' proved to be valuable to protect solvent-accessible free thiols in the sample. Moreover lower pH value and shorter reaction times helped in avoiding NEM reaction with lysine residues. Finally, analysis of NEM-blocked and HPDP treated

samples without pre-emptive DTT reduction shown low false-positive and confirmed effective blocking step (data not shown).

Selective reduction

When indirect or double labelling is performed, oxidised thiols are reduced to free thiols before the second labelling step (with HPDP). Generally two groups of chemical reagents are used for this: reduced thiols, especially DTT, the reaction of which is thermodynamically favoured by the formation of its cyclic intramolecular disulfide bond; and trialkylphosphines (TCEP). Since the presence of both of them in the labelling process impairs the attachment of the second probe to the thiols groups released, we need to remove the reducing agent before performing the labelling reaction with HPDP. This is why we preferred DTT instead of TCEP, despite higher reducing power and broader pH range-action: indeed we assessed the efficacy of reagent removal through desalting columns and TCEP demonstrated to be harder to remove, compromising HPDP further labelling. Thus we optimized DTT concentration by evaluating (by fluorescent-labelling of reduced thiols) the minimal amount (data not shown) and time required to fully reduce NEM-unreacted protein-thiols in the sample. DTT removal by means of buffer exchange was then confirmed with DTNB assay.

Affinity purification

Given the need for subsequent relative-quantification analysis by MS on extracted proteins, we choose to perform neutravidin-biotin HPDP affinity purification on intact proteins rather than on peptides (see above). Moreover we kept non-denaturing conditions throughout the reductive-elution step and subsequent IAM labelling so to avoid misleading reduction and labelling of potentially buried oxidised-thiols, which are not expected to be subject to functional redox switching. Thus elution volumes and time have been carefully evaluated to minimize samples variability: 5 mL along 10' proved sufficient to collect specifically bound proteins. Moreover further analysis confirmed that all proteins identified by this approach bear at least one cysteine residue in their sequence (even though not always the exact IAM-modified cys-containing peptide has been detected by MS/MS analysis – see after herein).

5.2.1 Label-free approach: computational analysis

It is nowadays clear the compelling need in the life sciences for studying of biological entities at the system level. In turn this requires analytical tools capable of identifying the component parts of the system and of measuring their responses to a changing environment. To this aim many classical proteomics quantification methods utilizing dyes, fluorophores, or radioactivity have provided very good

sensitivity, linearity and dynamic range, but they suffer from two important shortcomings: first, they require high-resolution protein separation typically provided by 2D gels, which limits their applicability to abundant and soluble proteins; and second, they do not reveal the identity of the underlying protein [Bantscheff et al., 2007]. Both of these problems are overcome by modern LC-MS/MS techniques and three main methods have been made available to perform quantitative LC-MS analysis: (1) quantification by spectral counting, (2) quantification via differential stable isotopic labelling, and (3) quantification by using the ion current in label-free measurements.

An obvious reason for choosing label-free approach over isotopic labelling is its cost-effectiveness. Among label-free quantification strategies, two widely used and fundamentally different approaches can be outlined: (a) measuring and comparing the mass spectrometric signal intensity of peptide precursor ions belonging to a particular protein and (b) counting and comparing the number of fragment spectra identifying peptides of a given protein. We will name the former “*features quantification*” and the latter “*spectral counting*”. In-depth analysis of both methodologies is beyond the topic of this discussion and exhaustive reviews can be found in Bantscheff and Mueller [Bantscheff et al., 2007, Mueller et al., 2008].

The choice of the features quantification approach

Briefly, the spectral counting approach is based on the empirical observation that the more of a particular protein is present in a sample, the more MS/MS spectra are collected for peptides of that protein. Thus, in contrast to quantification by peptide ion intensities, spectral counting benefits from extensive MS/MS data acquisition across the chromatographic time scale both for protein identification as well as protein quantification. Nevertheless, this represents also an intrinsic limit for this methodology, since the only peptides which will be quantified are the ones selected for fragmentation. Even at the scan rate of 3 spectra/second for MS/MS we adopted, and given the removal of noisy non-cys containing proteins from the sample prior to digestion (see above), spectral counting approach would result in poor sampling for accurate quantification. Indeed, such methodology is often coupled to hardware-burdensome 2D-LC pre-emptive to injection into the mass spectrometer. Moreover, to improve sampling (fragmentation) of lower abundant peptides, we took advantage of MS/MS dynamic exclusion after 2 spectra for 30”, thus increasing the number of peptides and proteins identified. Nevertheless dynamic exclusion violates in principle the random sampling approach required for spectral counting and its impact on quantification is still controversial. Indeed some authors state it is detrimental for accurate quantification [Old et al., 2005] while other show that it can be generally useful [Zhang et al., 2006, Zhang et al., 2009]. Our feature quantification approach does not suffer from the application of dynamic exclusion. In our approach peptide

signals are detected at the MS level and distinguished from chemical noise through their characteristic isotopic pattern. These patterns are then tracked across the retention time dimension and used to reconstruct a chromatographic elution profile of the peptide mass. It is worth to note that in this case the signal area integration within the mass spectrum utilize the sum of the areas of all the isotopomers of a peptide. This methodology despite being harder to implement computationally, is more sensitive and accurate in respect to the use of just the mono-isotopic peak area. The total ion current of the peptide mass, from now on called *feature* is then integrated and used as a quantitative measurement of the original peptide concentration. The extracted features are then mapped across multiple LC-MS measurements using their coordinates on the m/z and R_t dimension. All the workflow has been set-up to a good configurability and automation level based on OpenMS open source tools as reported in chapter 3, and we are looking forward to implement user-friendly graphical interface for larger usability too.

Reproducibility and relative-quantification criteria

Basically, the approach outlined here relies on reproducible LC separation of peptides across samples to be compared and gathering of high resolution MS data in order to generate ($m/z;R_t;intensity$) three dimensional raw maps from which features are extracted, aligned and quantified. Good accuracy of the steps involved is demonstrated in Fig. 4.i, giving < 5 seconds and < 0.014 Da differences among pairwise aligned features across samples to be compared. Multiple search engine of MS/MS data against a protein database enriched with commonly known crap/contaminant proteins and decoy strings is then used to obtain identification data (*peptide-spectrum matches* PSM) for peptides in the sample. False discovery rate and in turn posterior error probability are calculated for each result and used to filter unreliable matches. Peptide identification information are then merged to features intensities (relative-quantitative information) and multiple peptides (three most intense) are used to compute the relative-quantification of a protein in M2T over M2 pairwise comparison. Moreover we took advantage of three technical replicates for each biological replicate and multiply cross-aligned each M2T and M2 run in order to strengthen our data: only peptides reproducibly identified in both or in just one (i.e. presence/absence criteria) of the two samples have been used for quantification. Thus we were able to quantify about 27% of the identified proteins: indeed to identify and quantify a protein is a more complex task to achieve compared to identification only. Despite the fact that missing features (i.e. peptides missing in the quantification process) is a commonly known issue to face with in this kind of approach, we evaluated different missing features-imputation approaches (data not shown) and concluded that this would instead raise the number of false positives. Finally the good linearity of peak-area based quantification for a standard protein digest from 5 to 100 fmoles has been

demonstrated (Fig. 4.e) and good reproducibility of peptides relative-quantification between pairwise samples across technical replicates was demonstrated in the range of $\pm 40\%$ variability (Fig. 4.m). Finally, we put an effort against reduction of systematic and non-systematic variations between experiments by raising the number of biological replicates to five, while it is not uncommon that publications reporting results of proteomic experiments using quantitative MS base conclusions on measurements generated in one or two experiments [Bantscheff et al., 2007]. Higher number of replicates also helped us to relatively-quantify lower abundant peptides: since variation of change determination is a function of signal intensity [Bantscheff et al., 2007], we managed to avoid harsh signal-intensity threshold and rather strengthened measured relative-differences by virtue of their reproducibility. Paragraph 3.7.4 describes the criteria adopted through the procedure, which are in principle simply based on averaging of ratios to aggregate multiple measurements (indeed a criterion extensively applied and accepted in literature [Saito et al., 2007]). We also did not introduced inter-samples intensity normalization at the computational level: indeed after evaluation of different normalization approaches (not reported here) we managed to obtain 100% correct under/over-expression estimates on a benchmark sample (Fig. 4.l) without any data normalization. Moreover we took care of rigorous pre-digestion protein-quantity normalization between samples to be compared.

5.2.2 Limits and improvements of the approach

One of the consciously assumed limitations of this approach is that it cannot distinguish between the specific kinds of reversible oxidation borne by the selected cysteine residues: it could be a disulfide, rather than a glutathionylation, oxidation to sulfenic acid or sulfhydration. Operatively speaking, we catch by this methodology all those modification which can be reverted by DTT treatment. Nevertheless this method could be in principle easily adapted to the study of more or more specific oxidative modification like S-nitrosilation, by means of a different reduction step: for example including a pre-treatment with ascorbate and copper (see above).

Another assumed limit of the procedure we developed is that it does not allow direct evaluation of the oxidized/reduced ratio for a given protein *intra*-samples. This is due to the fact that affinity purification of oxidatively-modified cysteine-containing proteins hampers quantitative evaluation of the total protein content for given specie, which is instead prerogative of more classical MS-based quantitative approaches. Briefly, in a single experiment we are able to state if there is more of the oxidized form of a protein “x” in M2T sample in respect to M2 sample, but we cannot gather information on the total content of protein “x” in each of those samples. Nevertheless this information could be retrieved by different ways. First we developed the so called “totally reduced” control samples (§ 4.2.3) which

allow us to extract all of a specific cys-containing protein from the sample by simply avoiding the first blocking of available thiols with NEM: this provides information on the total protein “x” content independently from its oxidation status. Preliminary western blot (wb) data confirmed the results of this approach for glucose-6-phosphate dehydrogenase (see results), glyceraldehyde 3-phosphate dehydrogenase (see results) and peroxiredoxin-1 (not shown). Definitely information on the quantity for proteins of interest could be obtained as well by means of classical immunological approaches, thus validating results obtained by the methodology described here.

5.3 G6PDH as putative master regulator of redox equilibrium

We applied the methodology described above to the study of a cellular model of breast cancer derived from the breast cancer epithelial cell line MCF10A. Particularly M2 and M2T cells have been provided us by Prof. S. Piccolo laboratory and reproduce different grades of aggressiveness and malignancy of the tumour. Indeed M2T cells are engineered to express a constitutive active mutant of the transcription co-activator TAZ and reproduce higher grade malignancy and bear higher metastasizing potential in respect to their M2 counterpart. From our analysis 17 proteins were more oxidized into M2T cells, while 29 were more reduced in the same cell line in respect to M2 counterpart. Moreover we were able to quantify also other 45 redox sensitive proteins with unchanged oxidative status between the two samples. Numerous proteins known to be transcriptionally regulated by Nrf2 (see results) were mapped among both oxidatively unchanged and more reduced protein groups: specifically members of the unfolded protein response were unchanged while members of the antioxidant response were more reduced. On the other hand, among more oxidized proteins Hemicentin, Trophinin, Mucin-16, Usherin, and chondroitin sulphate proteoglycan share at different levels their function into cell adhesion and interaction with the ECM. We also mapped numerous oxidatively-modified cysteine-residues along those proteins sequence, both into cytoplasmic phosphorylative-regulatory domain (Mucin-16) and into EGF-like domain for the interaction with collagen (Usherin). Another interesting protein that we found to be more oxidized into more malignant cells was the enzyme glucose 6-phosphate dehydrogenase.

5.3.1 Cancer metabolism and ECM detachment

The initial recognition that cancer cells exhibit atypical metabolic characteristics can be traced to the work of Otto Warburg over the first half of the twentieth century [Koppenol et al., 2011]. Indeed, in the presence of oxygen, cells from most normal tissues use glucose through glycolysis producing pyruvate, and this is in turn mostly oxidized as Acetyl-CoA in mitochondria through the respiratory chain. On the other hand, in anaerobic conditions, normal tissues reduce pyruvate

from glycolysis to lactate, driving it away from mitochondrial oxidative phosphorylation. Then, in contrast to normal cells, rapidly proliferating ascites tumours metabolize pyruvate to lactate even in the presence of oxygen, despite the fact that this is energetically less “convenient” for the cell with respect to mitochondrial oxidation (almost 18-fold less ATP net production). It is still quite controversial if such metabolic switch is driven by impaired mitochondrial function in tumour cells, since it has been demonstrated that this organelle is still viable and functional even in cancer cells [de Oliveira et al., 2012]. Indeed neoplastic cells fermentative metabolism of glucose in the presence of oxygen has been proposed to serve more predominantly toward supporting biomass accumulation and redox maintenance in proliferating cells rather than to energetic functions [Cantor et al., 2012]. In this view glycolysis is interconnected with other metabolic pathways for synthesis of cellular building blocks: for example fructose-6-phosphate and glyceraldehyde-3-phosphate may be shunted into the non-oxidative arm of the pentose phosphate pathway (PPP) to generate ribose-5-phosphate (precursor in nucleotide biosynthesis). Alternatively glucose-6-phosphate can feed into the oxidative arm of the PPP to generate both ribose-5-phosphate and NADPH, which contributes to the cellular defence against oxidative stress. Oxidative stress is the rather generic term often used to describe an unbalance in cellular redox-homeostasis toward more oxidizing conditions. Even the role of this redox unbalance is not completely understood in reference to tumour etiology and progression: while oxidative DNA damage (see introduction too) could be culprit of the onset of genetic changes leading to neoplastic transformation, it seems that tumour cells need to raise some sort of defences against such oxidative stress in order to survive. Hence we can find a role for PPP activation in cancer. Nevertheless, focusing on the metabolic switch hallmark of tumour cells, it has been reported that also tumours developed in hypoxic environments have high glycolytic activity: in this case hypoxia can induce glycolysis and repress mitochondrial respiration to reduce oxygen consumption through hypoxia-inducible factor 1 (HIF-1). Moreover in hypoxic conditions mitochondria are reported to increase the production of superoxide (i.e. to favour mentioned oxidative stress) [Enns et al., 2012].

Tumour cells metabolic switch to aerobic glycolysis is also associated to increased glucose uptake. In relationship to this aspect, it has been demonstrated that ECM detachment could lead to *anoikis* (i.e. programmed cell death arising from loss of contact with the ECM) precisely via decreased glucose uptake [Schafer et al., 2009]. Indeed a model of ECM detachment developed with MCF10A cells demonstrated that breast cancer cells lacking ECM contact are selectively induced to *anoikis* [Fung et al., 2008] and Erb2 overexpression could confer *anoikis*-resistance by restoring glucose uptake through EGF receptor stabilization and PI3K activation [Kim et al., 2012]. In the mechanism proposed by Kim et al. *anoikis* resistance is basically obtained through the re-establishment of ATP production via restored glucose-uptake: in the proposed context this

involves the aerobic glycolytic pathway activated in tumour cells. Moreover, the same author demonstrates that *anoikis* resistance could be achieved also through antioxidant treatments of MCF10A cells in the above-mentioned model from Fung et al.: in this case resistance is obtained through re-establishment of ATP production via activation of the fatty acid oxidation, which is inhibited by high oxidant levels. Nevertheless, joining these data with the observations from de Oliveira and Cantor on mitochondrial activity in tumour cells (i.e. mitochondria are still the major source of intracellular ATP even in cancer cells), and the antioxidant function of the PPP shunted glucose-6-phosphate, it seems reasonable that the re-established glucose uptake could drive *anoikis* resistance through augmented NADPH production via oxidative PPP.

5.3.2 G6PDH redox regulation

Given a possible role for PPP in conferring resistance to *anoikis* in ECM detached tumour cells, it remains unclear the way by which this pathway could be activated. Mitsuishi et al. propose the direct activation of G6PD (the rate limiting enzyme of the PPP) by Nrf2 through the well conserved antioxidant response element (ARE) on its gene [Mitsuishi et al., 2012]. As already seen Nrf2 constitutive activation has indeed been associated with many tumours. But in our model NFE2L2 gene (i.e. Nrf2 gene) is even apparently down-regulated in M2T in respect to M2 cells. As NFE2L2 is regulated itself by the same Nrf2, it seems unlikely that this pathway is activated in our model. Moreover peroxiredoxin-1 western blotting showed that also this protein, known to be ARE regulated by Nrf2, is expressed at the same level in both M2T and M2 cells. Nevertheless we confirmed a globally even if slightly, more reduced status for M2T cells in respect to their M2 counterpart and we highlighted as well a pronounced unbalance toward a more oxidized status for the G6PD protein in the more malignant cells. The presence of different conformers of this enzyme is sustained also by reducing and non-reducing western blotting. However it cannot be stated at this point which are the causes for maintained G6PD oxidized status in M2T cells, but our experiments on the effect of redox status on this enzyme activity demonstrated that G6PD activity decrease in reducing conditions and that it re-oxidize itself quite rapidly (DTT removal, see results). Moreover, reduction and alkylation (with NEM) of G6PD further reduced its activity, thus showing that there is probably a less-active form of this enzyme lacking some required oxidation. Redox regulation of G6PD in organisms different from this human cell line has been extensively reported in the past [Udvardy et al., 1984, Gleason et al., 1996, Au et al., 2000, Née et al., 2009] and all agree on the reduction of activity consequent to enzyme reduction by DTT and thioredoxin. Finally, preliminary results from expression analysis don't detect any G6PD augmented transcription and western blotting, together with totally reduced controls confirmed nearly a twofold difference in protein quantity: probably the augmented activity of G6PD

in M2T cells could be ascribed to both its quantity *and* redox regulation. In a recent work from Halim et al., it has been demonstrated that prolonged H₂O₂ treatment (up to 10µM for 14 days) is able to rescue *anoikis* in non-small cell lung cancer and melanoma cells via over-expression of caveolin-1 [Halim et al., 2012]: even if not directly correlated with our observations, this study sustain once again a role for endogenous or exogenous produced electrophiles in conferring tumour cells an advantage toward survival, thus enriching the concept of “oxidative stress” mentioned above. Finally, another interesting observation arise from a less recent work on erythrocyte model system, where Scott et al. demonstrated that only G6PD-produced NADPH is able to decrease the oxidant sensitivity of those cells and not GSH [Scott et al., 1991], by correlating haemoglobin oxidant sensitivity to NADPH, but not to GSH. This is intriguing since it is known that Nrf2 pathway activation lead to increased GSH synthesis, while G6PD activation lead to increased NADPH synthesis, which is likely to be an interesting hypothesis in our model.

Finally, as for the outlined adhesion and ECM interaction molecules we found more oxidized into M2T cells, little could be said without further research. It is known indeed that oxidants could have a role into the induction of expression of adhesion molecules in mammalian vascular endothelial cells [Hurd et al., 2012] and that oxidants production to this aim could be localized by virtue of receptor mediated stimulation of membrane-NOX. Nevertheless there is no clear clue on the direct involvement of adhesion molecules oxidation into ECM-interaction processes. On the other hand, invasive cells could travel through various ECMs to extravasate, intravasate, and colonize target organs, but there is no unifying hypothesis to explain the mechanism used by cancer cells to cross these barriers [Díaz et al., 2012].

5.4 Concluding remarks

The work described here encompasses both the setting up of a complex analytical workflow and its application to the study of a cellular model. Thus, we were able to identify redox-sensible proteins which are differentially oxidized between M2T and M2 cells. M2T cells represent a more malignant breast cancer cellular model with higher metastasizing potential in respect to its M2 counterpart. M2T cells were demonstrated to contain more free thiols than M2 cells and so to be globally more reduced. Nevertheless, we identified proteins both more reduced and more oxidized into M2T cells, thus demonstrating a rather complex redox scenario in those cells. Particularly, among proteins more oxidized into M2T cells, we could identify proteins involved into ECM interaction and cell-adhesion processes and the PPP enzyme G6PD. While we are still looking to elucidate the significance of the formers, this latter enzyme is known to be a key player in redox homeostasis. Its oxidative activation together with increased expression could be culprit of

tumour cell response to ECM detachment induced oxidative stress, thus conferring aggressive cells survival advantage.

This work definitely lead to the generation of this hypothesis starting from the very development of a methodology and identified further research targets through a wider “omic” approach. Deeper studies on G6PD kinetic and redox-regulation and characterization of NADPH levels together with elucidation of Nrf2-pathway activation in this model, will provide further insights to the study.

6. REFERENCES

- Allison WS.** *Formation and reactions of sulfenic acids in proteins.* *Acc Chem Res* 1976;9(8):293-299
- Au SWN, Gover S, Lam VMS, Adams MJ.** *Human glucose-6-phosphate dehydrogenase: the crystal structure reveals a structural NADP⁺ molecule and provides insights into enzyme deficiency.* *Structure* 2000;8(3):293-303
- Bantscheff M, Schirle M, Sweetman G, Rick J, Kuster B.** *Quantitative mass spectrometry in proteomics: a critical review.* *Anal Bioanal Chem* 2007;389:1017-1031
- Barrett WC, DeGnore JP, Konig S, Fales HM, Keng YF, Zhang ZY, Yim MB, Chock PB.** *Regulation of PTP1B via glutathionylation of the active site cysteine 215.* *Biochemistry* 1999;38:6699-6705
- Barthel A, Ostrakhovitch EA, Walter PL, Kampkotter A, Klotz LO.** *Stimulation of phosphoinositide 3-kinase/Akt signaling by copper and zinc ions: Mechanisms and consequences.* *Arch Biochem Biophys* 2007;463:175-182
- Beckman KB, Ames BN.** *Oxidative decay of DNA.* *J Biol Chem* 1997;272(32):19633-19636
- Begg GE, Carrington L, Stokes PH, Matthews JM, Wouters MA, Husain A.** *Mechanism of allosteric regulation of transglutaminase 2 by GTP.* *Proc Natl Acad Sci USA* 2006;103(52):19683-8
- Bensadoun A, Weinstein D.** *Assay of proteins in the presence of interfering materials.* *Anal Biochem* 1976;70(1):241-250
- Bindoli A, Fukuto JM, Forman HJ.** *Thiol chemistry in peroxidase catalysis and redox signalling.* *Antiox Redox Signal* 2008;10(9):1549-1564
- Brandes N, Schmitt S, Jakob U.** *Thiol-based redox switches in eukaryotic proteins.* *Antiox Redox Signal* 2009;11(5):997-1014
- Brennan JP, Wait R, Begum S, Bell JR, Dunn MJ, Eaton P.** *Detection and mapping of widespread intermolecular protein disulfide formation during cardiac oxidative stress using proteomics with diagonal electrophoresis.* *Journal of Biological Chemistry* 2004;279(40):41352-41360
- Cantor JR, Sabatini DM.** *Cancer cell metabolism: one hallmark, many faces.* *Cancer Discov* 2012;2(10):881-98
- Chang F, Lee JT, Navolanic PM, Steelman LS, Shelton JG, Blalock WL, Franklin RA, McCubrey JA.** *Involvement of PI3K/Akt pathway in cell cycle progression,*

apoptosis, and neoplastic transformation: a target for cancer chemotherapy. Leukemia 2003;17:590-603

Chouchani ET, James AM, Fearnley IM, Lilley KS, Murphy MP. *Proteomic approaches to the characterization of protein thiol modification.* Curr Op Chem Bio 2011;15:120-128

Cordenonsi M, Zanconato F, Azzolin L, Forcato M, Rosato A, Frasson C, Inui M, Montagner M, Parenti AR, Poletti A, Daidone MG, Dupont S, Basso G, Bicciato S, Piccolo S. *The Hippo transducer TAZ confers cancer stem cell-related traits on breast cancer cells.* Cell 2011;147:759-772

Cumming RC, Andon NL, Haynes PA, Park M, Fischer WH, Schubert D. *Protein disulfide bond formation in the cytoplasm during oxidative stress.* Journal of Biological Chemistry 2004;279(21):21749-21758

Cuozzo JW, Kaiser CA. *Competition between glutathione and protein thiols for disulfide-bond formation.* Nat Cell Biol 1999;1:130-135

Denning TL, Takaishi H, Crowe SE, Boldogh I, Jevnikar A, Ernst PB. *Oxidative stress induces the expression of Fas and Fas ligand and apoptosis in murine intestinal epithelial cells.* Free Radic Biol Med 1992;33(12):1641-1650

Di Simplicio P, Cacace MG, Lusini L, Giannerini F, Giustarini D, Rossi R. *Role of protein -SH groups in redox homeostasis – The erythrocyte as a model system.* Archiv. Of Biochem Biophys 1998;355(2):145-152

Díaz B, Courtneidge SA. *Redox signaling at invasive microdomains in cancer cells.* Free Rad Biol Med 2012;52(2):247-256

Dickinson DA, Forman HJ. *Cellular glutathione and thiols metabolism.* Biochemical Pharmacology 2002;64(5-6):1019-1026

Enns L, Ladiges W. *Mitochondrial redox signaling and cancer invasiveness.* J Bioenerg Biomembr 2012;44(6):635-8

Esposito F, Chirico G, Gesualdi NM, Posadas I, Ammendola R, Russo T, Cirino G, Cimino F. *Protein kinase B activation by reactive oxygen species is independent of tyrosine kinase receptor phosphorylation and requires Src activity.* J Biol Chem 2003;278(23):20828-20834

Foster FM, Traer CJ, Abraham MJ, Fry J. *The phosphoinositide (PI) 3-kinase family.* J Cell Sci 2003;116:3037-3040

Franke TF, Cantley LC. *A Bad kinase makes good.* Nature 1997;390:116-117

- Fung C**, Lock R, Gao S, Salas E, Debnath J. *Induction of autophagy during extracellular matrix detachment promotes cell survival*. *Mol Biol of the Cell* 2008;19(3):797-806
- Gao X**, Xing Da. *Molecular mechanisms of cell proliferation induced by low power laser irradiation*. *J Biomed Sc* 2009;16(4):1-16
- Ghezzi P**. *Oxidoreduction of protein thiols in redox regulation*. *Biochem Society Transactions* 2005;33(6):1378-1381
- Giannoni E**, Buricchi F, Grimaldi G, Parri M, Cialdai F, Taddei ML, Raugei G, Ramponi G, Chiarugi. *Redox regulation of anoikis: reactive oxygen species as essential mediators of cell survival*. *Cell death differentiation* 2008;15:867-878
- Giles GI**, Tasker KM, Jacob C. *Hypothesis: The role of reactive sulfur species in oxidative stress*. *Free Radic Biol Med* 2001;31:1279-1283
- Gleason FK**. *Glucose-6-phosphate dehydrogenase from the cyanobacterium, Anabaena sp. PCC 7120: purification and kinetics of redox modulation*. *Archiv of Biochem and Biophys* 1996;334(2):277-283
- Go YM**, Jones DP. *Redox compartmentalization in eukaryotic cells*. *Biochim Biophys Act* 2008;1789:1273-1290
- Gorman JJ**, Wallis TP, Pitt JJ. *Protein disulfide bond determination by mass spectrometry*. *Mass Spectrometry Reviews* 2002;21(3):183-216
- Gupta SC**, Hevia D, Patchva S, Park B, Koh W, Aggarwal BB. *Upsides and downsides of reactive oxygen species for cancer: the roles of reactive oxygen species in tumorigenesis, prevention and therapy*. *Antioxid Redox Signal* 2012;16(11):1295-1322
- Halim H**, Chanvorachote P. *Long-term hydrogen peroxide exposure potentiates anoikis resistance and anchorage-independent growth in lung carcinoma cells*. *Cell Biol Int* 2012;36(11):1055-66
- Halvey PJ**, Watson WH, Hansen JM, Go YM, Samali A, Jones DP. *Compartmental oxidation of thiol-disulphide redox couples during epidermal growth factor signaling*. *Biochem J* 2005;386:215-219
- Higdon A**, Diers AR, OH JY, Landar A, Darley-Usmar VM. *Cell signalling by reactive lipid species: new concepts and molecular mechanisms*. *Biochem J* 2012;442:453-464
- Hurd TR**, DeGennaro M, Lehmann R. *Redox regulation of cell migration and adhesion*. *Trends Cell Bio* 2012;22(2):107-115

- Hurd TR**, DeGennaro M, Lehmann R. *Redox regulation of cell migration and adhesion*. Trends in Cell Biology 2012;22(2):107-115
- Hwang C**, Sinskey AJ, Lodish HF. *Oxidized redox state of glutathione in the endoplasmic reticulum*. Science 1992;257(5076):1496-14502
- Ikeda H**, Nichi S, Sajai M. *Transcription factor Nrf2/MafK regulates rat placental glutathione S-transferase gene during hepatocarcinogenesis*. Biochem J 2004;380:515-521
- Izquierdo-Álvarez A**, Martínez-Ruiz A. *Thiols redox proteomics seen with fluorescence yes: the detection of cysteine oxidative modifications by fluorescence derivatization and 2-DE*. J Proteomics 2011;75:329-338
- Kamata H**, Hirata H. *Redox regulation of cellular signaling*. Cell Signal 1999;11(1)1-14
- Kettenhofen NJ**, Wang X, Gladwin MT, Hogg N. *In-gel detection of S-nitrosated proteins using fluorescence methods*. Methods Enzymol 2008;441:53-71.
- Kim SK**, Yang JW, Kim MR, Roh SH, Kim HG, Lee KY. *Increased expression of Nrf2/ARE-dependent anti-oxidant proteins in tamoxifen-resistant breast cancer cells*. Free Radic Biol Med 2008;45:537-546
- Kim YN**, Koo KH, Sung JY, Yun UJ, Kim H. *Anoikis resistance: an essential prerequisite for tumor metastasis*. Int J Cell Biol 2012;2012:306879
- Kobayashi CI**, Suda T. *Regulation of reactive oxygen species in stem cells and cancer stem cells*. J Cell Physiol 2012;227:421-430.
- Koppenol WH**, Bounds PL, Dang CV. *Otto Warburg's contributions to current concepts of cancer metabolism*. Nat Rev Cancer 2011;11(5)325-37
- Käll L**, Storey JD, MacCoss MJ, Noble WS. *Posterior error probabilities and false discovery rates: two sides of the same coin*. J Proteome Res 2008;4:40-44
- Lambeth JD**. *NOX enzymes and the biology of reactive oxygen*. Nat Rev Immunol 2004;4:181-189
- Lau A**, Villeneuve NF, Sun Z, Wong PK, Zhank DD. *Dual roles of Nrf2 in cancer*. Pharmacol Res 2008;58(5-6):262-270.
- Le Moan N**, Clement G, Le Maout S, Tacnet F, Toledano MB. *The Saccharomyces cerevisiae proteome of oxidized protein thiols*. J Biol Chem 2006;281(15):10420-10430
- Leichert LI**, Jakob U. *Protein thiol modifications visualized in vivo*. PLoS Biol 2004;2(11):e333

- Leonard SE, Reddie KG, Carroll KS.** *Mining the thiol proteome for sulfenic acid modifications reveals new targets for oxidation in cells.* ACS Chem Biol 2009;4(9):783-799
- Lewis SD, Misra DC, Schafer JA.** *Determination of interactive thiol ionizations in bovine serum albumin, glutathione, and other thiols by potentiometric difference titration.* Biochemistry 1980;19(26):6129-6137
- Lind C, Gerdes R, Hamnell Y, Schuppe-Koistinen I, von Lowenhielm HB, Holmgren A, Cotgreave IA.** *Identification of S-glutathionylated cellular proteins during oxidative stress and constitutive metabolism by affinity purification and proteomic analysis.* Arch Biochem Biophys 2002;406:229-240
- Little C, O'Brien PJ.** *Mechanism of peroxide-inactivation of the sulphhydryl enzyme glyceraldehyde-3-phosphate dehydrogenase.* Eur J Biochem 1969;10(3):533-538
- Maiorino M, Ursini F, Bosello V, Toppo S, Tosatto SC, Mauri P, Becker K, Roveri A, Bulato C, Benazzi L, De Palma A, Flohé L.** *The thioredoxin specificity of Drosophila GPx: a paradigm for a peroxiredoxin-like mechanism of many glutathione peroxidases.* Journal of Molecular Biology 2007;365(4):1033-1046
- Martindale JL, Holbrook NJ.** *Cellular response to oxidative stress: signaling for suicide and survival.* J Cell Physiol 2002;192:1-15
- Mauri P, Toppo S, De Palma A, Benazzi L, Maiorino M, Ursini F.** *Identification by MS/MS of disulfides produced by a functional redox transition.* Methods in Enzymology 2010;473:217-225
- McCubrey JA, Steelman LS, Chappell WH, Abrams SL, Wong EWT, Chang F, Lehmann B, Terrian DM, Milella M, Tafuri A, Stivala F, Libra M, Basecke J, Evangelisti C, Martelli AM, Franklin RA.** *Roles of the Raf/MEK/ERK pathway in cell growth, malignant transformation and drug resistance.* Biochim Biophys Acta 2007;1773(8):1263-1284
- McDonagh B, Ogueta S, Lasarte G, Padilla CA, Bárcena JA.** *Shotgun redox proteomics identifies specifically modified cysteines in key metabolic enzymes under oxidative stress in Saccharomyces cerevisiae.* J Proteomics 2009;72:677-689
- McDonagh B, Requejo R, Fuentes-Almagro CA, Ogueta S, Bárcena JA, Padilla CA.** *Thiol redox proteomics identifies differential targets of cytosolic and mitochondrial glutaredoxin-2 isoforms in Saccharomyces cerevisiae. Reversible S-glutathionylation of DHBP synthase (RIB3).* J Proteomics 2011;74:2487-2497

- Mitsuishi** Y, Taguchi K, Kawatani Y, Shibata T, Nukiwa T, Aburatani H, Yamamoto M, Motohashi H. *Nrf2 redirects glucose and glutamine into anabolic pathways in metabolic reprogramming*. *Cancer Cell* 2012;22(1):66-79
- Mottley** C, Mason RP. *Sulfur-centered radical formation from the antioxidant dihydrolipoic acid*. *Journal of Biological Chemistry* 2001;276(46):42677-42683
- Mueller** L, Brusniak MY, Mani DR, Aebersold R. *An assessment of software solutions for the analysis of mass spectrometry based quantitative proteomics data*. *J Proteome Res* 2008;7:51-61
- Murphy** MP. *How mitochondria produce reactive oxygen species*. *Biochem J* 2009;417:1-13
- Murphy** MP. *Mitochondrial thiols in antioxidant protection and redox signalling: distinct roles for glutathionylation and other thiol modifications*. *Antioxid Redox Signaling* 2012;16(6):476-95
- Nagahara** N, Matsumura T, Okamoto R, Kajihara Y. *Protein cysteine modifications: (1) medicinal chemistry for proteomics*. *Curr Med Chem* 2009;16(33):4419-44
- Née** G, Zaffagnini M, Trost P, Issakidis-Bourguet E. *Redox regulation of chloroplastic glucose-6-phosphate dehydrogenase: a new role for f-type thioredoxin*. *FEBS Letters* 2009;583(17):2827-2832
- Nishikawa** M. *Reactive oxygen species in tumor metastasis*. *Cancer Lett* 2008;266:53-59
- Old** WM, Meyer-Arendt K, Veline-Wolf L, Pierce KG, Mendoza A, Sevinsky JR, Resing KA, Ahn NG. *Comparison of label-free methods for quantifying human proteins by shotgun proteomics*. *Mol Cell Proteomics* 2005;4:1487-1502
- Ozben** T. *Oxidative stress and apoptosis: impact on cancer therapy*. *J Pharm Sci* 2007;96(9):2181-2196
- Patel** KD, Zimmerman GA, Prescott SM, McEver R, McIntyre TM. *Oxygen radicals induce human endothelial cells to express GMP-140 and bind neutrophils*. *J Cell Biol* 1991;112(4):749-759
- Ralph** SJ, Enriquez SR, Neuzil J, Saavedra E, Sanchez RM. *The causes of cancer revisited: "Mitochondrial malignancy" and ROS-induced oncogenic transformation – Why mitochondria are targets for cancer therapy*. *Molecular Aspects of Medicine* 2010;31:145-170

- Requejo R**, Chouchani ET, James AM, Prime TA, Lilley KS, Fearnley IM, Murphy MP. *Quantification and identification of mitochondrial proteins containing vicinal dithiols*. Arch Biochem Biophys 2010;504(2):228-235
- Riederer BM**. *Oxidation proteomics: the role of thiol modifications*. Curr Proteomics 2009;6:51-62
- Rogers LK**, Leinweber BL, Smith CV. *Detection of reversible protein thiol modifications in tissues*. Anal Biochem 2006;358:171-184
- Romashkova JA**, Makarov SS. *NF- κ B is a target of AKT in anti-apoptotic PDGF signaling*. Nature 1999;401:86-90
- Saito A**, Nagasaki M, Oyama M, Kozuka-Hata H, Semba K, Sugano S, Yamamoto T, Miyano S. *AYUMS; an algorithm for completely automatic quantitation based on LC-MS/MS proteome data and its application to the analysis of signal transduction*. BMC Bioinformatics 2007;8:15
- Saitoh M**, Nishitoh H, Fujii M, Takeda K, Tobiume K, Sawada Y, Kawabata M, Miyazono K, Ichijo H. *Mammalian thioredoxin is a direct inhibitor of apoptosis signal-regulating kinase (AKS) 1*. The EMBO Journal 1998;17(9):2596-2606.
- Salmeen A**, Andersen JN, Myers MP, Meng TC, Hinks JA, Tonks NK, Barford D. *Redox regulation of protein tyrosine phosphatase 1B involves a sulphenylamide intermediate*. Nature 2003;423(6941):769-773
- Schafer ZT**, Grassian AR, Song L, Jiang Z, Gerhart-Hines Z, Irie HY, Gao S, Puigserver P, Brugge JS. *Antioxidant and oncogene rescue of metabolic defects caused by loss of matrix attachment*. Nature 2009;461(7260):109-113
- Scott MD**, Zuo L, Lubin BH, Chiu DT. *NADPH, not glutathione, status modulates oxidant sensitivity in normal and glucose-6-phosphate dehydrogenase-deficient erythrocytes*. Blood 2012;119(7):2059-2064
- Scott WA**. *Physical properties of glucose 6-phosphate dehydrogenase from Neurospora crassa*. J Biol Chem 1971;246(20):6353-6359
- Shigenaga MK**, Gimeno CJ, Ames BN. *Urinary 8-hydroxy-2'-deoxyguanosine as a biological marker of in vivo oxidative DNA damage*. Proc Natl Acad Sci USA 1989;86(24):9697-9701
- Singh A**, Misra V, Thimmulappa RK, Lee H, Ames S, Hoque MO. *Dysfunctional KEAP1-NRF2 interaction in non-small-cell lung cancer*. PLoS Med 2006;3(10):e420

- Stone JR.** *An assessment of proposed mechanisms for sensing hydrogen peroxide in mammalian systems.* Arch Biochem Biophys 2004;422(2):119-124
- Tosatto SCE, Bosello V, Fogolari F, Mauri P, Roveri A, Toppo S, Flohé L, Ursini F, Maiorino M.** *The catalytic site of glutathione peroxidases.* Antioxid Redox Signal 2008;10(9):1515-26
- Trotter EW, Grant CM.** *Non-reciprocal regulation of the redox state of the glutathione-glutaredoxin and thioredoxin systems.* EMBO 2003;Rep4:184-188
- Udvardy J, Borbély G, Juhasz A, Farkas G.** *Thioredoxins and the redox modulation of glucoase-6-phosphate dehydrogenase in Anabaena sp. strain PCC 7120 vegetative cells and heterocysts.* J Bacteriol 1984;157(2):681-683
- Ushio-Fukai M.** *Redox signalling in angiogenesis: role of NADPH oxidase.* Cardiovasc Res 2006;71:226-235
- Ushio-Fukai M., Nakamura Y.** *Reactive oxygen species and angiogenesis: NADPH oxidase as target for cancer therapy.* Cancer Lett 2008;266:37-52
- Valko M, Rhodes CJ, Moncol J, Izakovic M, Mazur M.** *Free radicals metals and antioxidants in oxidative stress-induced cancer.* Chem Biol Interact 2006;160(1):1-40
- Wardman P.** *Evaluation of the “radical sink” hypothesis from a chemical-kinetic viewpoint.* J Radioanal Nucl Chem 1998;232(1-2):23-27
- Watson WH, Pohl J, Montfort WR, Stuchlik O, Reed MS, Powis G, Jones DP.** *Redox potential of human thioredoxin I and identification of a second dithiol/disulfide motif.* J Biol Chem 2003;278(35):33408-33415
- Winterbourn CC, Metodiewa D.** *Reactivity of biologically important thiol compounds with superoxide and hydrogen peroxide.* Free Rad Biol Med 1999;27(3-4):322-328
- Woo HA, Yim SH, Shin DH, Kang D, Yu DY, Rhee SG.** *Inactivation of peroxiredoxin I by phosphorylation allows localized H₂O₂ accumulation for cell signaling.* Cell 2010;140:517-528
- Wouters MA, Fan SW, Haworth NL.** *Disulfides as redox switches: from molecular mechanisms to functional significance.* Antiox Redox Signal 2010;12(1):53-91
- Wouters MA, Iismaa S, Fan WS, Haworth NL.** *Thiol-based redox signalling: Rust never sleeps.* Int Journal of Biochem & Cell Biol 2011;43(8):1079-1085

- Zhang B**, VerBerkmoes NC, Langston MA, Uberbacher E, Hettich RL, Samantova NF. *Detecting differential and correlated protein expression in label-free shotgun proteomics*. J Proteome Res 2006;5:2909-2918
- Zhang H**, Liu H, Borok Z, Davies KJA, Ursini F, Forman HJ. *Cigarette smoke extract stimulates epithelial-mesenchymal transition through Src activation*. Free Rad Biol Med 2012;52:1437-1442
- Zhang Y**, Wen Z, Washburn MP, Florens L. *Effect of dynamic exclusion duration on spectral count based quantitative proteomics*. Anal Chem 2009;81:6317-6326
- Jaffe JD**, Mani DR, Leptos KC, Church GM, Gillette MA, Carr SA. *PEPPER, a platform for experimental proteomic pattern recognition*. Mol Cell Proteomics 2006;5(10):1927-41
- Fratelli M**, Demol H, Puype M, Casagrande S, Eberini I, Salmona M, Bonetto V, Mengozzi M, Duffleux F, Miclet E, Bachi A, Vandekerckhove J, Gianazza E, Ghezzi P. *Identification by redox proteomics of glutathionylated proteins in oxidatively stressed human T lymphocytes*. PNAS 2002;99(6):3505-10

Other studies carried out during PhD Program

During my PhD I also collaborated to projects encompassing the application of proteomics techniques to the study of Cisplatin resistance in cellular models and to the analysis of red blood cell membrane proteins. These works, not belonging to the thesis, have been published in: the *Journal of proteome research* (v.10; p.416-428, 2011) with the title “New insights into Neuroblastoma Cisplatin Resistance: A comparative proteomic and meta-mining investigation” and in the *Journal of chromatography A*, (v.1217; p.5328–5336, 2010) with the title “Extraction methods of red blood cell membrane proteins for multidimensional protein identification technology (MudPIT) analysis”. Finally, during the last year of my PhD I also gave my contribution to the MS-characterization of the redox-status of glutathione peroxidase 7 in the work recently submitted to “*Biochimica et Biophysica Acta*” with the title “Protein Disulfide Isomerase and Glutathione are alternative substrates in the one Cys catalytic cycle of Glutathione Peroxidase 7 within the endoplasmic reticulum”.

AKNWOLEDGMENTS

This thesis is the conclusion of three rich and compelling years dedicated to my PhD experience, and I hope this would represent the starting point for an even brighter and exciting future in research. Nevertheless, I would not have done much without the support that many people gave me, both in the working field and in private life.

First of all I would like to thank my tutor Professor Fulvio Ursini that gave me the opportunity to achieve this PhD and investigate the fascinating world of redox biochemistry, and Dr. Antonella Roveri for her irreplaceable help with experiments and wise suggestions in many fields. A special thank goes then to Dr. Marco Falda, member of the bioinformatics group of our lab, for his fundamental contribution to the data analysis workflow.

Then I would like to thank Prof. Stefano Piccolo for providing us the precious cellular model subject of this study, and Dr. Elena Tibaldi and Dr. Rina Venerando for their collaboration to the project.

I also want to thank the other members of the workgroup for the help they gave me both with experiments and fruitful discussions day after day: Prof. Matilde Maiorino and Dr. Valentina Bosello from the lab, and Dr. Stefano Toppo from the bioinformatics group.

Special thanks go to all the people from the Proteomics lab, where I met new friends and expert colleagues: first of all Dr. Giorgio Arrigoni, who shared his knowledge and prompted me through the engaging field of mass spectrometry. I would also like to thank Cinzia, Serena, Renato, and Lucia for all the funny moments we shared both in front of the instruments and tasting ethnic foods during lunchtime. A notice of gratitude goes then to Dr. Giovanni Miotto for his help with the often fickle mass spectrometers, and to Prof. Oriano Marin for his availability.

As I promised, I would like to thank also Massimo Guida for the availability and precious help in fixing my idiosyncrasy against bureaucracy.

Last, but not least, a special thank goes to my family and my friends for the constant support they gave me in these three years: Anna, Franco, Lorenzo, Francesco, and Michele.